xx(132593.1)

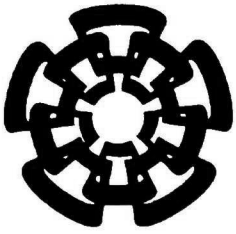

CINVESTAV

Centro de Investigación y de Estudios Avanzados del I.P.N.
Unidad Guadalajara

Valoración de la estabilidad robusta de sistemas de potencia de dimensión grande utilizando la teoría de valor singular estructurado

Tesis que presenta:
Rafael Castellanos Bustamante

para obtener el grado de:
Doctor en Ciencias

en la especialidad de:
Ingeniería Eléctrica

Director de Tesis
Dr. Arturo Román Messina

Guadalajara, Jalisco, Noviembre de 2006.

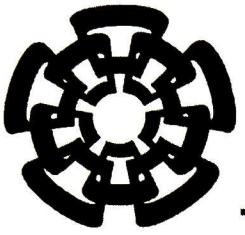

CINVESTAV

Centro de Investigación y de Estudios Avanzados del I.P.N.
Unidad Guadalajara

Robust Stability Assessment of Large Power Systems Using the Structured Singular Value Theory

A thesis presented by:
Rafael Castellanos Bustamante

to obtain the degree of:
Doctor in Science

in the subject of:
Electrical Engineering

Thesis Advisor:
Dr. Arturo Román Messina

Guadalajara, Jalisco, November 2006.

Valoración de la estabilidad robusta de sistemas de potencia de dimensión grande utilizando la teoría de valor singular estructurado

Tesis de Doctorado en Ciencias
Ingeniería Eléctrica

Por:
Rafael Castellanos Bustamante
Maestro en Ciencias en Ingeniería Eléctrica
Instituto Politécnico Nacional 1991-1992

Director de Tesis
Dr. Arturo Román Messina

CINVESTAV del IPN Unidad Guadalajara, Noviembre de 2006.

Robust Stability Assessment of Large Power Systems Using the Structured Singular Value Theory

Doctor of Science Thesis
In Electrical Engineering

By:
Rafael Castellanos Bustamante
Master in Science
Instituto Politécnico Nacional 1991-1992

Thesis Advisor:
Dr. Arturo Román Messina

CINVESTAV del IPN Unidad Guadalajara, November, 2006.

Acknowledgments

I thank God for give me health and power for going ahead

I would like to dedicate this thesis to the memory of my mother Maria Cruz. I would also like to thank my father Rafael for his love and encouragement

My wife Maribel deserves very special thanks for her love and valuable support that she has given me. Also, I wish to thank my sons Rafael and K. Rodrigo, and my little daughter Valeria for their love

The content of this thesis is strongly influenced by the ideas of Professor Messina. I wish to thank him for his constant encouragement, helpful discussions, and valuable comments and corrections

I like to thank all members of my thesis committee. Specially, I am grateful from Dr. Calderon for his valuable suggestions

Finally, I am grateful from Instituto de Investigaciones Electricas for its support

Valoración de la estabilidad robusta de sistemas de potencia de dimensión grande utilizando la teoría de valor singular estructurado

Resumen

En esta tesis, se propone un marco de trabajo analítico basado en la teoría de valor singular estructurado (SSV, por sus siglas en Inglés) y en la formulación de la transformación lineal fraccional (LFT), para el análisis de la estabilidad robusta y el comportamiento robusto de sistemas de potencia con respecto a una serie de incertidumbres paramétricas reales.

Se presenta una técnica general, la cual de manera precisa identifica la estabilidad robusta de sistemas de potencia complejos sometidos a incertidumbres en las condiciones de operación. En este procedimiento, las variaciones en las condiciones de operación del sistema de potencia son representadas mediante una transformación lineal fraccional discutiendo sus incertidumbres asociadas. También, se presentan criterios que mejoran tanto la evaluación del comportamiento dinámico del sistema de potencia de lazo cerrado en términos de su robustez en la presencia de estas incertidumbres como la identificación de los elementos con incertidumbre que dominan el comportamiento robusto. Se investigan la precisión de los estimados de robustez, reducción del tiempo de cómputo y del espacio óptimo de las condiciones de operación variantes.

Se propone un procedimiento sistemático para valorar la seguridad dinámica de los sistemas de potencia, el cual da el margen de estabilidad e información que es necesaria para garantizar una operación segura bajo condiciones de operación ante contingencias y en el diseño de controles preventivos y de emergencia, haciéndolo particularmente bien adaptado para aplicaciones en línea.

La metodología propuesta se prueba en dos sistemas: un sistema de potencia de dos áreas y un modelo dinámico de 6 áreas y 377 generadores del sistema interconectado Mexicano. Los resultados de las simulaciones de estos sistemas ante grandes variaciones en las condiciones de operación muestran que el método propuesto es preciso y flexible y que puede utilizarse para el análisis de estabilidad y control robusto de sistemas de potencia complejos de dimensión grande.

Robust Stability Assessment of Large Power Systems Using the Structured Singular Value Theory

Abstract

In this dissertation, an analytical framework, based on structured singular value (SSV) theory and the linear fractional transformation (LFT) formulation, is proposed for the analysis of robust stability and robust performance of power systems with respect to a set of *real*, parametric uncertainties.

A general technique is presented first, which accurately identifies robust stability of complex systems subject to uncertainties in operating conditions. In this procedure, variations in the operating conditions of the system are treated as LFT-based parametric uncertainty descriptions and incorporated into the SSV analysis framework. Techniques that explicitly address and treat multiple, interrelated uncertain parameters are given and efficient methods to generate LFT-based uncertainty descriptions for the model and its associated uncertainty are discussed. Improved criteria to evaluate the dynamics of the closed-loop power system model in terms of its robustness in the presence of these uncertainties as well as to identify the uncertain elements that dominate the robust performance, are also presented. Accuracy of the robustness estimates, reduced computational time, and optimal parameter space gridding are investigated.

A systematic procedure for dynamic security assessment of power systems is then proposed, that gives the stability margin and information which is necessary in ensuring secure operation under contingency conditions and in designing preventive and emergency controls, making it particularly well adapted for on-line applications.

The proposed methodology is tested on two test systems: a two-area test power system and, a 6-area 377-generator dynamic model of the Mexican interconnected system. Extensive simulation results of these systems for wide changes on operating conditions show that the proposed method is both, accurate and flexible, and can be used for robust stability and control analysis of very large power systems.

Contents

List of Figures

List of Tables

Chapter 1

Introduction

1.1. Introduction and motivation

Uncertain, large-scale interconnected networks are highly complex systems that defy predictions with any degree of certainty. Power systems, in particular, constantly experience sudden changes in operating conditions such as variations in generation and load patterns, as well as changes in network structure and configuration. High levels of uncertainty may lead to reduction of power system reliability and result in poor design of system controllers and unreasonable conservatism in power system operation. A systematic analysis of these uncertainties is therefore needed to determine their impact on both, robust stability and robust performance.

The evaluation of uncertainty effects on system dynamic performance is emerging as an area of increasing importance in the analysis of stability and control of power systems. Uncertainty modeling can contribute to better power system control by identifying and quantifying the sources of significant uncertainty in predicting system conditions that affect system behavior. In addition, accurate and efficient determination of small signal stability limits is fundamental, both to determining and interpreting worst case operating conditions as well as to ensure stable operation of the system and robustness of controllers to changing operating conditions.

With the increasing use of more complex control devices along with more variable and unpredictable operating conditions often dictated by economic issues, the influence of uncertainty on power system behavior is becoming more important and the requirements for more accurate predictive tools grow stronger. Uncertainties in the power system model can be unstructured (i.e. non-bounded parameter uncertainties) or structured associated with loading and other varying operating conditions [1] and can result in conservative assessment of system stability. In such cases, robustness is an important issue in control design as is also of interest to assess performance analysis. Although the parameters in the linear model change in a complex manner with the different loading and various operating

conditions, these variations are usually bounded and can be modeled as parametric uncertainties.

Existing techniques for the analysis of small signal stability such as eigenvalues analysis are based on a few selected points from the wide range of possible operating conditions [2, 3]. Based on engineering judgment, and experience, small signal stability limits can be approximately determined. Nevertheless, these techniques do not guarantee acceptable performance or even stability other than at the design condition. More importantly, the known methods do not produce an indication of the stability margin that is needed for the development of remedial measures [4].

Starting with a given operating scenario, the stress in the system is scaled up in finite steps until the instability condition is reached. In the first simulation a large change in stress is used. As the stress is increased, it is necessary to decrease the step size. This can be done for different load and transmission patterns or control settings. This approach, however, has several limitations:

- Large computer-based simulation models are often required to characterize uncertainty behavior with sufficient fidelity. Close to the instability condition, the steady state power flow solution may fail to converge or the resulting condition may be unstable. As a result, the degree of stress has to be reduced and a new solution is obtained. This may be time consuming.
- The handling of multiple uncertainties is very difficult and the computer solution of such models can be quite expensive.
- Accurate determination of small signal stability margins is based on experience, i.e. the approach is system-specific. Under severe uncertainty or in the presence of multiple, real interrelated uncertain parameters such approach may be ineffective.

These shortcomings may limit the range of applicability of conventional approaches or lead to conservative assessment of stability. Further, there is a general lack of specialized software to assess and ensure stability in the presence of uncertain system behavior.

The above discussions, point to the need for identification of techniques to estimate small-signal stability margins. This provides motivation to explore analytical techniques with the

ability to determine stability robustness of complex power systems. Such as an accurate prediction capability would significantly reduce the amount of computational resources required for assessing the maximum change in expected operating conditions to make the system unstable and provide important information needed in the design of system controllers.

1.2. Statement of the problem

Power system dynamic behavior is affected by the network structure, and operating conditions. An important problem that naturally arises in power system analysis is that of determining stability robustness with respect to *real* parameter variations associated with variations of operating conditions. In particular, uncertainties arising from varying operating conditions are of considerable practical engineering interest and the subsequent discussion of uncertainty will be restricted to the analysis of this problem.

A number of factors may contribute to uncertain system behavior. These include:

- Different load flow patterns and varying load levels during the day, week or year
- Load characteristics, and uncertainty in demand parameters such as voltage and frequency dependence, that might vary with seasons and time of day
- Uncertainty in the topology (structure) of the power system as some plants, transmission lines or transformers might be taken out for maintenance
- Inherent uncertainties in the dynamic models of power systems
- Changes in control parameters due to aging or control action

On top of these physical uncertainties, deregulation produces additional uncertainty in operating conditions. These uncertainties may be modeled in many forms and may be located at various points in the power system state-space representation. This makes the treatment and analysis of multiple uncertainties occurring simultaneously at various point of the control loop very difficult.

Furthermore, the choice of a particular representation is often problem-dependent or is associated with the specific type of uncertainty considered in the analysis. A framework is therefore needed that allows these effects to be represented in a more systematic manner.

This is a problem that has received limited attention by the power system community people.

Classical methods of small signal stability analysis present several limitations when applied to robust stability assessment of large systems. The first is that, for many physical systems, and in particular for small signal stability models in this research, the requirements for accurate representation of uncertainty makes reliable real state-space realizations very difficult to construct, especially for *real* uncertainty associated with physical changes in system parameters. Another drawback of conventional approaches is that multiple uncertainties occurring simultaneously are assumed to be uncorrelated. In practice, operating uncertainties may be related or have an interacting effect, for instance, on specific modes of oscillations which is not accounted for by existing techniques. Existing analytical frameworks for robustness analysis are therefore, grossly conservative and provide limited insight into the analysis and characterization of these interacting factors. A further disadvantage is that the high order of the models makes uncertainty analysis computationally intensive, especially as the number of uncertainties increases.

To circumvent these problems, this research explores the development of a new type of modeling framework that explicitly acknowledges and incorporates multiple, correlated uncertainty, and then use specialized numerical methods to evaluate stability margins and worst-case combinations of critical parameters given increased levels of uncertainty about forecasted or nominal conditions. The method extends previous LFT-based parametric uncertainty descriptions for the system model and its associated uncertainty to account for variations in power system operating conditions. More specifically, this research work addresses the more complex and less discussed problem of evaluating the range of damping of critical system modes and the associated small-signal stability uncertainty due to uncertainties in operating conditions. The resulting robustness tests provide definite worst-case guarantees of stability and performance robustness for uncertain systems and gives guarantee of finding the worst-case uncertainty combination in the parameter space.

The thesis also discusses the development of tools for on-line small-signal security assessment with the ability to estimate the damping ratio of critical system modes and the identification of remedial measures based on FACTS technologies. There are several novel

features. First, an analytical framework is introduced in which uncertainty-based modeling assists in the identification of critical ranges of damping of major inter-area modes and the critical sources of uncertainty thereby identified are used to produce remedial measures. Second, specialized techniques are devised to produce near, real-time preventive and emergency control actions that enhance small-disturbance angle stability and reduce the vulnerability of the system to changes in key system parameters by estimating the critical range of parameter variations. The method is of particular interest for stability and robustness analysis of large, complex systems and may be used to characterize most uncertainties associated with variations of operating conditions in both off-line and on-line environments. Finally, a systematic approach is proposed to determine both, worst-case operating conditions and the critical combination of system parameters that make the system unstable. This allows for a more effective utilization of control actions and results in increased system reliability.

1.3. Review of previous work

In recent years, the issue of plant uncertainty in power system models has been considered by several researchers. Several representations have been explored to characterize stability robustness including small signal stability and large performance stability. The following is a review of prior work relevant to the topic presented in this thesis.

1.3.1. Conventional analysis techniques

A number of analytical techniques exist in the power systems literature that enable the stability boundaries of a defined linear (nonlinear) system to be computed and the possible instabilities to be characterized. Conventional small signal simulations have been used for several decades to evaluate the stability of the power system. The theory has been covered extensively in the literature [4] and is no discussed here.

To date, these techniques have been used to design controllers using traditional multivariate techniques for a set of nominal operating conditions. These approaches, however, suffer from several drawbacks and may be ineffective, especially for the analysis of uncertainties occurring simultaneously. First, these techniques require considerable experience of the analysts. Second, it is very difficult to assess robust stability when multiple uncertainties

appear simultaneously. Lastly, they do not readily provide an indication of the stability margin.

1.3.2. Uncertainty modeling and characterization

Uncertainty modeling and characterization of stressed power systems has been the focus of many studies in the past decade. Robustness evaluation is also an importance issue because of the inherent uncertainty and the need to determine stability margins and the evaluation of the range of damping of critical system modes for a wide-range of operating conditions.

Various approximations have been utilized in the modeling of uncertain systems including polynomial approaches, Lyapunov state-space based procedures, probabilistic methods, and μ-synthesis. The various approaches also differ in how they mechanistically treat uncertainty.

The most general and accurate means of analyzing and characterizing the effect of uncertainty on robust performance and stability is the structured singular value framework developed by Doyle and other researchers [5,6]. This method provides simultaneous assessment of robust stability and performance and can be used to design power system controllers using μ-synthesis. The resulting robustness tests provide definite worst-case guarantees of stability and performance robustness for uncertain power system models.

In its original formulation, SSV theory was applied to complex uncertainty arising from neglected dynamics. Early applications of these methods were, at first, concerned with interpreting system uncertainty and were restricted to systems with unrealistically small and simple power system models [7-9]. These basic approaches were then extended to deal with multi-machine power systems using complex formulations [10-12]. A common feature shared by these approaches is the reliance on complex representations of uncertainty which is a subset of the full range of uncertainty that likely exist in most physical systems.

These previous attempts to characterize structured, real parametric uncertainty have, however, been limited in significant ways. First, a close examination of these works shows that existing formulations still result in conservative assessment of system stability. Second, the application of robustness analysis of large-scale systems has not been properly

investigated. Finally, quantitative descriptions of the uncertainty in operating conditions under real-time operation are needed.

Recently, several investigators have addressed the problem of uncertainty characterization arising from variations in physical parameters [12-15]. References [14-16] describe the first successful applications of these approaches to large power system models, particularly for systems with structured real parametric uncertainty arising from variations in operating conditions. However, a comprehensive treatment that considers all aspects of uncertainty in power system operation is in its formative stages.

1.3.3. Damping control design using robust techniques

The ability of a closed-loop control system to retain stability in the presence of parameter variations is an important aspect that is not guaranteed with conventional design techniques. Several representations have been explored over the last years to design system controllers which are robust to uncertain behavior and exhibit satisfactory performance.

The key issues among these works include (i) obtaining an uncertain model of the power system, (ii) establishing a framework for robust stability assessment, and (iii) developing a controller design framework that provides a guarantee of stability and robust performance within a set of model perturbations. Much of this research uses a linear fractional transformation (LFT) approach introduced by Doyle [5] to determine robust stability using a parametric uncertainty representation and structured perturbations.

In [10] an H_∞ controller for a thyristor controlled series capacitor to enhance the damping of an inter-area oscillation in a large power system was presented. The method enables robust coordinated tuning of PSSs for a variety of operating conditions and an arbitrary number of uncertainties in power system model parameters, but requires plant model reduction.

Parallel work by Chen and Malik [7], Zhao and Jing [8] explored the use of μ-synthesis techniques to design PSSs and FACTS controllers in small test systems. In addition, Yang [9], Taranto *et al.* [11], Djukanovic *et al.* [12,13], and Rios [17], have developed practical ways to design controllers in the presence of uncertainty as well as to analyze robustness of uncertain state-space models.

Other areas of research include the use of tabu search to design robust power system stabilizers for power systems working at various operating conditions [18]. In these approaches, the problem of selecting the stabilizer parameters is converted to a simple optimization problem with an eigenvalue-based objective function, which is solved by a tabu search algorithm. The objective function allows the selection of stabilizer parameters to optimally place the closed-loop eigenvalues on the left-hand side of the complex plane.

More recently, researchers have been exploring a wider range of applications with more complicated and more sophisticated control strategies, among them the application of Flexible AC Transmission Systems (FACTS) technologies and advanced excitation control [19-24]. Maslennikov *et al.* [20] discussed the use of an optimization-based framework for robust co-ordinate tuning of PSSs in the presence of uncertainty in operating conditions and uncertainty in model parameters. In [21], a bifurcation subsystem based model and controller order reduction method was proposed to design a robust μ-synthesis SVC control. Using a small, reduced-order bifurcation subsystem model of the full system, the SVC control system was designed to enhance damping of inter-area oscillations and voltage control.

Another interesting approach is based on the use of the Glover-McFarlane's H_∞ design procedure to tune PSSs [22]. The resulting PSS ensures the stability of a set of perturbed plants with respect to the nominal system and has good oscillation damping ability. Later, Ramos *et al.* [24] explored the use of decentralized output feedback controllers to damp electromechanical oscillations.

A significant disadvantage of these approaches is that they rely on model order reduction [10], which can result in additional uncertainty and does not guarantee robustness properties. For many applications, and in particular for the analysis of large interconnected power systems, these requirements may be problematic.

While these techniques have been successfully applied to design controllers in various test systems, to date no technique exists that can be directly applied to realistic power system models. Current techniques are also limited in their ability to analyze the combined effects of multiple, correlated parametric uncertainties on robust stability.

1.3.4. Assessment of robust stability and robust performance

Structured singular value (SSV) theory has recently been explored to determine stability robust with respect to parameter variations. A variety of general approaches to utilize uncertainty models for robustness analysis have been developed. In the bulk of these applications, SSV theory is used to design system controllers utilizing well-established, linear analysis techniques. There has been a lack of attention, however, to the study and characterization of real uncertainty arising from variations of power system operating conditions.

Previous work on the application of SSV theory has focused on the analysis of robust stability and robust performance of power systems characterized by operation over a wide range of conditions. In [13], the authors proposed a framework for robust stability assessment in multi-machine power systems using SSV theory. The essential part of this technique is a polynomial approximation of the varying coefficients of the state matrix which enables to characterize uncertainty. Reference [13] further extended the SSV formulation of [12] by fully accounting for real parametric uncertainty in the stability and robustness analysis and design framework. Both, individual and simultaneous appearance of uncertainty was considered.

In related work, Djukanovic *et al.* [25] extended this basic stability robustness framework to evaluate the effects of variations of specific uncertain parameters on the entries of the state matrix using first -and second-order sensitivity analyses.

In [26] the authors explored the application of selective direct control of loads for small-disturbance angle stability enhancement in power systems. In this approach, an analysis based on structure singular value theory is proposed, in which the controllable load range at selected buses that satisfies the desired stability robustness performance criterion is determined. The method is especially well suited for analyzing the stability robustness of power systems with parameter variations whose exact values are unknown but which are known to lie between some minimum and maximum values, and can be extended to include the representation of different types of uncertainties. Furthermore, the results of the analysis are seen to correspond closely with the evaluation of small signal stability margins using conventional eigen-analysis.

While the procedure is mathematically sound, the amount and complexity of the analyses required to extend this approach to the study of realistic systems increases rapidly with order. Also, some practical limitations may arise when the structure of the plant matrix is not known. In addition, the procedures are not general and may not be easily incorporated into existing commercial software. Finally, these methods are time consuming, especially from design point of view, where the effects of several varying parameters have to be studied.

Other recent research work has focused on the analysis and characterization of small signal stability in the face of uncertainty in operating conditions [12-16, 20]. In [15], the author proposed a numerically-based approach to estimate the varying coefficients of the state matrix using ideas from interval analysis. The main advantage of this formulation is its simplicity and the ability to handle very large models. These techniques have been shown to be effective and useful for uncertainty modeling even though some practical limitations arise when the number of operating conditions is too large.

Current research work concentrates on the analysis of multiple uncertain parameters occurring simultaneously in the control representation and the development of numerical techniques to determine upper and lower bounds for structured values. This latter problem has been studied recently [16], and analysis methods based on approximating the parameter space by low-order models have been developed. This uncertainty analysis method provides a systematic framework for making robust decisions under severe uncertainty, making it particularly well adapted for near real-time applications.

Some further benefits of these formulations, which are not typically obtained in other approaches, are also available. In particular, the analysis allows for the determination of the areas that are most vulnerable to system instability and the identification of the parameters with most influence on robust stability. Major research projects reflect current interest in this subject [27].

Other promising research areas currently underway relate to the analysis of stability robustness using v-gap metrics [28] and the use of developed techniques based on linear matrix inequalities [29]. Further advances are expected to lead to even more utilization of these techniques, especially for real-time security assessment and control.

1.4 Objectives of the thesis

The fundamental objective of this research is to develop a general, theoretical framework for robust stability assessment in multi-machine power systems subjected to severe, real parameter variations.

Other objectives identified are:

- To obtain an analytical model of uncertainty that can be used to explicitly treat and analyze variations in most practical physical parameters occurring in power systems. To extend existing uncertainty analysis methods based on linear fractional theory and μ - theory to deal with multiple sources of uncertainty and to evaluate and quantify the degree of robustness.
- To overcome the problems of conservatism by examining power-system model uncertainties from a physical perspective, and to express stability margins in a way that is familiar to engineers.
- To develop a near real-time uncertainty based methodology for small-signal security assessment based on on-line monitoring of key uncertain parameters
- To demonstrate the applicability of the propose method in the practical assessment of robust stability of realistic power system models

1.5. Contributions of this thesis

The main contributions of this thesis are:

- The development of a general real μ-analysis framework for modeling structured real-valued parametric perturbations that accounts for multiple, correlated uncertainty sources in the system, suitable for control design and analysis; the proposed formulation accounts for complex parameter dependence and is suitable for a wide range of problems. In this approach, variations in system operating conditions and system topology are modeled as real, state-space structured uncertainty and included in the nominal system representation. The method is based on a decomposition of perturbations into linear fractional transformations and is applicable to structured uncertainties in different points of the control loop.

- The extension of existing emergency and alert control strategies to account for security assessment with multiple disturbances. The proposed modeling framework explicitly treats and incorporates uncertainty and then uses these methods to evaluate secure operating regions. By continuously updating the forecasted values of parameters, the critical level of damping of critical modes and stability limits can be accurately predicted which results in improved coordination of remedial measures and the expansion of secure operating regions. Unlike previous approaches, security assessment can be performed on a near real-time basis. Such a strategy allows for a more detailed evaluation of the margin of safety before instability occurs and allows guaranteeing a reasonable performance over a wide range of uncertainty in operating conditions.

- A robust and efficient new numerical algorithm is, to this end developed, which reduces the dimension of the state-space realization while improving numerical accuracy, reducing computational requirements, and reducing run-time memory requirements. Such improvements are required for the realization of large scale, complex systems which are characterized by several simultaneous uncertainties.

- A new analytical technique for robustness analysis has been developed for this model which reduces the conservatism of the results. The developed methods are both general and easily incorporated into existing small signal stability software and are therefore convenient for robustness analysis and design of large, complex systems. The work presented here represents the first large-scale application of robustness to the analysis of realistic power system models.

- The incorporation of the developed procedures into a production-grade small signal stability software. The current methodology offers a practical way of translating real parameter uncertainty into general small-signal state representations in which no detailed information about the structure of the model is available.

1.6. Outline of the dissertation

This dissertation is organized as follows. Chapter 2 introduces and discusses robust control theory with particular emphasis on the derivation of linear fractional transformation models. In this context, the structured singular value, is presented and a general framework for robust stability assessment in multi-machine power systems is proposed.

In Chapter 3, a systematic analytical technique based on structured singular value is proposed to assess and quantify the robust stability of large power systems. In particular, variations in physical parameters such as power flow intertie and topological changes are represented as LFT based uncertainty descriptions. The procedures can be used to take into account the effect of several simultaneous varying parameters. Typical steps in the application of the algorithm are presented to illustrate how the modeling technique can be used to assess robust stability.

Chapter 4 discusses the application of the proposed analysis procedure to analyze stability robustness with respect to real parameter variations. First, a case study on a two-machine test system is presented and discussed. Then, the performance of the proposed method is verified through simulation studies on a large-scale test system. In particular, results for the systems are considered for an extensive range of uncertainties of operating conditions.

The validation is based on comparisons with results from repeated detailed eigenvalue analysis using a small signal stability program. Simulation results of this system for several changes in operating conditions show that the proposed method is both accurate and flexible and can be used for robust stability and control analysis in large power systems.

Chapter 5 discusses the development and application of near, real-time uncertainty-based control policies to the problem of evaluating dynamic security assessment in the presence of severe uncertainty in operating conditions. A general formulation for characterizing the effect of simultaneous variations of operating conditions on robust stability is presented. Robustness evaluation techniques are then used to produce on-line preventive and emergency control actions. Such improvements are required for the analysis of large-scale uncertain systems, which have a large number of parametric uncertainties.

Finally, Chapter 6 presents the overall conclusions drawn from this thesis and suggestions for future directions of research.

1.7. Publications

Refereed journal papers

1) R. Castellanos, A. R. Messina, H. Sarmiento, "Robust stability analysis of large power systems using the structured singular value theory", *International Journal of Electrical Power and Energy Systems*, vol. 27, no. 3, July 2005, pp. 389-397.

2) R. Castellanos, J.G. Calderon G., D. Olguin S., H. Sarmiento U., A. R. Messina, "Use of Power System Stabilizers for Damping Inter-Area Oscillations in the South systems of the Mexican Electrical Grid", *Electric Power Systems Research Journal*, vol. 76, no. 1, January 2006, pp. 180-193.

3) R. Castellanos, A. R. Messina, H. Sarmiento, "A μ-analysis Approach to Power Systems Stability Robustness Evaluation", to appear in *Electric Power Systems Research Journal*, 2006.

Papers on conference proceedings

4) R. Castellanos, C. Juarez T., A. R. Messina "Quantifying the Stability Robustness of Power Systems using Structured Singular Value Theory ", *IEEE PES General Meeting 2005, San Francisco, California, USA, June 2005.*

5) C. Juarez T., R. Castellanos, A. R. Messina "Analysis of Inter-Area Oscillations using Time-Varying One-Machine Infinite Bus Equivalents", *IEEE PES General Meeting 2005, San Francisco, California, USA, June 2005.*

6) R. Castellanos, C. Juarez T., J.H. Hernandez, A. R. Messina "Robustness Analysis of Large Power Systems with Parametric Uncertainties", *IEEE PES General Meeting 2006, Montreal, Quebec, Canada, June 2006.*

References

[1] S. Skogestad, I. Postlethwaite, "Multivariable Feedback Control: Analysis and Design", *John Wiley and Sons*, 1996, ISBN 0-471-94277-4.

[2] P. Kundur, "Power System Stability and Control", *EPRI Power Engineering Series*, New York: McGraw-Hill, Inc., 1994.

[3] E. V. Larsen, and D. A. Swann, "Applying power system stabilizers Parts I, II, and III", *IEEE Transactions on Power Apparatus and Systems*, vol. PAS-100, no. 6, June (1981), 3017-3046.

[4] CIGRE, "Analysis and Control of Power System Oscillations", *CIGRE*, Task Force 07 of Advisor Group 01 of Study Committee 38, December 1996.

[5] J. Doyle, "Analysis of feedback systems with structured uncertainty", *IEE Proceedings, Part D*, vol. 129, November 1982, pp. 242-250.

[6] A. Packard, J.C. Doyle, "The complex structured singular value", *Automatica*, vol. 29, 1993, pp. 71-109.

[7] S.Chen, O.P.Malik, "H∞- optimization–based power system stabilizer design", *IEE Proceedings Generation, Transmission, and Distribution*, vol. 142, No.2, March 1995, pp.179-184.

[8] Q. Zhao, J. Jiang, "Robust SVC controller design for improving power system damping", *IEEE Trans. on Power Systems*, vol.10, No.4, November 1995, pp.1927-1932.

[9] T.C. Yang, "Applying structured singular value to multi-machine power system stabilizer design", *Electric Power Systems Research*, vol. 43, 1997, pp. 113-123.

[10] M. Klein, L.X. Le, G.J. Rogers, S. Farrokhpay, N.J. Balu "H∞ Damping Controller in large Power Systems", *IEEE Trans. Power Systems*, vol.10, No. 1, February 1995, pp.158-166.

[11] G.N. Taranto, J.K. Shiau, J.H. Chow, H.A. Othman, "Robust decentralized design for multiple FACTS damping controller", *IEE Proc. Generation, Transmission, and Distribution*, vol. 144, No.1, January 1997, pp.61-67.

[12] M. Djukanovic, M. Khammash, V. Vittal, "Structured Singular Value theory based stability robustness of power systems", *Conference on Decision & Control*, San Diego California, December 1997, pp.2702-2707.

[13] M. Djukanovic, M. Khammash, V. Vittal, "Application of the structured singular value theory for robust stability and control analysis in multimachine power systems, Parts I and II", *IEEE Transactions on Power Systems*, vol. 13, no. 4, November 1998, pp. 1311-1322.

[14] R. Castellanos, A. R. Messina, H. Sarmiento, "Robust stability analysis of large power systems using the structured singular value theory", *International Journal of Electrical Power and Energy Systems*, vol. 27, no. 3, July 2005, pp. 389-397.

[15] R. Castellanos, C. Juarez T., A. R. Messina, "Quantifying the Stability Robustness of Power Systems using Structured Singular Value Theory ", *IEEE PES 2005 General Meeting*, San Francisco, California, USA, June 2005.

[16] R. Castellanos, C. Juarez, J. Hernandez, A. R. Messina, "Robustness Analysis of Large Power Systems with Parametric Uncertainties", *IEEE PES 2006 General Meeting*, Montreal, Quebec, Canada, June 2006.

[17] M. Rios, Nourdine Hadjsaid, R. Feuillet, A. Torres, "Power systems stability robustness evaluation by μ analysis", *IEEE Transactions on Power systems*, vol. 14, no. 2, May 1999, pp.648-653.

[18] Y. LAbdel-Magid, M.A. Abido, A.H. Mantawy, "Robust tuning of power system stabilizers in multi machine power systems", *IEEE Transactions on Power Systems*, vol.15, No.2, May 2000, pp.735-740.

[19] N. Yang, Q. Liu, J.D. McCalley, "μ analysis and synthesis for the uncertainties in static load modeling", *Electric Power Systems Research*, vol. 56, 2000, pp. 17-25.

[20] V.A. Maslennikov, S.M. Ustinov and J.V. Milanovic "Method for considering uncertainties for robust tuning of PSS and evaluation of stability limits", *IEE Proceedings Generation, Transmission, and Distribution*, vol 149, No.3, May 2002, pp.295-299.

[21] Meng Yue, Robert Schlueter, "A Model and Controller Reduction Method for Robust Control Design", *North American Power Symposium*, Rolla MO, October 20-21, 2003, pp.1-6.

[22] A. Swarcewicz, K.W. Swarcewicz, "Optimal Linear Control in Stabilizer Design", *IEEE Computer Applications in Power*, Vol. 15, No.4, October 2002, pp.51-56.

[23] C. Zhu, M. Khammash, V. Vittal, W. Qiu, "Robust power systems stabilizer Design Using H∞ Loop Shaping Approach", *IEEE Transactions Power Systems*, Vol. 18, No. 2, May 2003, pp.810-818.

[24] R. A. Ramos, L.F.C Alberto, N.G. Bretas, "Decentralized output feedback controller design for the damping of electromechanical oscillations", *Electric Power Systems Research*, vol. 26, 2004, pp. 207-219.

[25] M. Djukanovic, M. Khammash, V. Vittal, "Sequential synthesis of structured singular value based decentralized controllers in power systems", *IEEE Transactions on Power Systems*, vol. 14, no. 2, May 1999, pp. 635-641.

[26] Badri Ramanathan, and V. Vittal, "Small-Disturbance Angle Stability Enhancement Through Direct Load Control, Parts I and II", *IEEE Transactions on Power Systems*, vol. 21, no. 2, May 2006, pp. 773-790.

[27] Vijay Vittal, Badri Ramanathan, "Security Enhancement Through Direct Non-disruptive Load Control, Part II", *Power Systems Engineering Research Center*, PSERC Publication 06-02, Final Project Report, January 2006.

[28] S.L. Gatley, D.G. Bates, M.J. Hayes, I. Postlewaite, Robustness analysis of an integrated flight and propulsion control system using μ and the v-gap metric", *Control Engineering Practice,* vol. 10, 2002 , pp. 261-275.

[29] H. Werner, P. Korba, T.C. Yang, "Robust tuning of power system stabilizers using LMI-techniques", *IEEE Transactions on Control Systems Technology*, vol. 11, no. 1, January 2003, pp. 147-152.

Chapter 2

Robustness Analysis

Robustness design and evaluation of uncertain state-space models is an important issue in power system control processes because of the inherent uncertainty in system parameters and the need to determine stability margins for varying operating conditions. An efficient and accurate prediction of stability margins of an uncertain system subject to changes in operating conditions or varying structure requires a method that takes uncertainties into account.

This chapter introduces and discusses robust control theory with particular emphasis on the models and assumptions used in the analysis of uncertain, large-scale systems. Numerical issues associated with the broad application of robustness analysis are also discussed.

A concise review of current research activities in robustness analysis of uncertain linear systems with structured, real parameter variations is given. The main interest is focused on the study of robust stability problems associated with real parameter variations representing real physical quantities.

First, a general framework for robustness analysis is introduced. Then, a review of Linear Fractional Transformation (LFT) theory is provided which relies on the small-gain theorem. Lastly, stability robustness theorems are presented and μ-tests for robustness analysis are given.

2.1. Introduction

For many physical systems and system identification approaches, it is appropriate to consider a parametrized model of the system, possibly together with some unmodeled dynamics. This model may take the form of a state-space/differential equation or a transfer matrix. The unmodeled dynamics could be simply norm-bounded with an appropriate frequency weight as discussed below.

In order to address robustness problems for systems as above, researchers have developed a number of numerical and analytical techniques for both analysis and design. One of the most important and powerful approaches to the analysis of robust stability with respect to unstructured dynamic uncertainty is the small gain theorem introduced by Zames [1]. This approach provides an exact robust stability test with respect to unstructured dynamic uncertainty [2]. Subsequent work has resulted in analytical techniques allowing for single norm-bounded perturbations [3].

For many problems, however, it is necessary to exploit the structure of the problem to obtain a less conservative condition, especially for robust stability with respect to structured uncertainty. The structured singular value (SSV) framework introduced by Doyle [3] and co-workers [4] provides a systematic means of dealing with such type of problems. With this approach it is possible to consider systems subject to mixed real (e. g. parametric) and complex (e.g. dynamic) structured uncertainty in the μ-analysis framework. This theoretical research has introduced the use of both upper and lower bounds for such problems and stressed the need for viable methods of computation that led to the development of the μ-tools toolbox [4]. The complex μ-theory has been subsequently extended by Fan *et al.* [5] and other researchers [6-10] that considered the mixed μ analysis problem and explored the use of efficient computational schemes for both, upper and lower bounds rather than exact computation.

In this Chapter, we address several issues arising from the consideration of parametric uncertainty within the framework of μ-analysis. This approach allows for perturbations in the coefficients of the state-space model, and enables to examine the connection between system identification and robust control theories.

The starting point of the uncertainty modeling is the selection of a model structure in which uncertainties can be represented. Once a mathematical model of the uncertain is derived, stability robustness can be assessed using the SSV framework.

2.2. Model uncertainty representation

2.2.1. The notion of uncertainty

Uncertainty is an inherent characteristic of most phenomena or processes. In the most general sense, uncertainty refers to the lack of perfect understanding with regard to phenomena or processes. This may include the inability to perfectly model nature via mathematical models, deficiencies in simulation, or be associated to the nature of input, measurements or operating conditions. Further, physical quantities such as measurements and parameters are characterized by uncertainty. In such cases, robustness is an important issue in control design and is also of interest to assess performance analysis.

Uncertainties in a dynamic model can be broadly divided into two main categories:

1) Parametric uncertainty associated with uncertainty in a parameter used to generate the model. The parameter can appear explicitly in the state-space realization or, the matrices can be implicit functions of the parameters

2) Non-parametric uncertainty that cannot be captured by an uncertainty in one or more parameters. This type of uncertainty can capture modeling errors, lack of fidelity, etc.

Uncertainty modeling is increasingly finding use in the description and forecasting of uncertain behavior in control processes, and in various engineering fields. Characterization of system uncertainty, however, is a challenging problem. During the past two decades there has been significant progress in the development of analysis and design techniques for system with parametric uncertainties and unmodeled dynamics, using various analytical formulations.

The most general and accurate means of analyzing and characterizing the effect of uncertainty on robust performance and stability, is the structured singular value μ framework developed by Doyle and other researchers. This approach allows for the precise measurement of the effects of changes and operating conditions and uncertainty in model parameters on stability robustness and performance robustness.

2.2.2. *The parametric uncertainty modeling problem*

Consider a perturbed, parameter-dependent Linear Time Invariant (LTI) representation given by

$$\dot{\mathbf{x}}(t) = (\mathbf{A}(\mathbf{p}) + \Delta\mathbf{A}(\mathbf{p}))\mathbf{x}(t) \tag{2.1}$$

where $\mathbf{A} \in \Re^{nxn}$ is a known, stable matrix, $\Delta\mathbf{A} \in \Delta(\gamma) \subset \Re^{nxn}$ is an unknown real perturbation term, combining all uncertainties, that is assumed to be confined to a certain bounded set $\Delta(\gamma) := \{\Delta\mathbf{A} \in \Re^{nxn} : \|\Delta\mathbf{A}\| \leq \gamma\}$, and $\mathbf{p}$ is a vector of uncertain parameters.

Equation (2.1) may result from a linear model or be obtained from linearization about an equilibrium condition of a general nonlinear plant of the form $\dot{\mathbf{x}} = \mathbf{f}(\mathbf{x}(t), \mathbf{p})$. A question that naturally arises is whether the system (2.1) is stable for all possible parameter variations.

Uncertainty may be viewed as a possible perturbation of a given parameter around its nominal value. More formally, assume that a parameter p_i is allowed to vary within a certain interval $[p_i^{\min}, p_i^{\max}]$. Let now the nominal value, p_{i0}, be expressed as $p_{i0} = (p_i^{\max} + p_i^{\min})/2$ and let the separation between the upper and lower limits be expressed as $s_i = (p_i^{\max} - p_i^{\min})/2$. It then follows that the uncertain parameter p_i in the model can be rewritten as $p_i = p_{i0} + \Delta_{pi}$, where p_{i0} is the nominal value of the parameter and Δ_{pi} represents an unknown (independent) perturbation or varying parameter of the model. This perturbation is constrained to an uncertainty set which represents the possible values of the perturbation.

In practice, it is often desirable to let all the different uncertainties belong to the same uncertainty set. This is accomplished by introducing a scaling factor to each perturbation. Thus, for instance, parametric uncertainty may be quantified by assuming that each uncertain parameter, p_i is bounded within some region $[p_i^{\min}, p_i^{\max}]$ That is, there are parameter sets of the form

$$p_i = \frac{p_i^{\max} + p_i^{\min}}{2} + \frac{p_i^{\max} - p_i^{\min}}{2}\delta_i \tag{2.2}$$

where δ_i is any real scalar satisfying $|\delta_i| \leq 1$ which defines the range of possible values of the parameters. With this definition, it then follows that $p_i = p_i^{\max}$ if $\delta_i = 1$, and $p_i = p_i^{\min}$ if $\delta_i = -1$.

This thesis addresses the more complex problem of robust stability of linear models with real parametric uncertainty. In particular, we focus on the study of performance uncertainty associated with variations in power system operating conditions and variations in network structure. The following sections briefly review techniques for uncertainty representations and robustness analysis that will be especially important in our use of SSV theory.

2.3. General framework for robust stability analysis

2.3.1. Linear fractional transformation (LFT) uncertainty modeling

The μ approach to analyzing uncertain systems is based on the observation that problems involving the interconnection of linear time invariant systems with uncertain parameters and unmodeled dynamics can be reduced to considering the constant matrix feedback interconnection in Figure 2.1. Here, $\mathbf{M}(s)$ represents the generalized plant model, and $\mathbf{\Delta}$ represents the structured uncertainties in the system due to parameter variations or variations in the operating conditions [11]; the lower feedback loop is the control and stabilization loop and is often considered to be an inherent part of matrix $\mathbf{M}(s)$. The inputs and outputs corresponding to the uncertainties in the system are $\mathbf{w}$ and $\mathbf{z}$ respectively, and s is the Laplace variable.

Physically, the canonical diagonal perturbation system can be obtained by rearranging the uncertain parameters δ_i occurring simultaneously at several locations in the control system, into a diagonal structure. This framework allows treating and analyzing combined parametric and dynamic uncertainties.

The key fact of importance to us here is the LFT separates the uncertain or varying part of the system from the nominal system (plant and controller). This has several important and theoretical advantages as discussed below.

The definition of μ is dependent upon the underlying block structure of the uncertainties. Given a matrix $\mathbf{M} \in C^{nxn}$ the block structure $\mathrm{K}(m_r, m_c, m_C)$ is an m-tuple of positive integers

$$\mathrm{K} = (k_1, \ldots, k_{m_r}, k_{m_r+1}, \ldots, k_{m_r+m_c}, k_{m_r+m_c+1}, \ldots, k_{m_r+m_c+mC}) \tag{2.3}$$

where $\sum_{i=1}^{m} k_i = n$, the non-negative integers m_r, m_c, m_C specify the number of uncertain blocks of each type, i.e. real, complex and full complex, and $m = m_r + m_c + m_C$ specifies the dimensions of the perturbation blocks. The r denotes repeated scalar blocks.

The set of all allowable perturbations can thus be defined as:

$$\mathbf{X}_{\mathrm{K}} = \left\{ \begin{array}{l} \Delta = blockdiag\left(\delta_1^r I_{k_1}, \ldots, \delta_{m_r}^r I_{k_{mr}}, \delta_1^c I_{k_{mr+1}}, \ldots, \delta_{m_c}^c I_{k_{m_r+m_c}}, \ldots, \Delta_1^C, \ldots, \Delta_{m_C}^C\right): \\ \\ \delta_i^r \in \mathrm{R}, \ \delta_i^c \in C, \ \Delta_i^C \in C^{k_{m_r+m_c+i} x \, k_{m_r+m_c+i}} \end{array} \right\} \tag{2.4}$$

We remark that $\mathbf{X}_K \in C^{nxn}$ and that this block structure is general enough to allow for repeated real scalars $(\delta_i^r I)$, repeated complex scalars $(\delta_i^c I)$, and full complex blocks (Δ_i^C). The purely real case corresponds to $m_c = m_C = 0$.

Given this block structure we can now define uncertainties which are themselves stable dynamical systems. It is assumed that both $\mathbf{\Delta}$ and $\mathbf{M}(s)$ are stable and that the uncertainty $\mathbf{\Delta}$ belongs to the m-dimensional space of parameter variations

$$\mathbf{\Delta} = \left\{ diag\left(\Delta_1(j\omega), \ \ldots, \ \Delta_m(j\omega)\right): \sigma_{\max}\left(\Delta_i(j\omega)\right) \le \gamma \right\}, i = 1, \ldots, m \tag{2.5}$$

where γ defines an upper bound on the size of the maximum singular value of any uncertainty block $\mathbf{\Delta}_i$, and $\sigma_{\max}$ denotes its largest singular value. This is a direct generalization of the notion of a state-space realization, where a linear dynamical system is written as a feedback interconnection of a constant matrix and a very simple dynamic element made up of a diagonal matrix of delays or integrators.

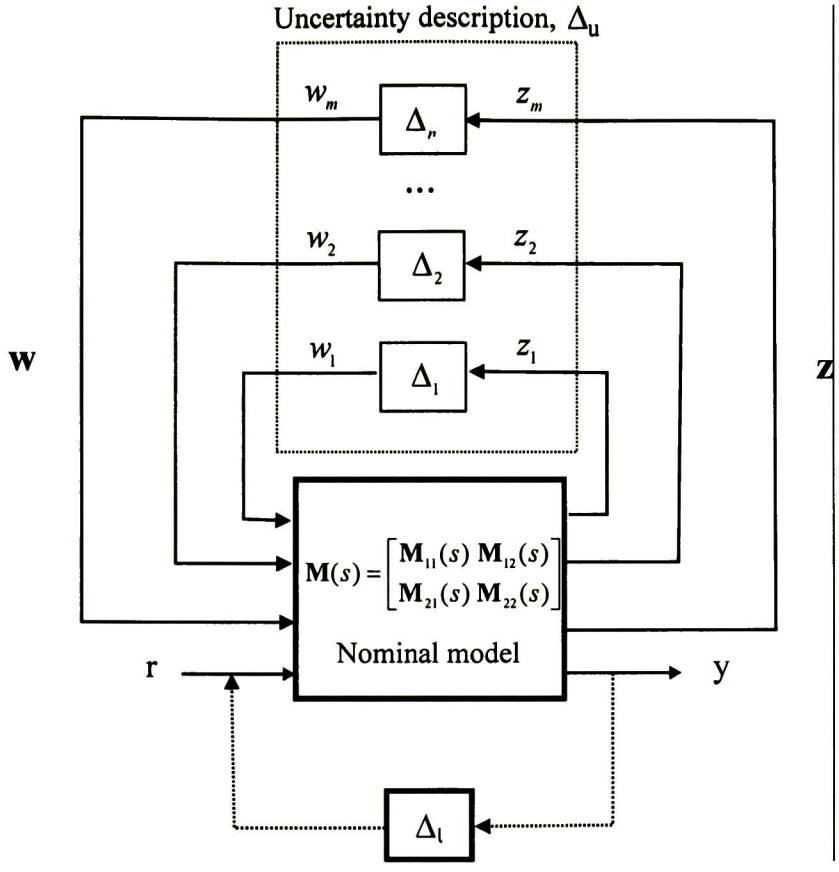

Figure 2.1. General feedback loop with structured perturbation

The resulting closed-loop system is defined by the linear fractional transformation of $\mathbf{M}$ closed with Δ. The LFT approach provides a representation of the matrices containing uncertain data preserving the structure of the uncertainties, and enables to deal with the uncertain part of the system separately from the nominal system.

To proceed further with the analysis, assume now that the matrix $\mathbf{M}$, of dimension $(n_1 + n_2)$ x $(m_1 + m_2)$, is partitioned as

$$\mathbf{M} = \begin{bmatrix} \mathbf{M}_{11} & \mathbf{M}_{12} \\ \mathbf{M}_{21} & \mathbf{M}_{22} \end{bmatrix} \tag{2.6}$$

and suppose that there is a defined block structure Δ_u, with dimension m_1 x n_1, which is compatible in size with $\mathbf{M}_{11}$ as shown in Fig. 2.1.

For any $\Delta_u \in \mathbf{\Delta}_u$, the input-output relationship becomes

$$\begin{bmatrix} \mathbf{z} \\ \mathbf{y} \end{bmatrix} = \mathbf{M} \begin{bmatrix} \mathbf{w} \\ \mathbf{r} \end{bmatrix} = \begin{bmatrix} \mathbf{M}_{11} & \mathbf{M}_{12} \\ \mathbf{M}_{21} & \mathbf{M}_{22} \end{bmatrix} \begin{bmatrix} \mathbf{w} \\ \mathbf{r} \end{bmatrix} \tag{2.7}$$

and

$$\mathbf{w} = \Delta_u \mathbf{z} \tag{2.8}$$

Solving for $\mathbf{z}$ in terms of $\mathbf{r}$ yields

$$\mathbf{z} = (\mathbf{I} - \mathbf{M}_{11}\Delta_u)^{-1}\mathbf{M}_{12}\mathbf{r} \tag{2.9}$$

Further, solving for the output signal $\mathbf{y}$ in terms of $\mathbf{M}$, Δ and $\mathbf{r}$ results in the upper LFT:

$$\mathbf{y} = \left[\mathbf{M}_{22} + \mathbf{M}_{21}\Delta_u (\mathbf{I} - \mathbf{M}_{11}\Delta_u)^{-1}\mathbf{M}_{12}\right]\mathbf{r} = \mathbf{F}_u(\mathbf{M}, \Delta_u)\,\mathbf{r} \tag{2.10}$$

where $\mathbf{F}_u(\mathbf{M}, \Delta)$ is the LFT which represents the closed-loop transfer matrix from $\mathbf{r}$ to $\mathbf{y}$ and u indicates that the upper Δ_u-loop is closed ($\mathbf{w} = \Delta_u \mathbf{z}$). It follows that the stability of the perturbed system is equivalent to:

$$\det(\mathbf{I} - \mathbf{M}_{11}\Delta_u) \neq 0$$

We can analogously define a lower LFT. Suppose now that Δ_l is a block structure compatible in dimension with $\mathbf{M}_{22}$. Physically, Δ_l may represent the stabilization and control loop or an integral loop as discussed in succeeding sections. Then, for $\Delta_l \in \mathbf{\Delta}_l$,

$$\mathbf{y} = (\mathbf{I} - \mathbf{M}_{22}\Delta_l)^{-1}\mathbf{M}_{21}\mathbf{w} \tag{2.11}$$

Hence, the lower LFT of Δ_l with matrix $\mathbf{M}$ is defined by the expression

$$F_l(\mathbf{M}, \Delta_l) = \left[\mathbf{M}_{11} + \mathbf{M}_{12}\Delta_l(\mathbf{I} - \mathbf{M}_{22}\Delta_l)^{-1}\mathbf{M}_{21}\right] \tag{2.12}$$

where l indicates that the lower loop is closed.

The relevant result is that $\mathbf{F}_u(\mathbf{M}, \Delta_u)$ contains a nominal component $\mathbf{M}_{11}$, and an uncertain component that depends on Δ_u. A useful interpretation of an LFT is that $F_u(\mathbf{M}, \Delta_u)$ has a

nominal mapping $\mathbf{M}_{11}$, and is perturbed by Δ_u, while $\mathbf{M}_{12}, \mathbf{M}_{21}, \mathbf{M}_{22}$ reflect a prior knowledge as how the perturbation affects the nominal mapping $\mathbf{M}_{11}$.

It is also interesting to observe that the linear interconnections of LFTs can be rewritten as one single LFT. This implies that LFTs can be used to separately model specific details of the system under consideration; the characteristics of the overall model can then be obtained by analyzing the composite system. Thus, for instance, a constant matrix (i.e. a feedback matrix), a scaling factor, or an integral loop can be treated algebraically like uncertain parameters.

More generally, several LFT-based descriptions can be added or manipulated. As a result, the LFT is very flexible in representing both, parametric uncertainty and unmodeled dynamics.

2.3.2. Well-posedness of solutions

The LFT is said to be well-posed if and only if $(\mathbf{I} - \mathbf{M}_{11}\Delta_u)$ is invertible, i.e. $\det(\mathbf{I} - \mathbf{M}_{11}\Delta_u) \neq 0$ When the LFT is not well posed, the gain from the input $\mathbf{r}$ to the other signals in Figure 2.1 is infinite, and the feedback loop is in some sense unstable[1] A problem of particular interest is to compute robust margins, defined as the maximum amount of model uncertainties, for which stability is satisfied.

With reference to figure 2.1, it is possible to write

$$\mathbf{w} = \Delta_u \mathbf{z},$$

and

$$\mathbf{z} = \mathbf{M}_{11}\mathbf{w},$$

or, equivalently,

$$\begin{cases} [\mathbf{I} - \mathbf{M}_{11}\Delta_u]\mathbf{z} = \mathbf{0} \\ [\mathbf{I} - \Delta_u\mathbf{M}_{11}]\mathbf{w} = \mathbf{0} \end{cases}$$

[1] We are interested here in the question of whether there is unique solution to the loop equations (2.7) and (2.8).

It immediately follows that, as long as $[\mathbf{I}-\mathbf{M}_{11}\Delta_u]$ is nonsingular, the only solution to the loop equations is $\mathbf{z}=\mathbf{w}=\mathbf{0}$. If $[\mathbf{I}-\mathbf{M}_{11}\Delta_u]$ is singular, then there are infinitely many solutions and the norms $\|\mathbf{z}\|$ and $\|\mathbf{w}\|$ can be arbitrarily large.

For practical implementation in current robust control algorithms, the LFT description must be obtained in a state-space model form and should be of low order. The formulation of an efficient $\mathbf{M}-\Delta$ model which accurately characterizes realist system uncertainties is very important, because the robustness results obtained using these formulations depend directly on the uncertainty model used in the analysis.

In robustness analysis, the size of the smallest destabilizing perturbation in Δ, is characterized by calculating the structured singular value of $\mathbf{M}$ as explained below. In what follows, a brief introduction to μ analysis is given, followed by the problem formulation for power system stability assessment. The theory and analysis methods can be easily generalized to other types of uncertainties.

2.3.3. Small-gain theorem

The small gain theorem was introduced by Zames [1] to analyze the stability of MIMO control systems in the presence of unstructured perturbations. To introduce this notion more precisely, we introduce the following definitions:

Definition 1. Consider an *m*-input, *n*-output transfer function matrix $\mathbf{G}(s)$. The singular values σ_i are defined as

$$\sigma_i[\mathbf{G}(s)]=\sqrt{\lambda_i[\mathbf{G}^T(s)\mathbf{G}(s)]} \qquad i=1,\cdots,p$$

where $\lambda_i[.]$ indicates the eigenvalue of a matrix, and $p=\min(m,n)$.

Definition 2. Consider the transfer function matrix $\mathbf{G}(s)$ defined above. The infinity-norm of $\mathbf{G}(j\omega)$ is defined as

$$\|\mathbf{G}(j\omega)\|_\infty=\max_\omega \sigma_{\max}[\mathbf{G}(j\omega)]$$

where $\sigma_{\max}[\mathbf{G}(j\omega)]$ is the largest singular value of the transfer function taken over all frequencies.

From these definitions, and the general structure 2.1, it is easy to derive the following theorem which can be seen as the basis of μ-analysis.

Theorem 1 (Small gain theorem). The system in Figure 2.1 is internally stable for all perturbations $\Delta_u(s) \in \mathbf{\Delta}$ with $\|\Delta_u(j\omega)\|_\infty \leq 1$ if and only if $\mathbf{M}_{11}(s)$ is stable, and

$$\sigma_{\max} \mathbf{M}_{11}(j\omega) \leq \gamma < 1 \qquad \forall \omega \tag{2.13}$$

or equivalently,

$$\|\mathbf{M}_{11}(j\omega)\|_\infty = \max_\omega \sigma_{\max} \mathbf{M}_{11}(j\omega) \leq \gamma < 1.$$

where $\sigma_{\max}(\mathbf{M}_{11}(j\omega))$ denotes the largest singular value of $\mathbf{M}_{11}(j\omega)$. In this case the system is said to be robustly stable. It should be stressed that there are no other limitations on the structure or form of the perturbation $\mathbf{\Delta}(s)$ except for the magnitude of its infinity norm. Therefore, $\mathbf{\Delta}(s)$ is referred to as an unstructured perturbation, i.e. the perturbation $\mathbf{\Delta}$ is assumed to be bounded but otherwise unknown.

This statement is referred to as the *small gain theorem* for unstructured uncertainty and states that a closed loop system will be stable provided that the maximum singular value of the loop gain is less than unity at all frequencies [3].

For structured and real uncertainty, however, the small gain theorem is known to be conservative since the block diagonal structure of the matrix is not taken into account. In words, we only get sufficient conditions for stability; we can violate these sufficient conditions and still be robustly stable. The structured singular value is defined below as an alternative measure of robustness and can be used to reduce the level of conservatism in robustness analysis.

2.4. The structured singular value

The structured singular value (SSV) can be used to analyze the robustness of the system to the structured uncertainty that enters in the feedback form.

Definition 3. The SSV, $\mu_\Delta(\mathbf{M})$, of an n x n complex transfer function $\mathbf{M}(s)$ with respect to the set Δ of allowable perturbations is a positive, real-valued function defined as

$$\mu_{\Delta}(\mathbf{M}) = \begin{cases} 0 & \text{if } \det(\mathbf{I} - \mathbf{M}\Delta) \neq 0 \quad \text{for all} \quad \Delta \in \mathbf{\Delta} \\ \dfrac{1}{\min_{\Delta \in \mathbf{\Delta}} \left\{ \sigma_{\max}(\Delta) \mid \det(\mathbf{I} - \mathbf{M}\Delta) = 0 \quad \text{for structured} \quad \Delta \right\}} & \text{else} \end{cases} \tag{2.14}$$

where $\mathbf{\Delta}$ is a subset of the allowable perturbations describing the uncertainty structure, i.e the set of all block-diagonal matrices with some specific structure.

Equation (2.14) defines a precise test for stability of a closed-loop system subject to structured uncertainty in terms of the maximum structured singular value of the matrix $\mathbf{M}_{11}$. The problem becomes that of studying the stability of the matrix $[\mathbf{I} - \mathbf{M}_{11}\Delta_u]$ or to test whether $\det([\mathbf{I} - \mathbf{M}_{11}\Delta_u])$ remains nonzero along the $j\omega$ axis.

Thus, if $\mathbf{M}$ is a stable closed-loop transfer function matrix , and $\mu_{\Delta}(\mathbf{M})$ is evaluated along the imaginary axis, then $\mu_{\Delta}(\mathbf{M})$ is a function of frequency that gives the size of the smallest allowable $\mathbf{\Delta}$ that moves a closed-loop pole (the zeros of $\det([\mathbf{I} - \mathbf{M}_{11}\Delta_u])$) to the imaginary axis.

With this definition of μ, the closed loop system is stable if and only if $\mu_{\Delta}(\mathbf{M}(j\omega)) < 1 \; \forall \omega$. In other words, at each frequency ω, the value of $\mu_{\Delta}(\mathbf{M}(j\omega))$, is the reciprocal of the smallest destabilizing perturbation in $\mathbf{X}_k$, i.e that turns the system unstable, where the size of a perturbation is measured in terms of the infinity norm.

We remark that:

1. In general, $\mu_{\Delta}(\mathbf{M}(j\omega))$ cannot be computed exactly. Instead, lower and upper bounds to $\mu_{\Delta}(\mathbf{M}(j\omega))$ can be computed
2. If $\mu(\mathbf{M}(j\omega))$ is an upper bound, such that $\mu_{\Delta}(\mathbf{M}(j\omega)) < \mu(\mathbf{M}(j\omega))$, then we have stability robustness if $\mu(\mathbf{M}(j\omega)) < 1 \; \forall \omega$
3. The usual technique to evaluate robustness consists of selecting a dense enough frequency grid, and evaluating the criteria $\mu_{\Delta}(\mathbf{M}(j\omega))$ for each chosen frequency.

This approach has been advocated by several researchers and adopted in many studies. For models of the type considered in this research, several problems arise with the above approach. Firstly, if the frequency grid is not dense enough, the robustness margin might not be determined accurately. Secondly, increasing the density of the frequency grid may result in high computational cost.

An alternative way of looking at this problem discussed in subsequent sections of this thesis, is to replace this criteria by a tractable one: the use of sensitivity-based analytical formulation for defining an approximate operating space.

As outlined in the introductory section of this chapter, the definition of $\mu_{\Delta}(\mathbf{M})$ is dependent on the block structure $\mathbf{\Delta}$, the underlying block structure of the uncertainties, and the matrix $\mathbf{M}$. This structure may be defined differently for each problem depending on the nature of uncertainty and performance objectives of the analysis.

In the bulk of these applications, the technique is used to analyze complex uncertainty. In this work, the set of all allowable repeated real uncertainties in the plant, $\Delta_u(s)$, (refer to equation (2.8)) to represent changes in the parameters will be considered to have a block diagonal structure of the form

$$\Delta_u = blockdiag\,(\delta_1^r I_{k_1},...,\delta_{m_r}^r I_{k_{m_r}}) \tag{2.15}$$

with $\delta_i^r \in \Re$ being the set of uncertain parameters, and $\sum_{i=1}^{m_r} k_i = n$. This allows the characterization of uncertainty of operating conditions associated with *physical* parameters, for instance, associated with changes in operating conditions.

In the work described subsequently in this thesis, it will be assumed that the uncertainty set, $\mathbf{\Delta}$, corresponds to the subset of all allowable distinct real uncertainties described by

$$\mathbf{\Delta} = \begin{bmatrix} \delta_1^r I_{k_1} & & \\ & \delta_2^r I_{k_2} & \\ & & \delta_{m_r}^r I_{k_{m_r}} \end{bmatrix} \tag{2.16}$$

where $\delta_i^r \in \Re$. Note that this structure corresponds to the case of real parametric uncertainty associated with real parameter variations.

In terms of this notation, the upper LFT can be rewritten in the form

$$F_u(\mathbf{M},\Delta_u) = \mathbf{M}_{22} + \mathbf{M}_{21}\begin{bmatrix} \delta_1^r I_{k_1} & & 0 \\ & \ddots & \\ 0 & & \delta_{m_r}^r I_{k_{rm_r}} \end{bmatrix}\left[\mathbf{I} - \mathbf{M}_{11}\begin{bmatrix} \delta_1^r I_{k_1} & & 0 \\ & \ddots & \\ 0 & & \delta_{m_r}^r I_{k_{rm_r}} \end{bmatrix}\right]^{-1}\mathbf{M}_{12} \quad (2.17)$$

The structured singular value provides a measure of the smallest structured Δ that causes instability of the feedback loop. As pointed out above, the computation of μ is a difficult problem, and in practice, it is convenient to compute upper and lower bounds, i.e. $\mu_l \le \mu(\mathbf{M}) \le \mu_u$. An upper bound gives a sufficient condition for the robustness whilst a lower bound gives sufficient conditions for when the robustness/performance will not be met.

With this technique, we can compute the maximum size of perturbations for which the system will remain stable.

In the developed approaches this is implemented in three steps:

1. Determine the LFT-based parametric uncertainty description using the procedures in section 2.3. This is the most complex and computationally demanding aspect of the problem
2. Once the state-space model of the uncertain system is obtained, compute upper and lower bounds for $\mu(\mathbf{M}(j\omega))$, and
3. Determine worst- and best-case measures of system stability and robust performance using the procedure in section 2.5.

Precise details of this implementation are given in subsequent chapters.

2.5. Robust stability in the presence of multiple structured uncertainties

The analysis of robust stability is concerned with finding out necessary and sufficient conditions on $\mathbf{M}(s)$ that guarantee the stability of the closed-loop system for all perturbations, $\Delta(s)$.

Referring to Figure 2.1, the nominal performance is obtained when $\Delta = 0$; the system is said to be robustly stable if the system is stable for all permissible $\Delta's$.

The size of the smallest matrix Δ which destabilizes the system is by definition, $1/\mu_{\Delta}(\mathbf{M})$. It follows that the system in Figure 2.1 is stable for all Δ in $\mathbf{\Delta}$, such that $\mu_{\Delta}(\mathbf{M}(j\omega)) < 1$.

This inequality defines a hypercube of perturbations for which the system is guaranteed to remain stable.

2.5.1. Robust-stability theorem

Theorem 2 (Robust stability [11]). Suppose $\mathbf{M}$ is a nominal stable system (otherwise the problem is trivial). Then, for all Δ in $\mathbf{\Delta}$ satisfying $\sigma_{\max} \leq \frac{1}{\gamma}$, the perturbed closed-loop system in Figure 2.1 is well-posed and internally stable if and only if

$$\max_{\omega \in \Re} \mu_{\Delta_s}(\mathbf{M}(j\omega)) \leq \gamma \tag{2.18}$$

Since it is always possible to scale the maximum singular value, $\sigma_{\max}(\Delta_i)$, to be equal to one, a value of $\mu_{\Delta}(\mathbf{M}(j\omega)) < 1$ for all ω implies that the system is stable for all possible uncertainties in the allowed set.

Several remarks are in order in the interpretation of this theorem.

Remark 1. The size of the smallest Δ which destabilizes the system in Fig. 2.1 is, by definition, $\gamma_{\max} = 1/\mu_{\Delta_s}(\mathbf{M}(j\omega))$ for $\omega \in (0, \infty)$; this is the multivariable small signal stability margin, or robustness margin.

Remark 2. The system in Fig. 2.1 is stable for all Δ in $\mathbf{X}_K$ such that $\max_i |\delta_i| \leq \gamma_{\max}$. This inequality defines a hypercube of perturbations for which the system is guaranteed to remain stable

Another important point is implicit in these observations. We have remarked that μ is dependent on the block structure of Δ; the robust stability properties computed by SSV will only be accurate if a realistic uncertainty operator is chosen.

The determination of the maximum Δ, that will drive the system unstable is an important practical problem and will be used in this thesis for the determination worst-case operating conditions.

Several refinements to this basic approach are possible and are discussed in our application of the technique. The modified analysis process is as follows:

- Compute an upper bound $\mu(\mathbf{M}(j\omega))$ for the μ criteria
- Select the frequency intervals, on which the upper bound is larger than a predetermine threshold, i.e. 0.9 For each of these intervals refine the computation of robustness measures.
- If necessary split the interval into smaller sections (ω_i, ω_{i+1}) and recalculate the upper bound

We will subsequently discuss the implications of these approximations for the analysis of complex systems.

2.5.2. Worst-case combination of parameters

Once the robustness margin has been computed, it is possible to determine a worst-case combination of uncertain parameters for the problem. Given $\gamma_{\max}$ we seek an estimate for the worst-case perturbation that drives the system unstable.

The worst-case perturbation (WCP) that drives the system unstable for the *i-th* varying parameter can therefore be expressed as

$$WCP_i = \frac{p_i^{\max} + p_i^{\min}}{2} + \frac{p_i^{\max} - p_i^{\min}}{2}(1/\mu_{\Delta}(\mathbf{M})) \tag{2.19}$$

To treat and analyze uncertainties occurring simultaneously at several locations in the control system, however, it is necessary to quantify the collective uncertainty in all the parameters.

In determining this measure, three separate issues have to be addressed:

(a) The determination of the uncertain elements which dominate the robustness measure

(b) The identification of interrelated uncertain parameters, and

(c) The identification of those elements which do not greatly affect the stability of the system

In what follows we briefly discuss the nature and relevance of these problems, and describe some recent extension of, and other developments related to, the practical use of these measures. A more detailed discussion of these issues is postponed until later chapters.

2.5.3. Identification of dominant uncertainties

The derivation of worst-case combinations of uncertain parameters also generalizes to functions of two or more uncertainties occurring simultaneously. Depending on the physical situation, weighting functions can be introduced to assess the relative contribution to the overall uncertainty. Based on the experience of the present author, weightings can also be used to determine which uncertain elements dominate the robustness measure.

Assume in order to introduce these ideas, that the block $\mathbf{\Delta}_i$ has been scaled through weighting functions. It then follows that the uncertainty parameter $\mathbf{p}_i$ can be rewritten in the form $\mathbf{p}_i = p_{i0}\left(1 + \hat{w}_i \delta_i\right)$, where the constant scalar $\hat{w}_i$ can be used to weight the uncertainty in the coefficient with respect to uncertainties in the other coefficients. Note that, several choices of the weighting coefficients are possible.

In our formulation, a frequency independent weighting matrix,

$$\hat{\mathbf{W}}(j\omega) = \begin{bmatrix} \hat{w}_1 & & \\ & & \\ & & \hat{w}_{m_r} \end{bmatrix}$$

is connected in series with the uncertainty representation in Fig. 2.1.

As in section 2.5.1, it can be readily proved that the closed loop system is stable for Δ_u in $\mathbf{X}_K$, such that

$$\max_{i=1,\ldots,m_r} \left|\hat{w}_i \delta_i\right| \leq \gamma_{\max} \tag{2.20}$$

As discussed in [13], this inequality defines and elongated hypercube of guaranteed stable perturbations. By comparing the robustness measures, the relative contribution of the uncertainty δ_i can be estimated.

Further, worst-case combinations of uncertain parameters for the system can be determined and the relative contribution of each parameter to the overall uncertainty can be readily estimated.

A drawback of this formulation, however, is that weighting coefficients lack physical meaning. Further, in treating uncertainties occurring simultaneously at several locations of the control loop, the physical nature of the variation in the real parameters must be accounted. This problem can be avoided if one chooses scaling appropriate to the physical phenomenon under study; this may require a separation of these matrices into input and performance weighting matrices.

2.6. Discussion

The use of LFT-based descriptions is a crucial first step in the characterization of uncertainty. In this Chapter, a broad overview, from an LFT perspective, of theoretical issues associated with robustness in the presence of real parametric uncertainty has been given. Attention has been focused on systems with real parametric uncertainties but the derived procedures are of general interest and could be used to analyze mixed systems subject to both real and complex uncertainties.

Similar to the case of stability robustness, the performance robustness problem is of interest but is not addressed here. This is an active area of research that is explored in succeeding chapters. In addition, techniques are needed to efficiently determine LFT-based uncertainty representations for realistic systems as well as to compute upper and lower bounds for real uncertainty.

Existing software for the analysis of uncertain systems assumes complex formulations. The analysis of the real case is more complex and few analytical approaches have been developed to address these problems. This is, again, an area of active research.

Details and the practical use of these methods are given in Chapter 3, along with specific algorithms to treat complex systems.

References

[1] G. Zames, "On the input-output stability of nonlinear time-varying feedback systems Part I: Conditions derived using concepts of loop gain, conicity and positivity", *IEEE Transactions on Automatic Control*, vol. AC-11, no. 2, April 1996, pp. 228-238.

[2] M.G. Safonov, "Stability and Robustness of Multivariable Feedback systems", *MIT Press: Cambridge*, MA, 1971.

[3] J. Doyle, "Analysis of feedback systems with structured uncertainty", *IEE Proceedings, Part D*, vol. 129, November 1982, pp. 242-250.

[4] G. Balas, J. Doyle , K. Glover , A. Pachard , R. Smith, "The μ analysis and Synthesis" *Toolbox MathWorks and MUSYN*, 1991.

[5] M.K. Fan, A.L. Tits, J.C. Doyle, "Robustness in the presence of mixed parametric uncertainty and unmodeled dynamics", *IEEE Transactions on Automatic Control*, vol. AC-36, No.1, pp.25-38, 1991.

[6] Bartlett, "Root locations of an entire polytope of polynomias: It suffices to check the edges", *In Mathematics of Control, Signal and Systems*, vol. 1, no. 1, 1988, pp. 61-71.

[7] D.D. Siljak, "Parameter space methods for robust control design: A guided tour", *IEEE Transactions on Automatic Control*, vol. 34, no. 7, July 1989, pp. 674-688.

[8] B.R. Barmish, H.I. Kang, "A survey of extreme point results for robustness of control systems", *Automatica*, vol. 29, no. 1, 1993, pp. 13-35.

[9] R. de Gaston, M.G. Safonov, "Exact Calculation of the multiloop stability margin", *IEEE Transactions on Automatic Control*, vol. AC-33, Feb. 1988, pp.156-171.

[10] A. Sideris, Ricardo S. Sanchez Peña, "Fast computation of the multivariable stability margin for real interrelated uncertain parameters", *IEEE Transactions on Automatic Control*, vol. 34, no. 12, December 1989, pp. 1272-1276.

[11] S. Skogestad, I. Postlethwaite, "Multivariable Feedback Control: Analysis and Design", *John Wiley and Sons*, 1996, ISBN 0-471-94277-4.

[12] A. Packard, J.C. Doyle, "The complex structured singular value", *Automatica*, vol. 29, 1993, pp. 71-109.

[13] Piero Miotto, James D. Paduano, "Application of real structured singular values to flight control law validation issues", Journal of Guidance, Control and Dynamics, vol. 19, no. 6, November-December, 1996, pp. 1239-1245.

Chapter 3

Power System Representation in the SSV Framework

In this chapter a framework for robust stability assessment in multimachine power systems using LFT theory and μ-analysis is suggested. The model builds upon the state-space representation of a linearized power system model and can be used to analyze robust stability of large interconnected power systems.

Techniques for treating uncertainty are revised and discussed. A general technique for treating uncertainty in power system behavior and the computation of LFT-based power system representations is then proposed. In this procedure, variations in system parameters are represented as LFT-based parametric uncertainty descriptions and incorporated into a SSV based framework for robust stability analysis. Unlike previous approaches, deviations from nominal behavior are determined using a numerical rather than analytical approach. This enables the analysis of large scale systems.

Several assumptions are introduced in order to formulate an efficient analytical procedure. These assumptions are consistent with current small signal stability analysis practices used by the industry and lead to computer codes that are numerically efficient while at the same time provide accurate solutions.

The developed characteristics have been assembled into a simulation program with the ability of determining stability robustness to varying operating conditions as well as to assess worst-case parameter conditions. The procedures are general and can be used to treat and analyze multiple uncertainties.

3.1. Problem statement

3.1.1. The perturbed state-space system

Consider a general nonlinear uncertain system described by the state-space model

$$\dot{\mathbf{x}} = \mathbf{A}(\mathbf{p})\mathbf{x} \tag{3.1}$$

where $\mathbf{p} = [p_1 \;\; p_2 \;\; \ldots \;\; p_m]$ is the set of uncertain parameters which are known to vary within some practical limits $p_k^{\min} \le p_k \le p_k^{\max}$ about the nominal value.

The aim is to obtain a linear parametric representation of the system model suitable to generate a LFT-based parametric uncertainty description.

Several approaches to transform the model in (3.1) into a convenient form for μ-analysis have been proposed in the literature, including symbolic linearization methods and numerical techniques. We next review some existing approaches to treat uncertainty in the system model (3.1).

3.1.2. Analytical approaches

Assume that the elements a_{ij} of the state matrix $\mathbf{A}(\mathbf{p})$ are analytic functions of the parameters p_k $(k = 1,\ldots,m)$, and that they can be represented accurately by their Taylor series expansion. The second-order Taylor series expansion of each varying element a_{ij} can be expressed in the form

$$a_{ij} = a_{ij}(p_{ko}) + \sum_{k=1}^{m} \frac{\partial a_{ij}}{\partial p_k} \Delta p_k \bigg|_{p_{ko}} + h.o.t \tag{3.2}$$

where p_k, $k = 1,\ldots,m$ denotes the varying parameters and $h.o.t$ stands for higher order terms. It immediately follows from (3.2) that the first order approximation of the system can be rewritten in matrix form as

$$\dot{\mathbf{x}} \approx \left[\mathbf{A}_o + \sum_{k=1}^{m} \mathbf{A}_k \Delta p_k \right] \mathbf{x} = \left[\mathbf{A}_o + \Delta\mathbf{A}(\mathbf{p}) \right] \mathbf{x} \tag{3.3}$$

where

$$\mathbf{A}_o + \Delta\mathbf{A}(\mathbf{p}) = \mathbf{A}(p_{ko}) + \left.\frac{\partial \mathbf{A}_k}{\partial p_k}\right|_{p_{ko}} \Delta p_k + \ldots \tag{3.4}$$

In the equations above, $\mathbf{A}_o$ describes the nominal system (a stable system), while matrices $\mathbf{A}_k$, $k = 1,\ldots,m$ describe unknown deviations from the nominal system depending on the normalized physical uncertain real value, p_k confined to a certain bounded set Δ (the real structured uncertainties). Variations of this approach are presented in [1].

Under parameter perturbations, the plant matrix, $\mathbf{A}_o$, changes to $\mathbf{A}_o + \Delta\mathbf{A}$; an important problem in control analysis is that of determining bounds on the elements of $\Delta\mathbf{A}$ that guarantee stability of the perturbed system. This is the subject of this research.

The derived analytical formulation can then be converted to a form suitable for robust stability analysis. With this approach, it becomes possible to study robust stability properties in an analytical setting where repeated numerical linearizations are conducted to uncover the robustness properties in the state-space as function of system parameters.

3.1.3. Parametric uncertainty modeling

A key issue in applying robustness theory is allowing for the role of parameter variations whose exact values are unknown but which are known to lie between some minimum and maximum values. In robust stability theory, uncertainty is represented by a scalar perturbation to the nominal model. Assume in order to introduce this notion, that each entry of the system matrix $\mathbf{A}$ is described as a rational linear (nonlinear) function of the uncertain parameter vector. Then, the (i, j) coefficient of the system $\mathbf{A}$-matrix can be approximately expressed as

$$a_{ij}(p_k) = f_{ij}(p_k, \mathbf{x}) = a_{ij}\Big|_{p_{ko}} + \left.\frac{\partial a_{ij}}{\partial p_k}\right|_{p_{ko}} (p_k - p_{ko}) + \frac{1}{2}\left.\frac{\partial^2 a_{ij}}{\partial p_k^2}\right|_{p_{ko}} (p_k - p_{ko})^2 + \ldots \tag{3.5}$$

where a_{ij} denotes the varying coefficient, and the first- and second-order sensitivities of the coefficients of the $\mathbf{A}$-matrix with respect to the varying parameter are given by [1]

$$\left.\frac{\partial a_{ij}}{\partial p_k}\right|_{p_{ko}} = \sum_{r=1}^{n}\left(\left.\frac{\partial a_{ij}}{\partial x_r}\right|_{p_{ko}}\right)\left(\left.\frac{\partial x_r}{\partial p_k}\right|_{p_{ko}}\right)$$

$$\left.\frac{\partial^2 a_{ij}}{\partial p_k^{\,2}}\right|_{p_{ko}} = \sum_{r=1}^{n}\sum_{r=1}^{n}\left(\left.\left(\frac{\partial H^i_{rj}}{\partial x_s}\frac{\partial x_s}{\partial p_k}\right)\right|_{p_{ko}}\left(\left.\frac{\partial x_r}{\partial p_k}\right|_{p_{ko}}\right) + \left.H^i_{rj}\right|_{p_{ko}}\left.\frac{\partial x_r}{\partial p_k}\right|_{p_{ko}}\right)$$

where H^i_{rj} are the elements of the Hessian matrix. The extension to the multiparameter case follows along similar lines.

Once an analytical model has been obtained, a procedure is needed to transform uncertainties in the model (3.5) into a form a form that is suitable for robustness analysis.

Thus, for instance, if a parameter p_k, such that $p_k^{\min} \le p_k \le p_k^{\max}$ has a nominal value p_{ko}, but an uncertainty of $\pm r$ then the parametric uncertainty can be expressed as a parameter set of the form

$$p_k = \bar{p}_k(1 + r_k\delta_k), \quad k = 1,...,m \tag{3.6}$$

in which

$$\bar{p}_k = \frac{(p_k^{\min} + p_k^{\max})}{2} \qquad r_k = \frac{p_k^{\max} - p_k^{\min}}{p_k^{\min} + p_k^{\max}}. \quad p_k \in [p_k^{\min}, p_k^{\max}]$$

where $\bar{p}_k$ is the mean parametric value and r_k is the relative uncertainty in the parameter; δ_k is a real scalar such that $-1 \le \delta_k \le 1$. In this way, the varying parameter p_k is decomposed into a nominal part p_{ko}, the scaling factor $(p_k^{\max} - p_k^{\min})/2$, and the normalized real-valued perturbation δ_k.

With this notation in mind, we note that $p_k = p_k^{\max}$ for $\delta_k = 1$, and $p_k = p_k^{\min}$ for $\delta_k = -1$. From the previous definition it follows that the uncertain system representation can be written in terms of the nominal and perturbed parameters as

$$a_{ij} = a_{ij_o} + a_{ij1}\delta_k + a_{ij11}\delta_k^2 \tag{3.7}$$

where

$$a_{ijo} = a_{ij}\Big|_{p_{k_o}} - \frac{\partial a_{ij}}{\partial p_k}\Big|_{p_{k_o}} p_{k_o} - \frac{\partial a_{ij}}{\partial p_k}\Big|_{p_{k_o}} \bar{p}_{k_o}^2$$

$$a_{ij1} = \frac{\partial a_{ij}}{\partial p_k}\Big|_{p_{k_o}} (\bar{p}_k + \bar{p}_k r_k) - \frac{\partial^2 a_{ij}}{\partial p_k^2}\Big|_{p_{k_o}} (\bar{p}_k p_{k_o} + \bar{p}_k p_{k_o} r_k)$$

$$a_{ij11} = \frac{1}{2}\frac{\partial^2 a_{ij}}{\partial p_k^2}\Big|_{p_{k_o}} (\bar{p}_k^2 r_k^2)$$

Applying the same procedure to each varying element, the uncertain system representation becomes

$$\dot{\mathbf{x}} = \mathbf{A}(\mathbf{p})\mathbf{x} = [\mathbf{A}_o(\mathbf{p}_o) + \mathbf{A}_1(\delta_k) + \mathbf{A}_{11}(\delta_k^2)]\mathbf{x} \tag{3.8}$$

where matrix $\mathbf{A}_o$ represents the nominal plant dynamics, $\mathbf{p}_o = [p_{1o}\ p_{2o}\ \cdots\ p_{mo}]$ is the uncertain parameter vector at the linearization point, and matrices $\mathbf{A}_{\neq o}$ describe deviations from the nominal system; the scalar uncertainty, δ_k, represents an unknown varying coefficient whose values belong to an uncertainty interval $\delta_k^{\min} \le \delta_k \le \delta_k^{\max}$

Referring to Eq. (3.6) it is to be noted that the local parametric uncertainty can be expressed by an upper LFT defined by [2]

$$p_k = F_u(\mathbf{M}, \Delta) = F_u\left(\begin{bmatrix} 0 & r_k\bar{p}_k \\ 1 & \bar{p}_k \end{bmatrix}, \delta_{p_k}\right) = \mathbf{M}_{22} + \mathbf{M}_{21}\Delta(\mathbf{I} - \mathbf{M}_{11}\Delta)^{-1}\mathbf{M}_{12} \tag{3.9}$$

where $\Delta = \delta_{pk}$, and

$$\mathbf{M} = \begin{bmatrix} M_{11} & M_{12} \\ M_{21} & M_{22} \end{bmatrix} = \begin{bmatrix} 0 & r_k\bar{p}_k \\ 1 & \bar{p}_k \end{bmatrix}$$

Due to the high dimensionality of the plant, however, the general calculation of analytical models may become prohibitive, or precise models relating the effects of the parameter p_k on the original nonlinear system may not readily available. This is particularly true when variations of operating conditions are treated as structured uncertainty [3-6].

Further, since linearization is performed in the neighborhood of the equilibrium point, these methods essentially provide local information.

An alternative to introducing uncertainty in the system model is to repeatedly perform numerical linearizations over several points in the expected range of operating conditions in the system [3,4]; the resulting change in several system parameters is then approximated by a second (or higher) order polynomial approximation using a least-squares minimization technique.

Let p_k be a given uncertain parameter. From (3.6), it then follows that the variation of this parameter will result in a change of each varying element of each state matrix, a_{ij}^{var} that can be expressed in the form

$$a_{ij}^{\text{var}}(p_k) = f_{ij}(\delta_k) \approx a_{ij}^{o} + a_{ij_k}^{av}\delta_k \tag{3.10}$$

where $a_{ij_o} = (a_{ij}^{\min} + a_{ij}^{\max})/2$ and $a_{ij}^{av} = (a_{ij}^{\max} - a_{ij}^{\min})/2$. This enables the uncertainty description to be represented by an affine parameter-dependent representation.

We point out that in this formulation, the parameters δ_k are artificially introduced; they represent the effect of physical parameters indirectly. While this approach is well suited for the analysis of practical systems, the model is conservative since it neglects the coupled effect of joint parameter dependence in the formulation. This limits its applicability for robust stability assessment of complex power systems. In the following sections, we explore techniques to reduce the level of conservatism in this description and proposed a general algorithm for generating the uncertain description.

3.2. Least-squares computation of analytical parameters

To illustrate the details of the proposed procedure consider the case of a single varying parameter, $\mathbf{p} = \mathbf{p}_1$, which can be related to variations in the power system parameters such as loading or changes in tie-line structure. For each varying element of each state-space matrix, this variation can be expressed as $a_{ij}^{\text{var}} = f_{ij}(p_1)$ where the nonlinear functionals, f_{ij}, are analytical mathematical expressions to be determined.

We remark that, in interpreting parameter variations two fundamental operations are involved: (a) identifying the varying elements of the state-space matrix **A** affected by a change in the set of uncertain parameters, and (b) introducing an uncertain representation of such a change in the nominal plant model. Both problems are addressed here.

To quantify the extent to which a parameter $a_{ij} \in \mathbf{A}$ is modified by the change in operating conditions we use the metric

$$\frac{\left\| a_{ij}^{nom} \right| - \left| a_{ij}^{\neq nom} \right\|}{\left| a_{ij}^{nom} \right|} > \varepsilon \tag{3.11}$$

in which a_{ij}^{nom} represents the coefficient, a_{ij}, that corresponds to the nominal state matrices, and $a_{ij}^{\neq nom}$ is the numerical value of the coefficient associated with the other state matrices; the parameter ε is an appropriate accuracy criterion.

The resulting change in a given coefficient a_{ij}^{var} can then be approximated by the polynomial function

$$f(a_{ij}^{o}, p_1) = a_{ij_o} + a_{ij_1} p_1 + a_{ij_{11}} p_1^2 \tag{3.12}$$

where $p_1^{min} \le p_1 \le p_1^{max}$ and p_1^{max} p_1^{min} are the maximum and minimum values, respectively of the varying element.

In the adopted approach, each parametric uncertainty can then be expressed as a parameter set of the form

$$p_k = \bar{p}_k (1 + r_k \delta_k) = \frac{p_k^{max} + p_k^{min}}{2} + \frac{p_k^{max} - p_k^{min}}{2} \delta_k = \bar{p}_k + s_k \delta_k \tag{3.13}$$

in which

$$\bar{p}_k = \frac{p_k^{max} + p_k^{min}}{2} \; ; \qquad r_k = \frac{p_k^{max} - p_k^{min}}{p_k^{max} + p_k^{min}}$$

where r_k is the relative uncertainty in the parameter, and $\delta_k \in \Re$ is a real scalar such that $-1 \le \delta_k \le 1$.

Substitution of eq. (3.13) into eq. (3.12) results in the perturbed model

$$f(a_{ij}^{o}, \delta_1) = \hat{a}_{ij_o} + \hat{a}_{ij_1}\delta_1 + \hat{a}_{ij_{11}}\delta_1^2 \tag{3.14}$$

where

$$\hat{a}_{ij_o} = a_{ij_o} + a_{ij_1}\bar{p}_1 + a_{ij_2}(\bar{p}_1)^2$$
$$\hat{a}_{ij_1} = a_{ij_1}\bar{p}_1 r_1 + 2a_{ij_2}(\bar{p}_1)^2 r_1$$
$$\hat{a}_{ij_{11}} = a_{ij_2}(\bar{p}_1)^2 (r_1)^2$$

The variation in the nominal state matrix can then be expressed as

$$\mathbf{A} = \mathbf{A}_o + \delta_1 \mathbf{A}_1 + \delta_1^2 \mathbf{A}_{11}$$

Analogous expressions can be defined for the case of several varying parameters.

We emphasize that (3.14) represents a typical polynomial function of the form $y = a_o + a_1 t + \sum_{i=1}^{n-1} a_{1i} t^{i+1}$ where n denotes the order of the approximation. Given t and y, the unknown coefficients, a_o, a_1 and a_{11} can be easily determined by doing a least squares solution fit which minimizes the sum of the squares of the deviations of the data from the model.

Based on this representation, a systematic procedure to compute the polynomial function is proposed for the case of a single varying parameter δ_1.

Computation of the coefficients $\hat{a}_{ij_o}, \hat{a}_{ij_1}, \hat{a}_{ij_{11}}$ is then straightforward:

(i) For each operating condition, r, and an associated level of uncertainty δ_{1_r}, compute the variation in the ij element of matrix $\mathbf{A}$. This defines a data pair $(\hat{a}_{ij}^{\text{var}}, \delta_{1_r})$. In our simulations, the variation in the parameter-dependent state matrix, a_{ij}^{var} is obtained from numerical simulation of the system model; for each operating condition, a power flow simulation is performed and the magnitude of the varying entries is obtained.

(ii) Repeat the above procedure for a number of operating conditions, $r = 1,...,ne$. The coefficients of the quadratic approximation for each varying element, ij. of each state-space matrix are determined by solving the following set of (usually over-determined) system of linear equations

$$\begin{bmatrix} 1 & \delta_{1_1} & \delta_{1_1}^2 \\ 1 & \delta_{1_2} & \delta_{1_2}^2 \\ \vdots & \vdots & \vdots \\ 1 & \delta_{1_{ne}} & \delta_{1_{ne}}^2 \end{bmatrix} \begin{bmatrix} a_{ij_o} \\ a_{ij_1} \\ a_{ij_{11}} \end{bmatrix} = \begin{bmatrix} a_{ij_1}^{\text{var}} \\ a_{ij_2}^{\text{var}} \\ \vdots \\ a_{ij_{ne}}^{\text{var}} \end{bmatrix} \tag{3.15}$$

or, in compact form

$$\mathbf{X}\mathbf{a}_{ij}^{\text{var}} = \mathbf{y} \tag{3.16}$$

where $\mathbf{X}$ is the matrix of uncertainties, ne represents the number of operating conditions, $\mathbf{a}_{ij}^{\text{var}}$ is the vector of unknown polynomial coefficients, and $\mathbf{y} = \left[a_{ij_1}^{\text{var}} \quad a_{ij_2}^{\text{var}} \quad \ldots \quad a_{ij_{ne}}^{\text{var}}\right]^T$ is the vector of variations corresponding to the ij element of the state matrix $\mathbf{A}$.

(iii) Solve for the polynomial coefficients $\mathbf{a}_{ij}^{\text{var}}$ using an appropriate technique

The above model can be easily extended to the case of various simultaneously varying parameters. Let $\boldsymbol{\delta} = \left[\delta_1 \quad \delta_2 \cdots \delta_m\right]^T$ be the vector of varying parameters. From (3.15), we obtain

$$\begin{bmatrix} 1 & \delta_{1_1} & \delta_{2_1} & \delta_{1_1}^2 & \delta_{2_1}^2 & \delta_{1_1}\delta_{2_1} \cdots \\ 1 & \delta_{1_2} & \delta_{2_2} & \delta_{1_2}^2 & \delta_{2_2}^2 & \delta_{1_2}\delta_{2_2} \cdots \\ \vdots & \vdots & \vdots & \vdots & \vdots & \vdots \\ 1 & \delta_{1_{ne}} & \delta_{2_{ne}} & \delta_{1_{ne}}^2 & \delta_{2_{ne}}^2 & \delta_{1_{ne}}\delta_{2_{ne}} \cdots \end{bmatrix} \begin{bmatrix} a_{ij_o} \\ a_{ij_1} \\ a_{ij_2} \\ a_{ij_{11}} \\ a_{ij_{22}} \\ a_{ij_{12}} \\ \vdots \end{bmatrix} = \begin{bmatrix} a_{ij_1}^{\text{var}} \\ a_{ij_2}^{\text{var}} \\ \vdots \\ a_{ij_{ne}}^{\text{var}} \end{bmatrix} \tag{3.17}$$

The main consideration is then how efficiently this implementation may be performed. Several critical issues arise in the practical implementation of the method:

- The order of the polynomial function, n, and
- The number of operating conditions, ne, i.e. *the parameter space* needed to determine the polynomial coefficients.

The first issue is of importance since a linear approximation may result in a conservative assessment of system stability. The error incurred in the approximation will depend upon the nature of the nonlinear functional dependency and the operating condition. This is illustrated in figure 3.1 that shows the functional dependency of the ij element of the state matrix. As illustrated, linear approximations may fail to characterize instability associated with variations in operating conditions.

The accuracy of approximation depends upon both, the operating condition and the approximating function. At a given operating condition, δ_k^r, this can be estimated from

$$error = \left| f\left(\delta_k^r\right) - \left(\hat{a}_{ij_o} + \hat{a}_{ij_1}\delta_k^r\right) \right|$$

Alternate approaches to the determination of the accuracy of the estimate through use of an innovative algorithm, will be discussed in section 3.5.

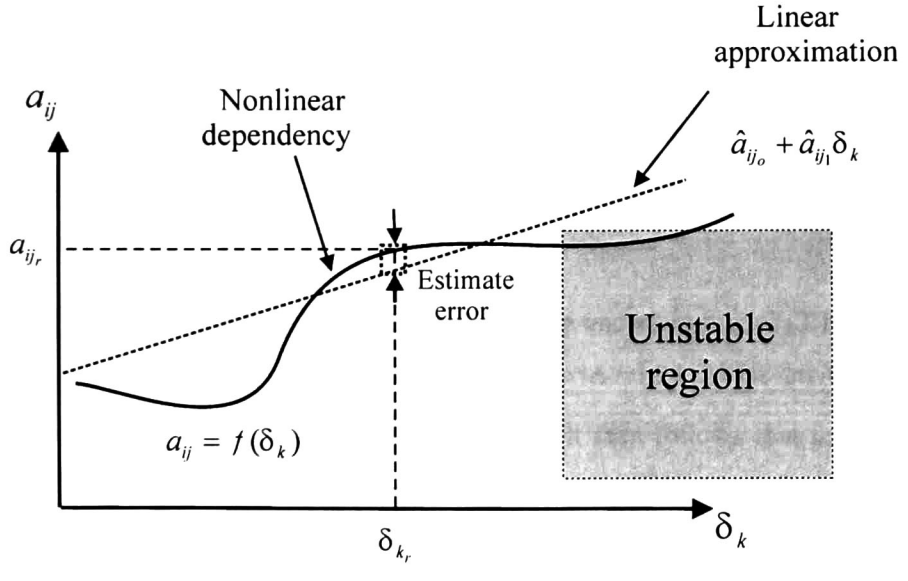

Figure 3.1. Conceptual illustration of the functional dependency of an element of the state matrix **A** *on the order of approximation*

The second issue is also of importance because a low number of operating conditions may result in a poor estimate to the true solution. A suitable choice of the number of operating conditions depends of various interaction factors such as the distance to instability and the specific problem at hand. We note that, in the case of two varying parameters the above representation can be interpreted as a surface which is approximated by a two-dimensional plane. In the case of m uncertain parameters, the approximation can be interpreted as a multidimensional regression plane.

This latter aspect is dealt with in section 3.5 of this chapter.

3.3. Formulation of the optimization problem

Consider the problem of finding a solution $\mathbf{a}_{ij}^{\text{var}}$ to the overdetermined set of equations (3.16). The solution for the unknown vector, $\mathbf{a}_{ij}^{\text{var}}$ is obtained here using a least-squares solution. Straightforward computation yields:

$$\mathbf{a}_{ij}^{\text{var}} = (\mathbf{X}^T\mathbf{X})^{-1}\mathbf{X}^T\mathbf{y} \tag{3.18}$$

The least fit minimizes the residual $\|\Delta\mathbf{y}\|$ subject to $\mathbf{Ax} = \mathbf{b} + \Delta\mathbf{b}$. Several techniques to deal with this representation are available based on conventional analysis and robust least-squares techniques. As discussed in [7], however, the accuracy of the optimization problem is sensitive to perturbation in the data matrices $(\mathbf{A},\mathbf{b})$. This provides motivation for the work to follow.

On the basis of our previous results, we assume that the uncertain model (3.14) is given by a family of matrices $(\mathbf{A} + \Delta\mathbf{A}(\delta), \mathbf{b} + \Delta\mathbf{b}(\delta))$, where $\Delta = [\Delta\mathbf{A}, \Delta\mathbf{b}]$ is an unknown, but bounded matrix such that $\|\Delta\| \le \gamma$ where γ is given. It then follows that for $\mathbf{x} \in R^m$ the worst-case residual can be defined as [7]

$$r_S = (\mathbf{A},\mathbf{b},\gamma,x) = \max_{\|\delta\|} \|\mathbf{A}(\delta)x - \mathbf{b}(\delta)\| \tag{3.19}$$

This problem can be practically solved using robust least-squares regression. The details of the practical implementation are omitted.

Having derived the expressions for $\mathbf{a}_{ij}^{var}$ in (3.18), the LFT uncertainty description can be obtained.

In what follows, the derivation of an uncertainty model is described and details of the implemented algorithm are provided in the context of the robust least-squares regression discussed previously.

3.4. Uncertainty Representation

The framework for robust stability analysis requires that the uncertain system in (3.14) be written as a LFT of the uncertain parameter δ To motivate our analysis of uncertainty, and the calculation of an LFT based representation, we briefly review pertinent results demonstrating the applicability of the proposed technique.

In order to introduce the notation used in the analysis, we start with the case of a single varying parameter. To obtain the uncertain model in the robustness framework let the uncertain plant with structured uncertainty in (3.14) be described by

$$\begin{aligned} \dot{\mathbf{x}} &= \mathbf{A}_o\mathbf{x} + \mathbf{A}_1(\delta\mathbf{I}) + \mathbf{A}_{11}(\delta^2\mathbf{I}) = \mathbf{A}_o\mathbf{x} + \Delta\mathbf{A}(\delta) \\ \mathbf{w} &= \Delta\mathbf{z} \end{aligned} \tag{3.20}$$

where $\mathbf{A}_{o[nve,nve]}$ represents the nominal plant, and the matrix $\Delta\mathbf{A}(\delta)$ accounts for structured uncertainties in the model; the matrix of uncertainties in the model is given by

$$\Delta = \left\{ \begin{bmatrix} \delta & \\ & \delta^2 \end{bmatrix}; \delta \in \Re \right\} \tag{3.21}$$

In order to construct the LFT, the quadratic dependence of the coefficients of the matrix $\mathbf{A}$ has to be incorporated. There are several approaches to deal with this dependence. Here, we extend the approach in [3,4] to account for large scale application of the method.

Defining $\mathbf{z}_1 = [z_{11} \quad z_{21}]^T$ and $\mathbf{w}_1 = [w_{11} \quad w_{21}]^T$ as the vector of inputs and outputs to the uncertainty block, one has $\mathbf{w}_1 = \delta\mathbf{I}_2\mathbf{z}_1$, where $\mathbf{I}_2$ is the *2x2* identity matrix.

The quadratic dependence is then obtained from

$$\mathbf{w}_2 = \delta\mathbf{I}_2\mathbf{z}_2 = \delta\mathbf{I}_2\mathbf{w}_1 = (\delta\mathbf{I}_2)(\delta\mathbf{I}_2)\mathbf{z}_1 = \mathbf{R}(\delta\mathbf{I}_2)(\delta\mathbf{I}_2)\mathbf{x} \tag{3.22}$$

where $\mathbf{R}$ is a matrix composed of 1's of appropriate dimensions; the rows of $\mathbf{R}$ correspond to those columns of the state-space matrix $\mathbf{A}$, that change following a variation in the uncertain parameter. The vector $\mathbf{z}_2$ is a fictitious vector needed in the development of the robustness framework.

With these definitions, and omitting intermediate derivations, the linear and quadratic dependence can be expressed in matrix form as $\Delta\mathbf{A}(\delta) = \mathbf{L}^T\mathbf{A}_1\mathbf{w}_1 + \mathbf{L}^T\mathbf{A}_{11}\mathbf{w}_2$, where $\mathbf{L}$ is an *rAcxnve* matrix composed of 0's and 1's, and $\mathbf{A}_{1[rAc,cAc]}$, $\mathbf{A}_{11[rAc,cAc]}$ represent varying matrices combining all uncertainties. In this notation, rA_c cA_c denote the number of rows and columns of the state matrix $\mathbf{A}$ that change due to varying operating conditions.

Combining these equations, the LFT representation of the system with structured uncertainties becomes

$$\begin{bmatrix} \dot{\mathbf{x}} \\ \mathbf{z}_1 \\ \mathbf{z}_2 \end{bmatrix} = \left[\begin{array}{c|cc} \mathbf{A}_0 & \mathbf{L}^T\mathbf{A}_1 & \mathbf{L}^T\mathbf{A}_{11} \\ \hline \mathbf{R} & \mathbf{I} & \mathbf{0} \\ \mathbf{0} & \mathbf{0} & \mathbf{0} \end{array}\right] \begin{bmatrix} \mathbf{x} \\ \mathbf{w}_1 \\ \mathbf{w}_2 \end{bmatrix} \tag{3.23}$$

in which $\mathbf{A}_{*o} = 0$ yields the nominal linearized model of the system model, and

$$\begin{aligned} \mathbf{A}_0 &= \mathbf{A}_0^{\text{var}} + \left[\mathbf{A}_{10}^{\text{var}} + \mathbf{A}_{110}^{\text{var}} p_a\right] p_a \\ \mathbf{A}_1 &= \left[\mathbf{A}_1^{\text{var}} + 2\mathbf{A}_{11}^{\text{var}} p_a\right] p_b \\ \mathbf{A}_{11} &= \mathbf{A}_{11}^{\text{var}} p_b \\ p_a &= \bar{p}_1 \\ p_b &= \bar{p}_1 - p_1^{\min} \end{aligned}$$

Also, using the above approach, it is straightforward to show that

$$\mathbf{A} = \mathbf{A}_0 + \mathbf{L}^T\left[\mathbf{A}_1\delta_1 + \mathbf{A}_{11}\delta_1^2 + \cdots + \mathbf{A}_{1n}\delta_1^n\right]\mathbf{R} \tag{3.24}$$

where n is the order of the polynomial approximation.

Using (3.24), the uncertainty description of the system can then be expressed in the form

$$\begin{aligned}
\dot{\mathbf{x}} &= \mathbf{A}_0\mathbf{x} + \mathbf{L}^T(\mathbf{A}_1\mathbf{w}_1 + \mathbf{A}_{11}\mathbf{w}_2 + \ldots + \mathbf{A}_{1n}\mathbf{w}_n) \\
\mathbf{z}_1 &= \mathbf{R}\mathbf{x} \\
\mathbf{z}_2 &= \mathbf{I}\mathbf{w}_1 \\
&\vdots \\
\mathbf{z}_n &= \mathbf{I}\mathbf{w}_{n-1}
\end{aligned} \tag{3.25}$$

where

$$\mathbf{x} = \frac{1}{s}\dot{\mathbf{x}}$$

Figure 3.2 shows the adopted robust stability framework for the case of one varying parameter. The basic idea here is often referred to as "pulling out of the Δ's" [8,9]. That is, all uncertain elements have been pulled out of the system and placed in the Δ block.

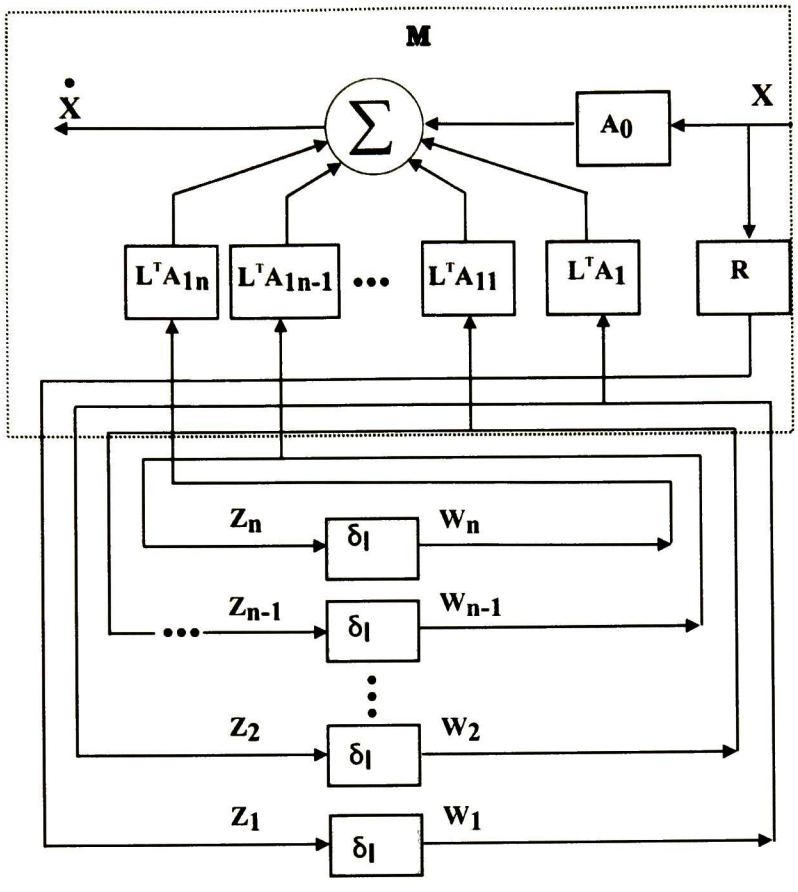

Figure 3.2. Pulling out of the Δ's. One varying parameter case

In pursuit of further generalization assume now, that p parameters are varied simultaneously. Generalizing the previous approach, one has

$$\mathbf{A} = \mathbf{A}_{\cdot} + \sum_{i=1}^{m} \mathbf{A}_i \delta_i + \sum_{i=1}^{m} \mathbf{A}_{ii} \delta_i^2 + (if \quad m > 1 \quad then \quad \sum_{i=1}^{m-1} \sum_{j=i+1}^{m} \mathbf{A}_{ij} \delta_i \delta_j) \tag{3.26}$$

Figure 3.3. shows the LFT representation of the system. Employing the above formulation, and noting that $\Delta_2 = \frac{1}{s}\mathbf{I}$, the transfer function from $\mathbf{w}$ to $\mathbf{z}$ can be expressed as a LFT of a constant matrix $\mathbf{M}_{11}$ on the frequency variable s, as

$$F_l(\mathbf{M}, \Delta(\delta)) = \mathbf{M}_{11} + \mathbf{M}_{12}\Delta_2 (\mathbf{I} - \mathbf{M}_{22}\Delta_2)^{-1}\mathbf{M}_{21} = \mathbf{M}_{11} + \mathbf{M}_{12}\frac{1}{s}\mathbf{I}\left(\mathbf{I} - \mathbf{M}_{22}\frac{1}{s}\mathbf{I}\right)^{-1}\mathbf{M}_{21} \tag{3.27}$$

such that $\mathbf{z} = F_u(\mathbf{M}, \Delta)\mathbf{w}$ In interpreting this expression we emphasize that, the LFT representation of the feedback term $\frac{1}{s}\mathbf{I}$, is $F_l = \left(\begin{bmatrix} \mathbf{0} & \mathbf{I} \\ \mathbf{I} & \mathbf{0} \end{bmatrix}, \frac{1}{s}\mathbf{I}\right)$.

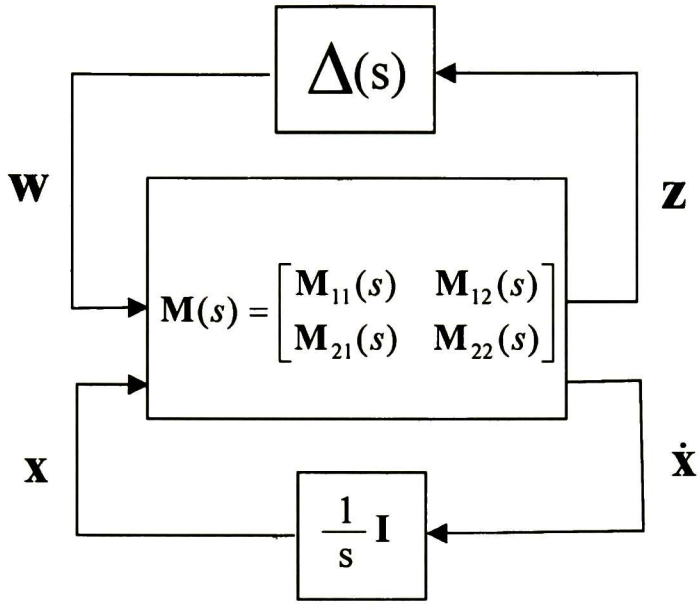

Figure 3.3. Linear fractional description for robust stability analysis

Once the LFT-based description has been defined, robust stability of the closed-loop system is then evaluated using μ-analysis techniques within the MUSYN software [2], modified to compute tight bounds on the real SSV [10]. This approach is applicable to a variety of uncertainties of operating conditions.

3.5. Effect of multiple uncertainties

When analyzing several uncertainties it is of especial interest to determine which uncertain elements dominate the robustness measure, which elements are interrelated, and which elements do not greatly affect the stability of the system.

3.5.1. Parameter space

A critical aspect in the derivation of the model is the definition of a suitable operating space. Based on the simple uncertainty case considered in the previous section, we propose a technique to treat and analyze multiple uncertainties.

The set of uncertain parameters which are assumed to vary within practical limits is defined by the expressions,

$$\begin{aligned}
\mathbf{p}_1(\delta_1) &= [p_{11} \quad p_{12} \quad p_{13} \quad \cdots \quad p_{1ne}] \\
\mathbf{p}_2(\delta_2) &= [p_{21} \quad p_{22} \quad p_{23} \quad \cdots \quad p_{2ne}] \\
\vdots \quad &= [\vdots \quad \vdots \quad \vdots \quad \ldots \vdots \quad] \\
\mathbf{p}_m(\delta_m) &= [p_{m1} \quad p_{m2} \quad p_{m3} \quad \cdots p_{mne}]
\end{aligned} \tag{3.28}$$

where m is the number of varying parameters, and ne defines the number of uncertain parameters, i.e the number of operating conditions.

As an example of the calculation of uncertainty representations, we consider a two-dimensional set of two uncertain parameters, $m = 2$, with three different operating conditions. More precisely, we assume each parameter set to consist of three terms ($ne = 3$) corresponding to different operating conditions (refer to figure 3.3). Using the above representation results in the parameter space

$$\begin{aligned}
\mathbf{p}_1(\delta_1) &= [p_{11} \quad p_{12} \quad p_{13}] \\
\mathbf{p}_2(\delta_2) &= [p_{21} \quad p_{22} \quad p_{23}]
\end{aligned}$$

More precisely, figure 3.4 shows the grid of points in the parameter space for the case of two simultaneous varying parameters. Each point on the grid of operating conditions is defined by one entry corresponding to each varying parameter. Simultaneous analysis of two varying parameters requires nine operating conditions.

Practical approaches in this dissertation are based on a few operating conditions, namely three for each one of the varying parameters.

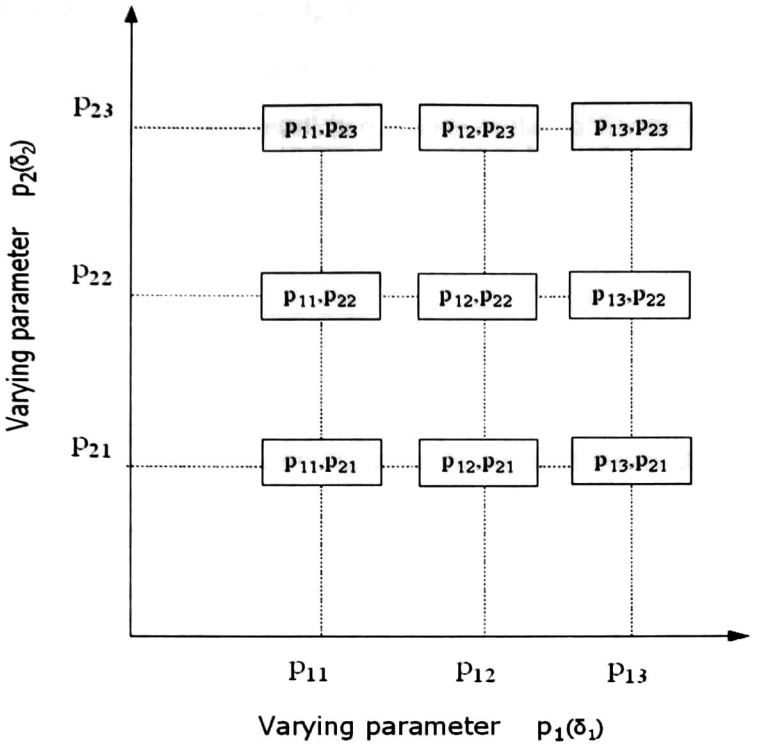

Figure 3.4. Grid of points in the parameter space for two uncertainty sources

Assuming further that each parameter lies between some minimum (a) and maximum value (b) it is possible to construct a representation with the nominal $(a+b)/2$ value, and an additional extra input and output pair through which the variation of the nominal value enters to the system.

Using these assumptions, a very simple but powerful procedure for the modeling of real parameter uncertainties is proposed.

For each combination of the uncertain parameters, p_{1j}, p_{2j}, we generate a grid of operating conditions that approximates the parameter space (refer to Table 3.1).

Table 3.1. Grid of operating conditions for parameter sets p_1, p_2

	p_{21}	p_{22} *	p_{23}
p_{11}	A_I	A_{II}	A_{III}
p_{12} *	A_{IV}	A_V	A_{VI}
p_{13}	A_{VII}	A_{VIII}	A_{IX}

* Nominal operating points

Here, the state matrices $A_{II}, A_{IV}, A_{V}, A_{VI}$, and A_{VIII} are associated with the nominal values p_{12} and p_{22}, and are defined as nominal state matrices. It follows that the simultaneous variation of these parameters will result in a change in the coefficients of the **A** matrix of the form

$$a_{ij}^{\text{var}} = f_{ij}(p_1, p_2) \tag{3.29}$$

where the nonlinear functional, f_{ij}, are analytical mathematical expressions to be determined. It is important to emphasize that the parameters p_1, p_2 can be independent or be correlated as discussed below and discussed in our numerical simulations.

3.5.2. Sensitivity/uncertainty analysis

The relative importance of the uncertainties in operating conditions can be determined using sensitivity or uncertainty analysis. Inspired by work on sensitivity analysis in the analysis of differential equations we explore a simple methodology for approximation and quantification of multiple, interrelated uncertainties.

From (3.29), if $\mathbf{p} = [p_1 \quad p_2]$ is perturbed by Δp, the change in the coefficients of matrix **A** may be approximated using a first order Taylor series expansion

$$a_{ij}^{\text{var}}(p + \Delta p_o) = a_{ij}(p_o) + \frac{\partial f_{ij}}{\partial p_1}\Delta p_1\bigg|_{p_{1o}} + \frac{\partial f_{ij}}{\partial p_2}\Delta p_2\bigg|_{p_{2o}} \tag{3.30}$$

where the sensitivity coefficients $\partial f_{ij}/\partial p_k$, $k = 1,2$ are computed assuming that all other parameters are fixed.

Clearly

$$\left| a_{ij}^{\text{var}}(p + \Delta p_o) - a_{ij}^{\text{var}}(p_o) \right| \le \sum_{i=1}^{m} \left| \frac{\partial f_{ij}}{\partial p_k}\Delta p_k\bigg|_{p_{ko}} \right| \tag{3.31}$$

Figure 3.5 shows a two-dimensional view of the model surface showing the region of uncertainty for the case of two varying parameters. The assumed upper and lower limits produce a region of uncertainty (dark area) in the $p_1 - p_2$ plane.

Physically, the sensitivity of the **A**-matrix elements, $\partial f_{ij}/\partial p_k$ to parameter variations evaluated at p_1^{av}, p_2^{av} represent the local gradient of the model surface at point P, with respect to each parameter.

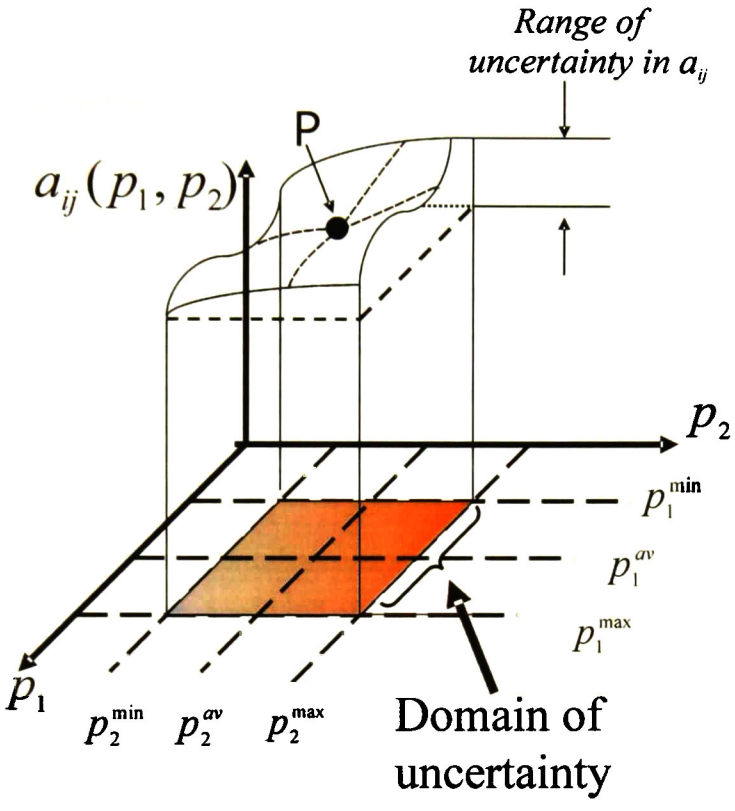

$$p_k = (p_k^{\min} + p_k^{\max})/2 + p_k^{av}\delta_k$$

Figure 3.5. Schematic of the model surface, showing the region of uncertainty in two parameters, $\mathbf{p}_1$ *and* $\mathbf{p}_2$.

Two approaches are possible to determine the sensitivity coefficients. The first is based on knowledge of the system structure of matrix **A**. The second is based on numerical analysis of the state-space matrix. This latter approach is explored here.

The method proceeds as follows:

a). For each expected operating scenario $(p_1, p_2, ..., p_m)$ determine numerical (or analytical) first-order sensitivity coefficients, $\partial f_{ij}/\partial p_k$. Owing to the coupled nature of uncertainty, however, attempts to compute the sensitivity coefficients varying

one parameter at a time while holding all the other parameters fixed at some specific values become prohibitive, especially for large systems.

b). Once a mathematical model of the system has been constructed, a quantitative estimate of the overall estimate can then be obtained using (3.30). In this research study, an alternative formulation for the numerical computation of the variations, a_{ij}^{var} that considers multiple parameter variations can be obtained from the numerical determination of matrices $\mathbf{A}^{var}$ using a small signal stability software or using automatic differentiation. See Castellanos *et al.* [5,6] for details.

The aforementioned approach allows studying the effects of large deviations from the nominal parameter values on the uncertainty representations and can be used to identify the uncertainties with most influence in the model. In addition, since various parameter values can be varied simultaneously, one can explore regions of the parameter space where certain combinations of values of parameters deviate substantially from their nominal values.

A heuristic way to verify the numerical accuracy of the method would be to: (i) Compute variations in the coefficients (or sensitivity) of the $\mathbf{A}$-matrix elements using the normalized norm (3.11), and (ii) Generate the associated $\mathbf{A}_k$ matrices using the procedures in sections 3.3 and 3.3. A suitable choice of the truncation order will depend upon the pre-selected accuracy criterion ε. Generating the required perturbation matrices in this manner may make the results of the analysis more accurate.

Subsequent transformation of this description to the standard form for μ analysis is straightforward and is not discussed here.

3.5.3. General polynomial function

The foregoing two-dimensional example can be readily extended to higher dimensions. Experience indicates [4-6] that using a second-order polynomial function ($n = 2$ in eq. 3.24) accurate enough results can be obtained. Using these assumptions, we extend the second-order polynomial function to the case of m varying parameters. It is easily verified from (3.24) that

$$p(\delta_1,\delta_2,...,\delta_m)=\begin{cases} A_o+\sum_{i=1}^{m}A_i\delta_i+\sum_{i=1}^{m}A_{ii}\delta_i^2 & if \quad m=1 \\ A_o+\sum_{i=1}^{m}A_i\delta_i+\sum_{i=1}^{m}A_{ii}\delta_i^2+\sum_{i=1}^{m-1}\sum_{j=i+1}^{m}A_{ij}\delta_i\delta_j, & if \quad m>1 \end{cases} \tag{3.32}$$

The derivation of the LFT representation is then straightforward and the details are omitted. We discuss this point further in our numerical simulations.

3.5.4. Optimal combination of operating conditions

As noted in this and in the preceding section, one of the basic open issues yet to be resolved, is the determination of the optimum number of operating conditions or power flow solutions, which are necessary to obtain practical results. With m given by (3.28), we find

$$noc = ne^m$$

where noc is the number of power flow solutions, ne is the number of entries in each varying parameter, and m represents the number of varying parameters.

Table 3.2 shows the maximum number of power flow solutions, noc, required to capture the effects of uncertainty in large power systems, using a parameter set with three terms ($ne=3$). In the case of one varying parameter, the method requires three power flow solutions whereas for the case of two varying parameter formulation, nine power flow solutions are needed. Results indicate [4-6] that both approximations are sufficiently good for all practical purposes and overcome computational limitations associated to large power systems. Several examples of one and two varying parameters assessment are shown in Chapters 4 and 5.

Table 3.2. Number of power flow solutions, noc, as a function of the number of varying parameters, m.

m	*1*	*2*	*3*	*4*	...	*m*
noc	3	9	27	81	...	3^m

It is worth emphasizing that in the case of three varying parameters the application of the method requires twenty-seven power flow solutions with one state matrix associated to each one.

Clearly, the computer requirements as well as the high number of power flow solutions (twenty-seven) required may not represent a practical solution for robust stability assessment of large power systems.

3.6 Computational algorithm

The procedure aforementioned has been implemented in Matlab using the μ-analysis framework toolbox, Musyn [2]. An overview of the algorithm utilized for assessing robust stability is shown in Figure 3.6, illustrating the combined application of conventional small signal analysis and μ-synthesis techniques for robust stability assessment of power systems.

Notice that step 1 in Figure 3.6 is performed using commercially available small-signal stability software.

The robust stability technique is implemented as follows.

1. Define a set of parameter variations $\mathbf{p}_1, \mathbf{p}_2, .., \mathbf{p}_m$. For each varying parameter defines a range of operating conditions, including here the nominal condition. For each operating condition, included in the range, perform a load flow simulation and obtain the associated state matrix $\mathbf{A}_i$.

2. To quantify the extent to which a parameter $a_{ij} \in \mathbf{A}$ is modified by the change in operating conditions compute the metric (3.11).

3. Compute the parameters for each varying element of the state-space matrices by solving the set of equations (3.15).

4. Generate the $\mathbf{M} - \Delta$ structured by using equations (3.25) and (3.26). Express the effect of varying parameters and changing operating conditions as structured uncertainties, Δ. Evaluate matrices $\mathbf{M}_{11}, \mathbf{M}_{12}, \mathbf{M}_{21}$ and $\mathbf{M}_{22}$ using the procedure given in section 3.4.

5. Evaluate stability robustness using μ analysis. Compute an upper bound for $\mu_{\Delta}\mathbf{M}(j\omega)$ using the optimal multiplier algorithm of [10]. Select worst-case uncertainty combinations and determine the size of the smallest Δ (limiting of small signal stability) which destabilizes the system by computing $\delta_1 = 1/\mu_{upper}$.

6. The robustness analysis results obtained before can be used to define uncertainty-based control policies. As discussed in Chapter 5, the robust stability limit can represent the starts of a small-signal stability emergency zone. This point, also, may be used to define the finish of an alert zone.

Finally, in order to construct the whole control strategy we use the conventional linear analysis to define a small-signal stability margin, for instance, 5 % damping ratio for critical contingencies conditions.

Based on the concept of structure uncertainty representation outlined above, it is possible to determine worst-case operating conditions as well as to identity which elements dominate the robustness measure.

Also, these results can be used to define uncertainty-based control strategies. Further work on the approach considered follows on these lines in Chapter 5.

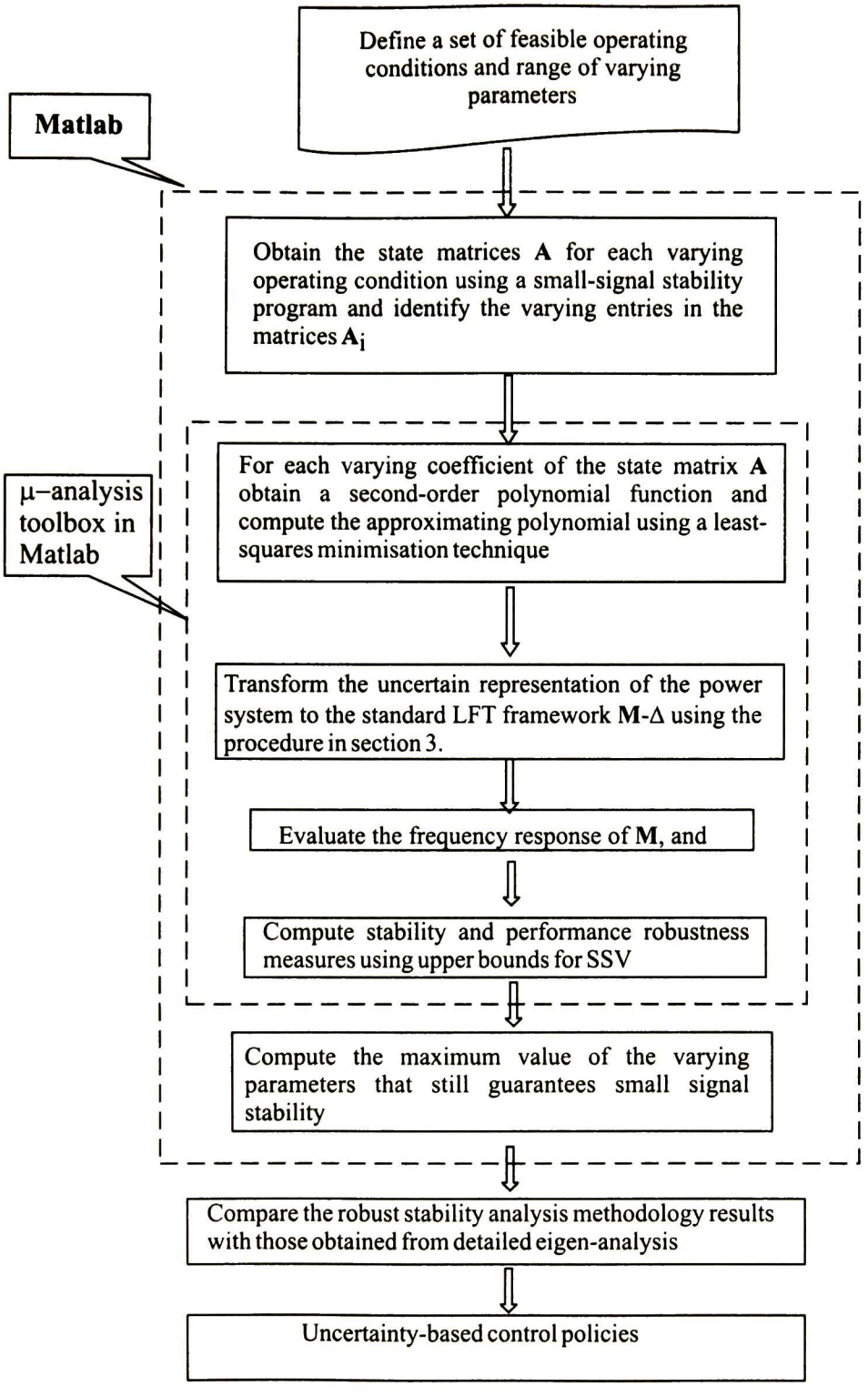

Figure 3.6. Overview of the algorithm for computing robust stability using μ-analysis

3.7 Discussion

In this chapter a framework for robust stability assessment in multi-machine power systems using LFT theory and μ-analysis is suggested. Two strong advantages of this method are its generality, and the fact that it can be applied to both numerical and analytical derivations. The approach is general enough to include the representation of complex systems and can be used in conjunction with efficient techniques for the analysis of large sparse linear systems.

While the process has some conservatism, it can deal with practical networks. More importantly, the proposed procedure constitutes one of the first attempts to treat real parametric variations.

In the following chapters we discuss how this algorithm is implemented and discuss practical details concerning its numerical implementation.

References

[1] M.B. Djukanovic, M. H. Khammash, V. Vittal "Sensitivity based structured singular value approach to stability robustness of power systems", *IEEE Transactions on Power Systems,* vol. 15, no. 2, May 2000, pp. 825-830.

[2] G.J. Balas, J.C. Doyle, K. Glover, A. Packard, R. Smith, "μ-Analysis and Synthesis Toolbox, Matlab" *MUSYN Inc. and The MathWorks, Inc. V. 3.05 (Release 12),* January 2001.

[3] M. Djukanovic, M. Khammash, V. Vittal, "Application of the Structured Singular Value Theory for Robust Stability and Control Analysis in Multimachine Power Systems", Parts I and II. *IEEE Transactions on Power Systems,* vol. 13, no. 4, 1998, pp. 1311-1316.

[4] R. Castellanos, A. R. Messina, H Sarmiento, "Robust stability analysis of large power systems using the structured singular value theory", *International Journal of Electrical Power and Energy Systems,* vol. 27, no. 3, June 2005, pp. 389-397.

[5] R. Castellanos, C. Juarez, A. R. Messina, "Quantifying the Stability Robustness of Power Systems using Structured Singular Value Theory", *IEEE PES 2005 General Meeting,* San Francisco, California, USA, June 2005.

[6] R. Castellanos, C. Juarez, J. Hernandez, A. R. Messina, "Robustness Analysis of Large Power Systems with Parametric Uncertainties", *IEEE PES 2006 General Meeting,* Montreal, Quebec, Canada, June 2006.

[7] L. El Ghaoui, H. Lebret, "Robust solution to least-squares problems with uncertain data", *SIAM Journal of Matrix Analysis and Applications,* vol. 18, no. 4, October 1997, pp. 1035-1064.

[8] B. Morton and McAfoos, "A μ test for real parameter variations", *In: Proceeding of the ACC,* pp. 135-138, 1985.

[9] *T.* Mannchen, K.H. Well, "Uncertainty Bands Approach to LFT Modelling", *Advances Techniques for Clearance of Fly Control Laws.* LNCIS, 2002, pp. 211-220.

[10] M.J. Hayes, D.G. Bates, I. Postlethwaite, "New tools for computing tight bounds on the real structured singular value", *Journal of Guidance, Control and Dynamics,* vol. 24, no. 6, November-December 2001, pp. 1204-1213.

Chapter 4

Application of SSV Theory for Robust Stability Analysis

The practical treatment of systems with parameter uncertainties has become an increasingly important problem in many areas of power system dynamic analysis. Uncertain behavior under closed-loop operation of power systems can originate from a variety of sources. These include, changes in load flow patterns, varying load levels, load characteristics and control characteristics. Network robustness is also of importance as, for instance, the loss of major generation and transmission resources widens the electrical distances between interconnected areas leading to increased angular deviations and reduced small signal stability margins.

This chapter discusses the results of analytical studies conducted to examine the applicability of the proposed analysis procedures to assess stability robustness with respect to real parametric variations. In particular, uncertainties in the nominal plant model arising from two distinct sources are considered; variations in the levels of power transfer between interconnected areas, and variations in the topology of the power system. These uncertainties are represented as LFT-based parametric uncertainty descriptions to analyze stability robustness.

The proposed analysis procedure is tested on two power networks derived from actual power systems. The first network is a two-area four-machine test system used by several researchers in the study of small signal stability. The second system is a six-area, 377-generator, and 3759-bus dynamic equivalent of the Mexican interconnected system. Detailed nonlinear time-domain simulations are presented and discussed to check the accuracy of the proposed analysis procedure. A brief summary in section 4.3 concludes this chapter.

4.1. Four-machine system results

As a first example of the application of the method we consider a two-area, four-generator power system from Ref. [1]. This model has been used extensively for comparing study techniques and investigating small signal behavior. Figure 4.1 shows a one-line diagram of this system. The test power system consists of two similar areas connected by a weak tie, 4 generators, 8 transmission lines, 4 transformers and 2 loads. In addition, fixed shunt compensation and dynamic voltage support by means of Static VAR Compensators (SVCs) are used to support system voltage.

For the purpose of analysis, the four generators are represented by a two-axis model and equipped with a fast exciter [1]. The load model used is constant current for the real component and constant impedance for the reactive component. This representation results in a system model with 48 states.

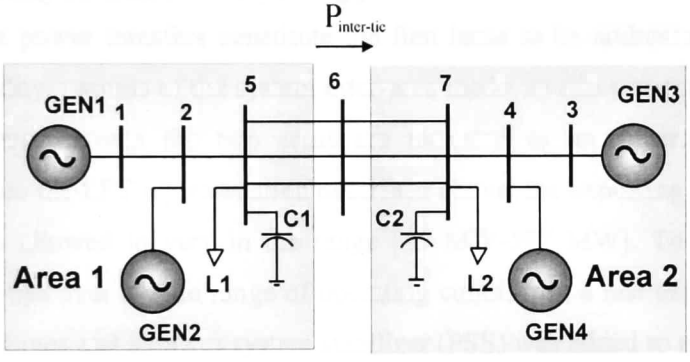

Figure 4.1. Four-machine, two-area test power system

The system exhibits three electromechanical modes of concern [1,2]:

- An inter-area mode with a frequency of 0.70 Hz involving the exchange of oscillating energy between Areas 1 and 2, and
- Two local modes associated with the local dynamics between generators in each area

Attention in the following is focused on determining robust stability for varying operating conditions and uncertainties in the structure of the power system. Specifically, the developed technique is used to estimate the effects of variations in the parameters of the major system intertie on the nominal stability of the 0.70 Hz inter-area mode.

The validation is based on comparisons with results from conventional eigen-analysis using a commercial small-signal stability software.

4.1.1. Study objectives and assumptions

The effectiveness of the proposed technique is demonstrated through three case studies. In the first case study (*Case study 1*), the exporting power from Area 1 to Area 2 is modeled as a varying uncertain parameter. In the second case (*Case study 2*), the interconnecting tie-line reactance is considered as an uncertain quantity. In the last case (*Case study 3*), both the interconnecting tie-line reactance and the power transfer between Areas 1 and 2 are modeled as uncertain parameters. For clarity, single and multiple uncertainties are analyzed separately.

4.1.2. Robustness evaluation; one parameter variation

4.1.2.1. Case study 1: Maximum exporting power

High inter-area power transfers constitute the first issue to be addressed as they result in decreased stability margins of the system inter-area mode. In this test case, variations in the exporting power between the two areas are modeled as an uncertain parameter and incorporated into the LFT representation described above; the exporting power from Area 1 to Area 2 was allowed to vary in the range [45 MW-597 MW]. To maintain adequate stability properties over a wide range of operating conditions, a fast excitation system was used in all machines and a power system stabilizer (PSS) was added to machine GEN3. For comparison, the linear stability limits were determined by increasing gradually the tie-line transfer to Area 2. At each operating condition the system eigenvalues were computed until instability was detected.

Table 4.1 gives the frequency and damping ratio of the inter-area mode as a function of the intertie power flow computed using conventional eigenanalysis. Stressing the system by increasing the power flow shows that the inter-area mode is stable. Note that, the nominal interface flow is 285 MW.

In order to confirm these results, μ-analysis was performed for the critical stability condition (597 MW) using the proposed procedure. Following the procedures outlined in Chapter 3, we transform the linear model of the system into an LFT form for μ-analysis.

Table 4.1. Inter-area mode eigenvalue as a function of the power transfer level, $P_{inter-tie}$

Power Flow (MW)	Eigenvalue	Damping ratio (%)	Frequency (Hz)
45	-0.1343± j 4.5365	2.96	0.7220
80	-0.1270±j 4.6797	2.71	0.7448
180	-0.1259±j 4.6510	2.70	0.7402
285	-0.1226±j 4.6008	2.66	0.7322
360	-0.1165±j 4.5239	2.58	0.7200
490	-0.1069±j 4.4110	2.42	0.7020
597	-0.0919± j 4.2377	2.17	0.6744

As a further validation of the above results, robust stability limits were computed using the proposed approach. Table 4.2 synthesizes the exact and estimated critical power flow using conventional eigenvalue analysis and the robust stability assessment tool. Robust stability results in Table 4.2 indicate that using a high number of operating conditions (7 in this case) we may obtain accurate enough results even when the system is far from the small signal stability limit (approximately 50%, for this case).

Note worthily, the error estimate using the proposed procedure is less that 2.2% with respect to the results of conventional small signal analysis. We emphasize that the accuracy of this prediction is superior to other approaches based on conventional polynomial approximations. As pointed out in our subsequent analysis, however, a reduced operating space often suffices to provide sufficiently accurate results for many practical applications.

Table 4.2. Robust stability assessment – Case study 1

μ upper bounds	0.4792
Estimated ω (rad/s)	4.58
Exact ω (rad/s)	3.75
Estimated (exact) power flow (MW)	**904.5 (886)**
Exact eigenvalue	-0.009± j3.7468
	ζ = 0.02 %
Error (%)	2.1

In turn, examination of the μ upper bound in Figure 4.2, shows a value less than one at the frequency of concern indicating that the system is stable for this range of power transfer. These results are in good agreement with those obtained by conventional eigenanalysis (refer to Table 4.1).

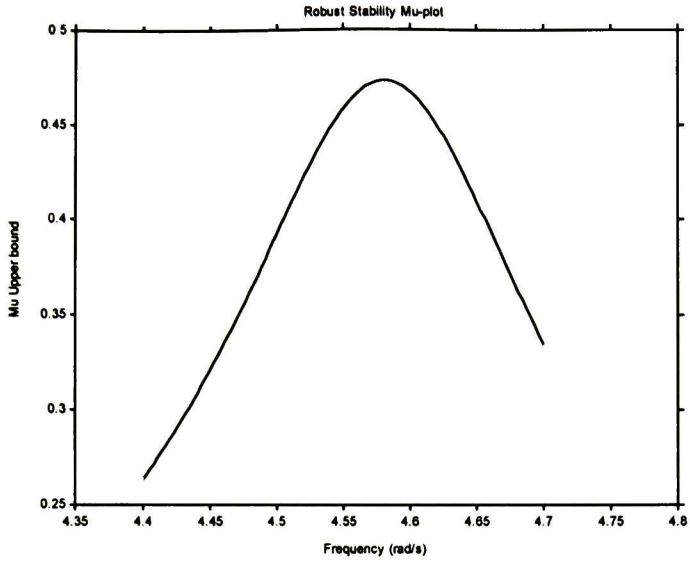

Figure 4.2. Robust stability μ - plot (frequency-sweep around the critical frequency). Case study 1

4.1.2.2. Case study 2: Maximum interconnecting tie-line reactance

In this study, the interconnecting tie-line reactance, $X_{tie-line}$, was treated as an uncertain parameter and allowed to vary in the range [0.073 p.u.-0.22 p.u.] by connecting and disconnecting parallel paths. For the purposes of the study, fast static exciter models were used in all generators and an SVC, with supplementary damping control, was added at the midpoint between the two areas; the corresponding nominal tie-line power flow is 400 MW.

Following the same approach as that used in the previous case, the tie-line reactance was adjusted in small steps and the inter-area mode eigenvalue was computed for each operating condition. Table 4.3 shows the damping ratio and frequency of the inter-area mode as a function of equivalent reactance. It is seen from these simulations that, the inter-area mode remains stable for the physically expected range of tie-line reactances.

Table 4.3. Inter-area mode eigenvalue as a function of the tie-line reactance

Equivalent reactance (pu)	Eigenvalue	Damping ratio (%)	Frequency (Hz)
0.073	-0.2172±j 4.8126	4.51	0.7660
0.11	-0.2700±j 4.2625	6.32	0.6784
0.22	-0.1920± j 2.8855	6.64	0.4592

In turn, the upper-bound μ-plot in Figure 4.3 shows an upper bound of 0.9395, suggesting that the system is robustly stable for the uncertainty range of operating conditions considered. Since the value of μ is quite close to 1, however, only small levels of additional uncertainty can be allowed before instability of the inter-area mode can occur.

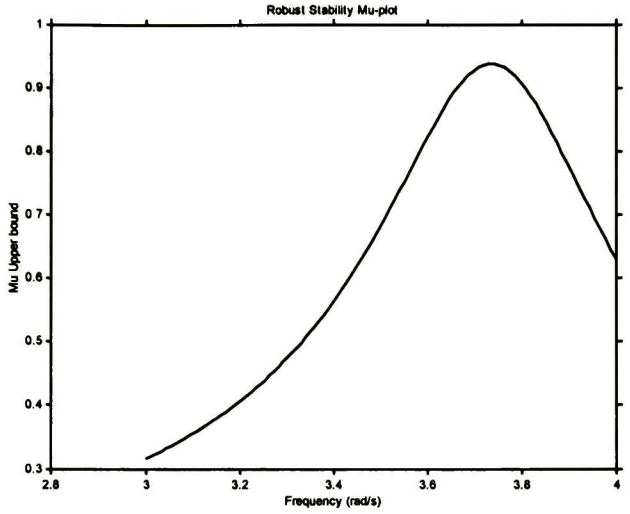

Figure 4.3. Robust stability μ plot. Case study 2

Table 4.4 shows the exact and estimated critical value of $X_{tie-line}$ determined iteratively using conventional eigen-analysis along with the eigenvalue computed at the limiting condition. Again the results show a small error between the estimated and computed limits.

Table 4.4. Robust stability assessment – Case study 2

μ upper bounds	0.9395
Estimated ω (rad/s)	3.7307
Exact ω (rad/s)	2.4997
Estimated (exact) $X_{tie-line}$ (p.u.)	**0.2247 (0.2282)**
Exact eigenvalue	-0.0288± j2.4997
	ζ = 1.15 %
Error (%)	-1.53

4.1.3. Case study 3; Two parameter variation

To further illustrate the potential usefulness of the developed method, we consider a case with two varying parameters. In this study the tie-line equivalent reactance is allowed to vary in the range [0.073 p.u.-0.22 p.u.] and the inter-area power flow is allowed to vary in the range [102 MW-510 MW]. For this case, slow excitation systems without PSSs, and an

SVC with Supplementary Damping Control (SDC), installed at the midpoint of the intertie are assumed. Appendix A provides dynamic data for the SVC.

The analysis of the upper bound in figure 4.4 shows a peak bigger than one implying that the system is unstable. Table 4.5 gives the damping ratio and frequency of the inter-area mode as a function of the equivalent reactance and power flow. Also shown in Table 4.5 is the damping associated with the limiting operating conditions. As can be seen, the analysis enables us to confirm that the system is stable for all operating conditions, except for the limiting condition (0.22 p.u., 500 MW), for which a feasible solution was not attained.

Table 4.5. Damping of critical inter-area mode as a function of the interconnecting reactance and power flow

Equivalent reactance (p.u.)	Power flow (MW)		
	102	301	510
0.073	-0.0726± j4.1590 f = 0.6619 Hz ζ = 1.74 %	-0.1824± j4.2016 f = 0.6687Hz ζ =4.34%	-0.299± j4.1634 f= 0.6626 Hz ζ = 7.16 %
0.11	-0.0635± j3.6972 f = 0.5884 Hz ζ = 1.72 %	-0.1761± j3.7124 f = 0.5908 Hz ζ = 4.74%	-0.2598± j3.5251 f= 0.5610 Hz ζ =7.35 %
0.22	-0.0462± 2.8465 f = 0.453 Hz ζ = 1.62%	-0.1357± j2.7546 f = 0.4384 Hz ζ = 4.92%	**power flow no solved**

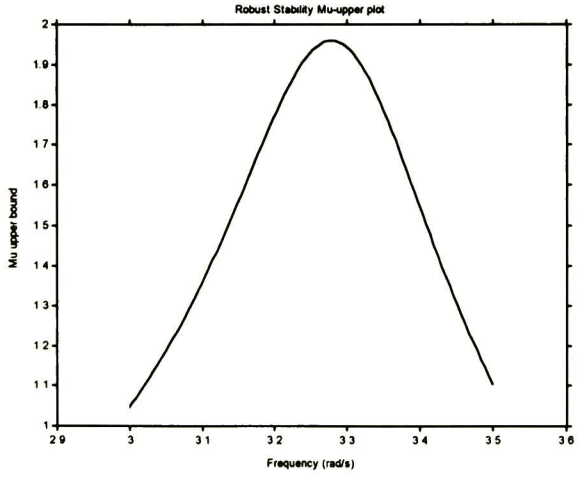

Figure 4.4. Robust stability μ plot for two varying parameters. Case study 3.

In order to validate our uncertainty modeling, we computed the exact value of reactance at which instability is detected.

Table 4.6 shows the estimated and exact equivalent reactance and power flow along with the eigenvalues calculated at the exact instability condition.

From the results summarized in Table 4.6, we see that the errors between the exact and estimated parameter are –7.6% for the tie-line reactance, $X_{tie-line}$, and -1.41% for the inter-area power flow. As emphasized in our previous simulations, the accuracy of the approximate eigenvalues is acceptable for any practical use, especially in view of the fact that the range of uncertainty is very high.

Table 4.6. Robust stability assessment – Case study 3

μ upper bound	1.9593
Estimated ω (rad/s)	3.2248
Exact ω (rad/s)	2.1798
Estimated (exact) $X_{tie-line}$ (p.u.)	**0.1868 (0.2010)**
Error (%)	*-7.6*
Estimated (exact) power flow (MW)	**417.8 (423.7)**
Error (%)	-1.41
Exact eigenvalue	0.0077± j2.1798 ζ = - 0.35 %

These results provide a useful numerical background for an analysis of more complex systems. The analysis is also relevant to the study of multiple uncertainties occurring simultaneously.

This issue is investigated in more detail in our numerical simulations and results in Chapter 5.

4.2. Application to a large scale system

To further illustrate the potential usefulness of the proposed method, we consider as a second example a 6-area model of the Mexican interconnected system (MIS). Figure 4.5 shows, schematically, a simplified representation of this system indicating the nature of the varying operating conditions considered in the studies. The study is based on a dynamic model of the MIS that includes the detailed representation of 377 generators, 3759 buses, 2936 branches and 1986 transformers. More details of this system and modeling considerations are given in Castellanos *et al.* [3].

The base case condition is the summer peak-load 2002; the overall state-space model of the system has 2250 states.

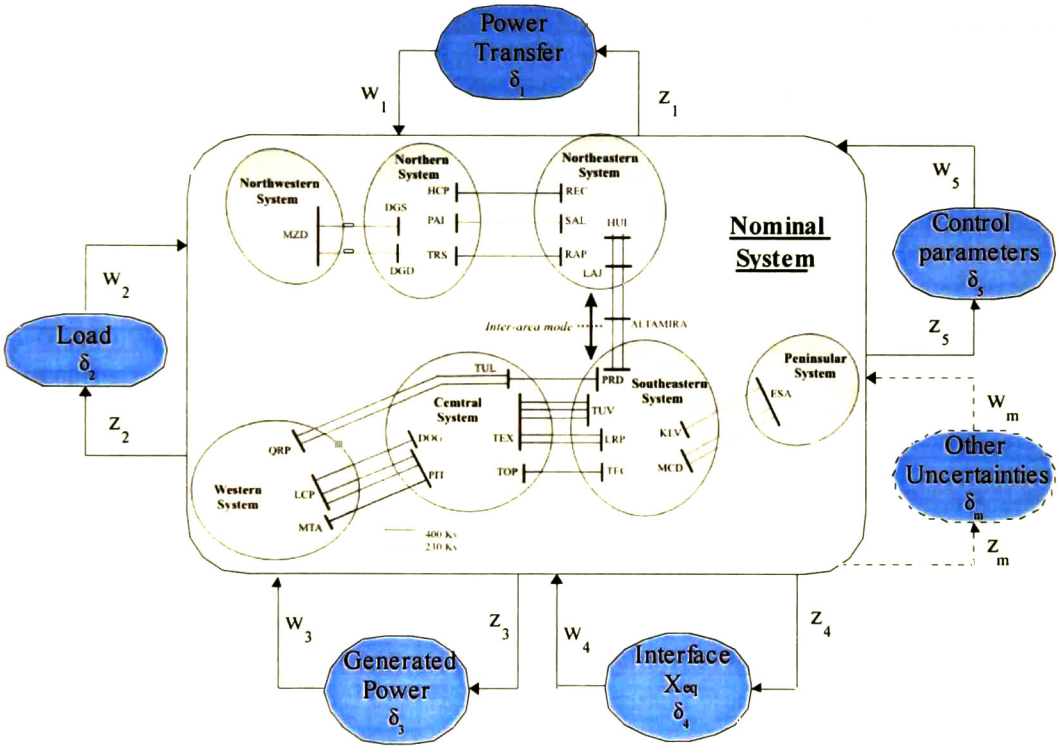

Figure 4.5. Simplified one-line diagram of the Mexican Interconnected System showing typical uncertain parameters

In this representation, 25 machines are equipped with PSSs. Further, loads are represented as 70% constant current and 30% constant impedance characteristics for both active and reactive power.

4.2.1. Small signal characteristics

The 6-area MIS model has a complex dynamic behavior involving the participation of several machines and their controllers spread out over a large geographical area. Table 4.7 summarizes the main characteristics of the slowest electromechanical modes showing their oscillation pattern and swing frequency.

Major factors contributing to low damping in the system include:

a) The use of high gain, high speed excitation systems without stabilizing feedback.
b) Operation of the power system with high power transfers over relatively weak interconnections.
c) Outages of major generation or delivery sources.
d) Topological changes due to contingencies or transmission paths taken out for maintenance.

Table 4.7. Critical inter-area modes of the 6-area MIS model

Mode description	Eigenvalue*	Freq. (Hz)	Swing pattern
Inter-area mode 1	-0.222±j 2.19	0.32	North systems vs. South systems
Inter-area mode 2	-0.028±j 3.28	0.52	Peninsular system vs. Western and Southeastern systems
Inter-area mode 3	-0.0466±j 3.906	0.62	Northern system vs. Northeastern system
Inter-area mode 4	-0.0814±j 4.960	0.78	Western system vs. Southeastern system
Mode 5	-0.1677±j 5.794	0.92	Local mode to the Northeastern system
Mode 6	-0.292±j 7.62	1.21	Local mode to the Peninsular system
Mode 7	-0.601±j 9.38	1.49	Local mode to the Southeastern system

*Real part in (1/s); imaginary part in (rad/s)

The study focuses on the analysis of the effects of varying parameters on the stability of the slowest modes in the MIS model.

Eigenvalue analysis of the MIS system identified four critical inter-area modes with damping ratios below 5%. Figure 4.6 gives a graphical interpretation of the oscillation process showing main regions and machines involved. To facilitate their identification, system modes are classified as inter-area modes indicating their geographical location.

Inter-area mode 1 involves machines in the north systems (North and Northeastern systems) swinging coherently against machines in the Center, Western, Southeastern and Peninsular systems of the MIS. This mode is referred to as the 0.32 Hz north-south inter-area mode 1.

Observability of inter-area mode 1 is high at machines in the North and Northeastern systems, namely the generators MTY, SYC, MZD, RIB and CBD and at the north-south interface. Consequently, adding power system stabilizers on these units might enhance damping of the 0.32 Hz inter-area mode 1.

The 0.52 Hz East-west mode 3, on the other hand, shows the interaction of machines located in the Western and Southeastern systems swinging against machines in the Peninsular system. The observability of the 0.52 Hz inter-area mode 3 appears primarily related to machines in the south systems and is hence highly observable in the tie-lines linking the Southeastern network with the Central and Western systems and the Peninsular system.

Also of concern, the 0.78 Hz Western–Southeastern inter-area mode involves machines in the Western system swinging against the machines in the Southeastern regions of the system. The high participation factors and mode shape of the DEL machines in the Western system (refer to Figure 4.6) suggest that adding supplementary controls on these units will produce a better dynamic performance on the system.

Other low-frequency electromechanical modes are in the MIS associated with more localized phenomena as discussed in our case studies.

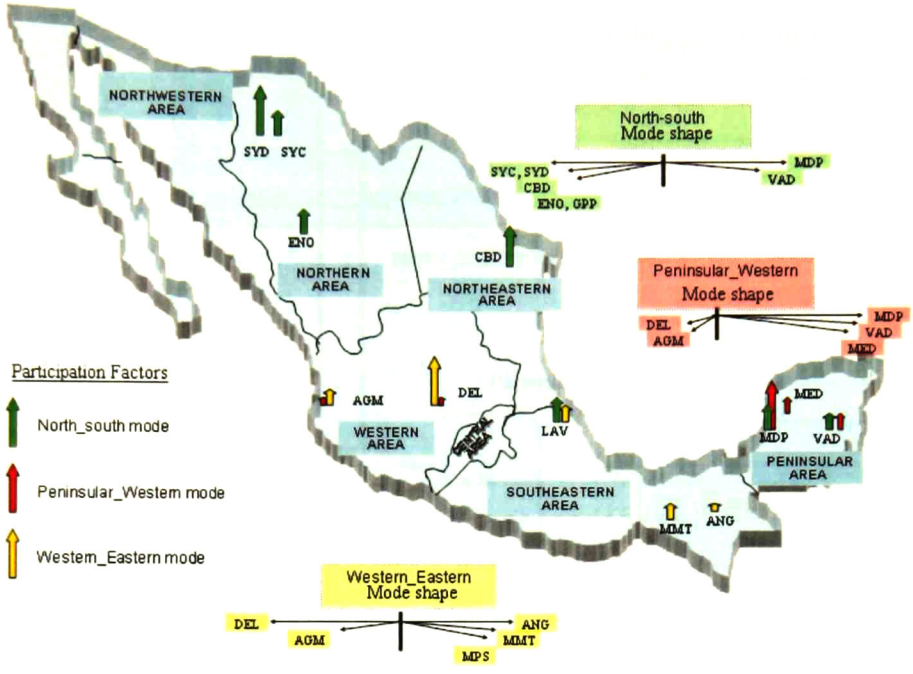

Figure 4.6. Participation factors and mode shape of critical inter-area modes

4.2.2. Test scenarios

Three critical system parameters were used to assess the influence of uncertainty of operating conditions on the nominal stability of the critical inter-area modes, namely the north-south power transfer LAJ-PRD 400 kV, the north-south intertie reactance, and the active power generated at Merida Dos (MDP) power station (refer to Figure 4.5). These operating conditions are known from previous studies to excite the slowest inter-area modes.

Figure 4.7 illustrates, schematically, the nature of the varying operating conditions considered in the studies. Among the several interconnections, the north-south tie-line GUE-PRD and the Peninsular-Southeastern interface (ESA-MCD) play a critical role on the damping of the two slowest inter-area modes. The weak nature of these interties poses a limit to power transfers between the north and south systems and east and west systems and is a major cause of the onset of low-frequency oscillations in the system.

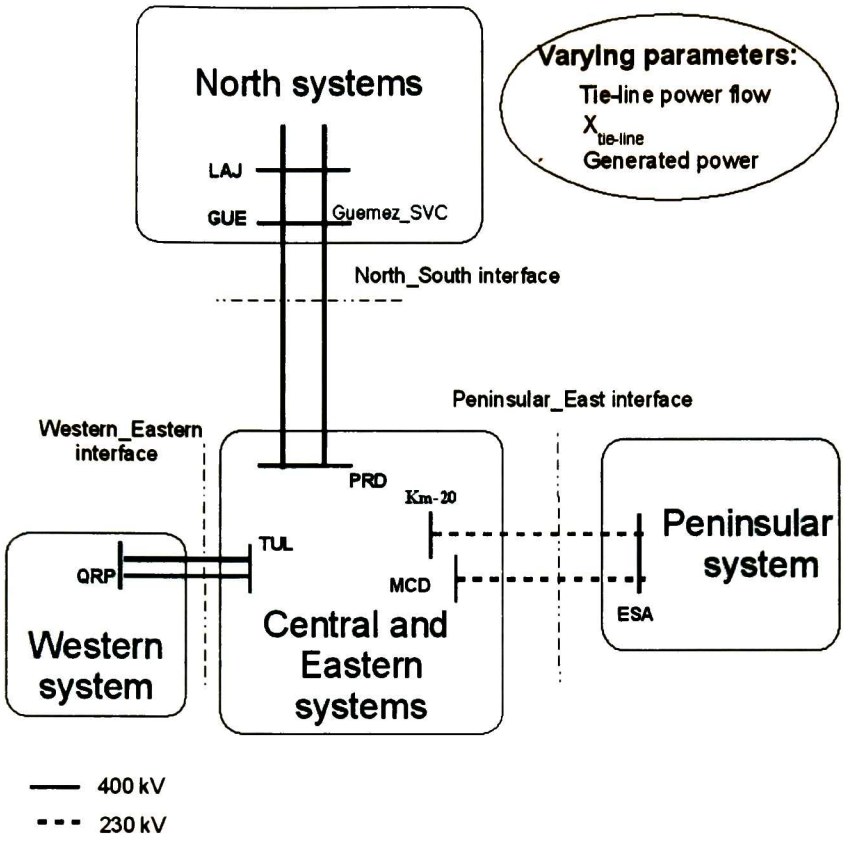

Figure 4.7. Schematic representation of several interfaces showing varying parameters used in the analysis

The next subsections describe a number of studies aimed at analyzing stability robustness with respect to real parameter variations. The validation is based on comparisons with results from conventional eigen-analysis using SSAT, a commercial small-signal stability software [4].

4.2.3. Robustness analysis; one parameter variation

4.2.3.1. Robust stability assessment of limiting tie-line reactance

In this study, the interconnecting tie-line reactance, $X_{tie-line}$ was allowed to vary in the range [0.03532 p.u.-0.07532 p.u.] representing, respectively, operating conditions with the two circuits of the 400 kV HUI-LAJ transmission line in service, and a stressed system

condition associated with the loss of one the circuits of the of the 400 kV HUI-LAJ transmission line (refer to Figure 4.7). The base-case (nominal) condition corresponds to 875 MW north-south intertie power transfer with all PSSs considered.

To determine the limiting condition, successive small-signal studies were conducted for increasing values of the tie-line reactance, $X_{tie-line}$, until an unstable condition was detected. Eigenvalues associated with the critical 0.33 Hz north-south inter-area mode 1 for different values of the interconnecting reactance are listed in Table 4.6. As expected from physical considerations, the analysis reveals that as the interconnecting reactance is increased, the damping ratio of the critical inter-area mode drops off rapidly. Note, however, that the conventional determination of the critical parameter comes at a high computational expense due to the large number of simulations required to estimate the stability limit.

Table 4.8. Damping of the 0.32 Hz north-south inter-area mode 1 as a function of the interconnecting tie-line reactance.

Tie-line reactance (pu)	Eigenvalue	Damping ratio (%)	Frequency (Hz)
0.03532	-0.3646±j 1.839	19.44	0.2928
0.05532	-0.1716±j 1.6313	10.46	0.2529
0.07532	-0. 0343± j 1.3801	2.48	0.2197

Based on these observations, the tie-line reactance, $X_{tie-line}$ was modeled as a structured uncertainty using the procedures developed in Chapter 3. In the study, a grid of operating conditions was determined from a parameter space of the form $\mathbf{p}_1 = [p_{11} \quad p_{12} \quad p_{13}]$, corresponding to various sections of the north-south interface out of service. The first value, p_{11}, corresponds to the normal operating condition with all circuits in service, whilst the second and third values, p_{12}, p_{13} correspond to the case with one and two circuits out of service, respectively. This basic approximation is found to yield accurate enough results.

From the μ plot in Figure 4.8, we can see that μ has a dominant peak at about 0.30 Hz, which is the 0.30 Hz north-south inter-area mode 1. The magnitude of the peak is greater than 1 suggesting that the system is unstable.

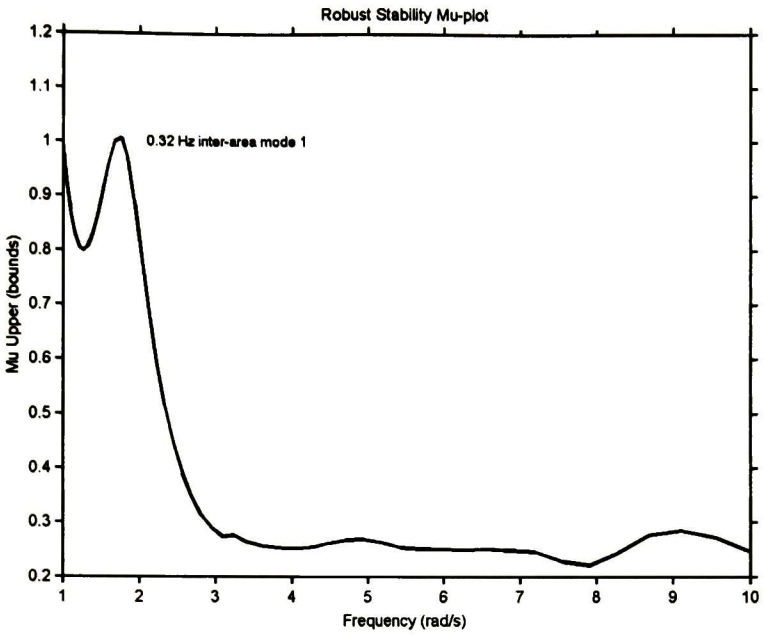

Figure 4.8. μ-upper bound for robust stability assessment of limiting tie-line reactance

Table 4.9 compares the exact tie-line reactance at which instability is detected, with the estimated reactance using μ-analysis. For reference and comparison, the eigenvalue calculated at the exact limiting condition using SSAT is also included. It can be seen that uncertainty analysis gives a good prediction of the highest limiting reactance. The error in the maximum reactance estimate is below 6 % indicating the accuracy of the proposed method. We remark that this case corresponds to nearly a 100% increase (variation) in the interconnecting tie-line reactance.

Table 4.9. Robust stability assessment of the limiting tie-line reactance case

μ upper bounds	1.0082
Estimated ω (rad/s)	1.7269
Estimated $X_{tie-line}$ (p.u.)	0.0752
Exact ω (rad/s)	1.3130
Exact $X_{tie-line}$ (p.u.)	0.0795
Exact eigenvalue	-0.0024± j1.3130 ζ = 0.19 %
Error (%)	- 5.72

4.2.3.2. Robust stability assessment of maximum power transfer

High southwards power transfers across the north-south interface are known from previous studies to strongly stimulate the 0.3 Hz north-south inter-area mode 1. To assess the limiting loading condition, the north-south power transfer level was varied from the low-stress operating condition (528 MW) to a stressed system condition with a high power flow representing the critical load transference (1171 MW). The base case (nominal) condition corresponds to a double circuit north-south inter-tie with all PSSs on; the nominal power transfer flow is 873 MW.

Several operating scenarios to stress the system are possible that result in decreased stability margins for the slowest inter-area mode. Among these alternatives, we favor the use of controllability-based scenarios since they enable to consider generation patterns that affect the mode of concern. To stress the system, the generation was increased in machines in the Northern and Northeastern systems determined from modal analysis. The generation at selected machines in the south systems was decreased accordingly to achieve a given level of power transfer across the north-south interface. The objective was to supply the demand in the Central system which is the main load center in the system.

Table 4.10 depicts the damping of the critical north-south inter-area mode as a function of the inter-tie power flow. The analysis reveals that the critical inter-area mode becomes unstable at a transfer level of about 1171 MW. The analysis of the μ-plot in Figure 4.9, on the other hand, shows two dominant peaks suggesting a more complex behavior; a peak at about 0.30 Hz associated with the critical inter-area mode 1 and a peak at about 0.81 Hz associated with the critical inter-area mode 3. The magnitude of the peak for the 0.3 Hz inter-area mode 1 and the 0.78 inter-area mode 4 is greater than 1 showing that the system is robustly unstable.

Table 4.10. Damping of the 0.32 Hz north-south inter-area mode 1 as a function of the southward power transfer

Power Flow (MW)	Eigenvalue	Damping ratio (%)	Frequency (Hz)
528	-0.3186±j 2.4635	12.83	0.3921
873	-0.2219±j 2.1906	10.08	0.3486
1171	0.0007± j1.9492	- 0.040	0.3102

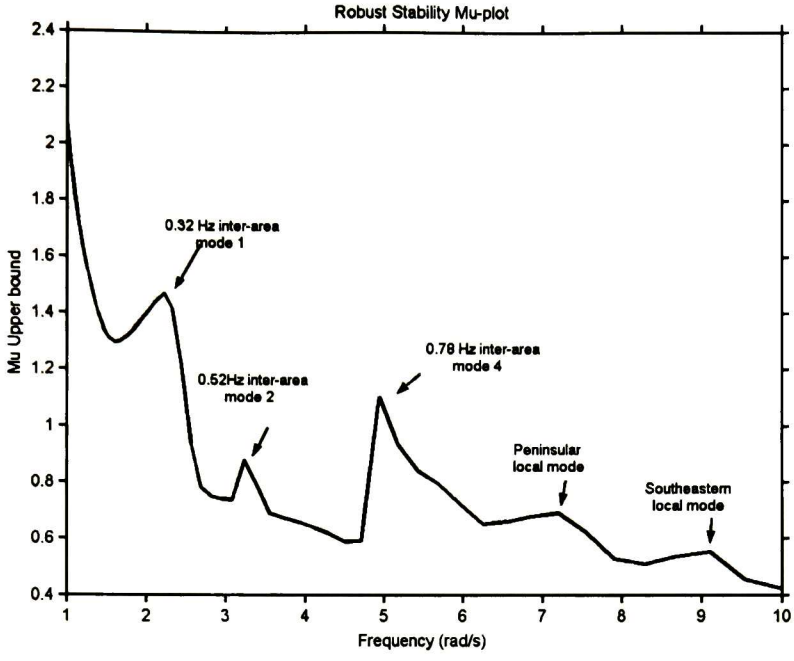

Figure 4.9. μ-upper bound for robust stability assessment of limiting transfer power

Table 4.11 shows the estimated and exact equivalent power flow along with the eigenvalue calculated at the exact power flow. By using μ-analysis, the limiting loading condition can be estimated with reasonable accuracy. As can be seen from Table 4.11, uncertainty analysis gives a good prediction of limiting loading conditions even for the most stringent operating conditions.

Table 4.11. Robust stability assessment of the limiting tie-line power case

μ upper bounds	1.4676
Estimated ω (rad/s)	2.2332
Estimated power flow (MW)	1,068.6
Exact ω (rad/s)	1.9492
Exact power flow (MW)	1160
Exact eigenvalue	-0.0069± j1.9591
	ζ = 0.35 %
Error (%)	-7.88

4.2.4. Robustness analysis; uncertainty in two parameter values

4.2.4.1. Modeling of parameter space

In the light of single uncertainty analysis in Chapter 2 and in an attempt to maximize the preciseness of the model, we extend our formulation to treat the effects of simultaneously varying parameters over an expected range of varying values. Again, we assume that upper and lower bounds on the parameter values are known and that simulation variations are uncorrelated.

To characterize uncertainty we selected a physically expected range (or forecasted values) of varying parameters. From this representation, the parameter space is then approximated using a few operating conditions. More specifically, we assume that each varying parameter can be described by the interval vectors

$$\mathbf{p}_1 = [p_{11} \quad p_{12} \cdots \quad p_{1ne}]$$

and

$$\mathbf{p}_2 = [p_{21} \quad p_{22} \cdots \quad p_{2ne}]$$

where *ne* is the number of interval parameters.

Figure 4.10 illustrates the process of generating a grid of operating conditions for the case of two varying parameters. As pointed out in Chapter 3, each point on the grid represents one steady-state operating condition characterized by the corresponding power flow solution, and defines a region of uncertainty in the parameter space.

For reasons to be described later in this document, the operating space is divided into regions or zones representing adequate levels of system performance. Chapter 5 describes in more detail the nature of robustness-based operating policies employed in this research to construct the admissible operating space.

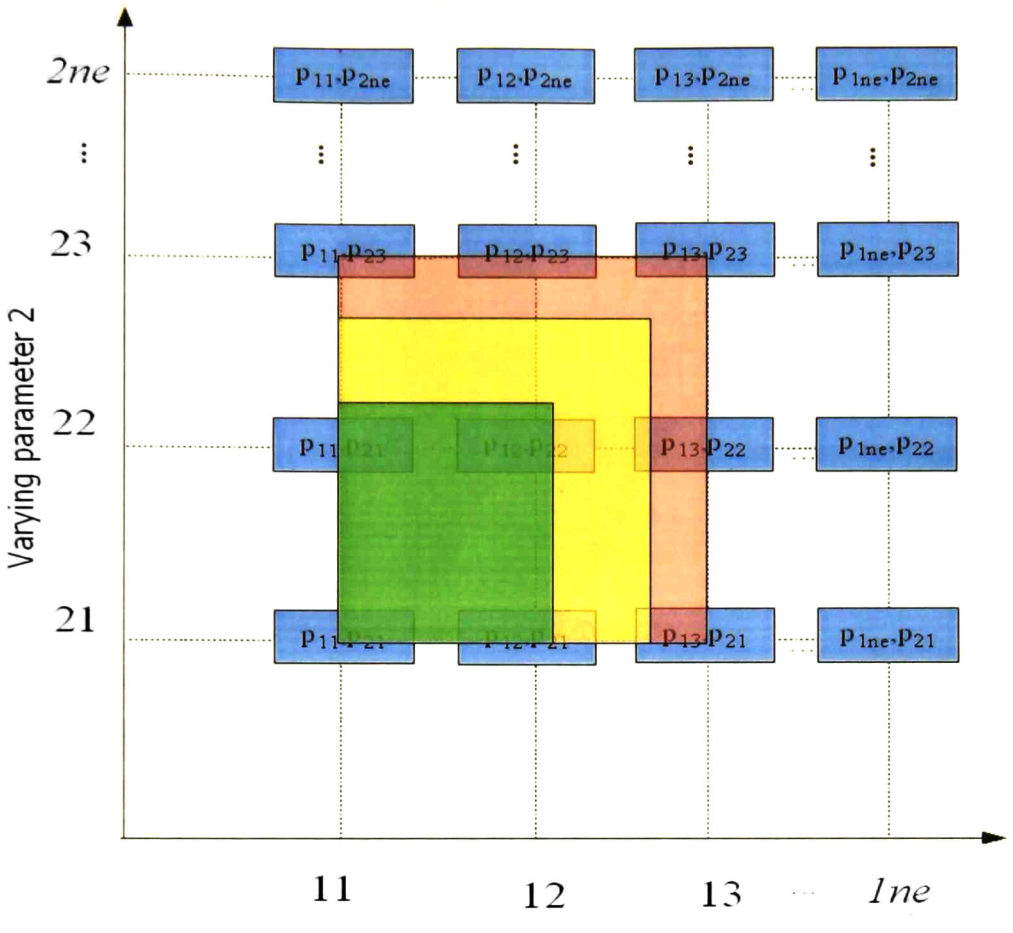

Figure 4.10. Grid density for two uncertainty sources

The extension of this approach to account for a larger number of variations of operating conditions is straightforward. Figure 4.11 shows a schematic diagram of the solution surface for the case of three varying parameters. For illustration, it is assumed that $n = 3$; this results in a tri-dimensional plot with 27 points. The assumed varying parameters produce several regions of uncertainty in $\mathbf{p}_i, \mathbf{p}_j$ planes which result in a range of uncertainty in the small signal stability margin.

Using the results of this analysis allows us to construct a solution surface in parameter space with the parameters varied systematically.

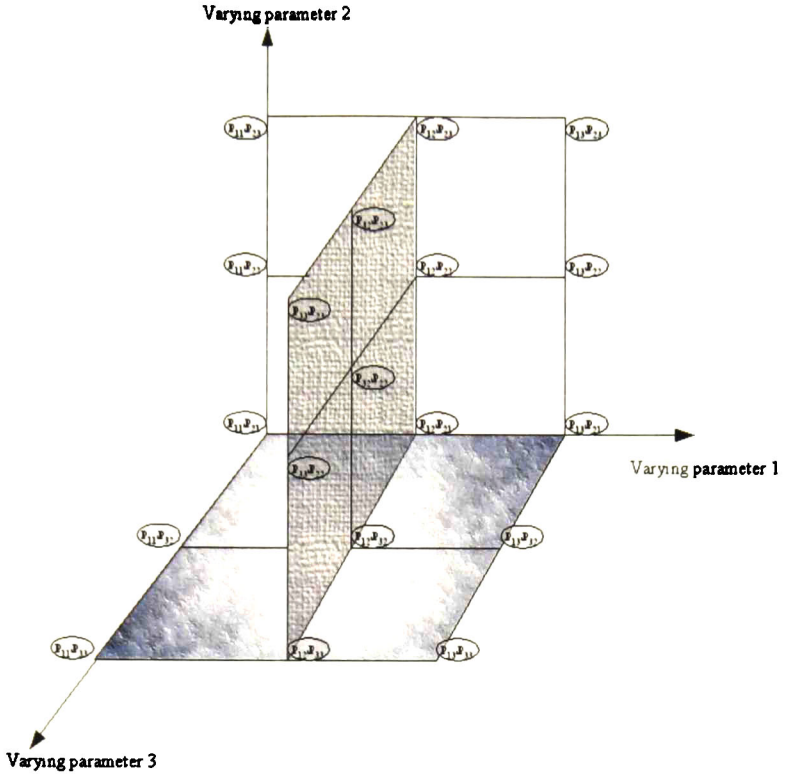

Figure 4.11. Schematic of the solution surface n_j, showing the region of uncertainty in three parameters, $\mathbf{p}_1, \mathbf{p}_2$, and $\mathbf{p}_3$.

Once the parameter space is defined, robustness analysis can be applied to determine robust stability margins. From the set of solutions a number of quantities can be derived which may be compared directly with available small signal stability. This approach allows us to more precisely evaluate the dynamic behavior of power systems in which multiples uncertainties occur simultaneously.

4.2.4.2. Robust stability assessment of simultaneous varying parameters

This study examines robustness to simultaneous variations in the north-south power flow and the Peninsular-Southeastern interface flow. At the nominal operating condition, the power flows are predominantly from the north systems to the south systems and from the Peninsular system to the Southeastern system [5]. Increased power flow on these interties (high stress conditions) reduces the stability margins of inter-area modes 1 and 2 as shown in Figure 4.12. To increase the transfer capabilities of these interfaces, PSSs were added at Merida unit U3, and at Carbon Dos units U1-U3.

Table 4.12 gives the damping ratios and frequency of oscillation of these oscillation modes as a function of the north-south power flow intertie and the generated active power at Merida station whilst Figure 4.12 shows the oscillation modes as a function of the north-south interface power transfer and the active power generation at MDP power station for two scenarios: the normal (nominal) base case condition (528, 583 MW) and a high-stress condition (1170, 727 MW) obtained by increasing the north-south power transfer and the generation at MDP. The results from these studies show that both, the 0.32 Hz inter-area mode 1 and the 0.52 Hz inter-area mode 2 become unstable at the highly stressed condition.

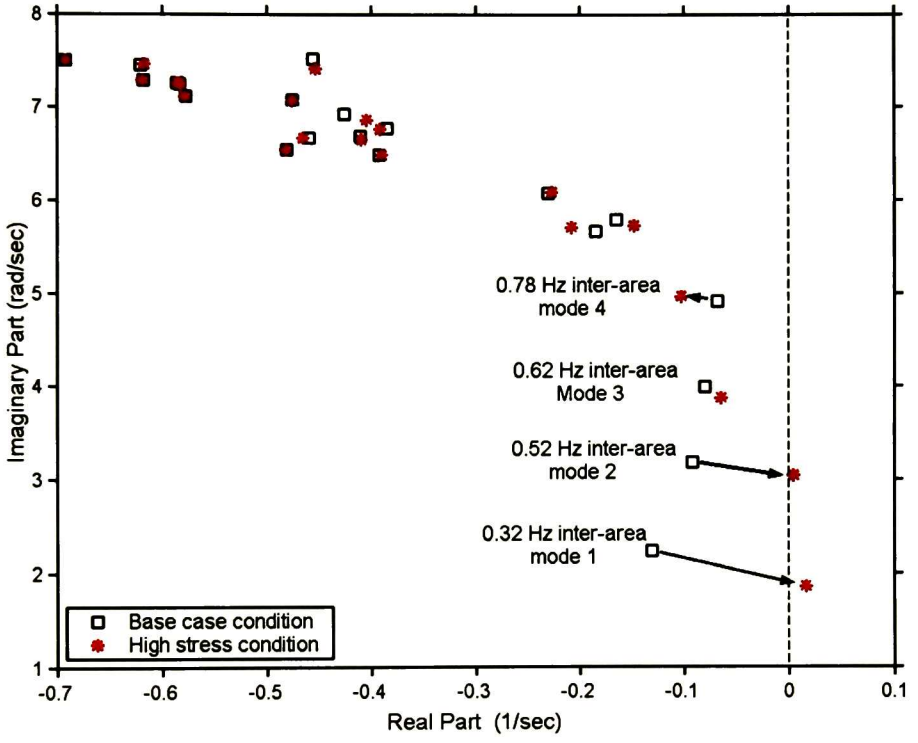

Figure 4.12. Plot of critical inter-area modes for the base case and the high-stress conditions

The analysis of the μ plot in Figure 4.13, on the other hand, shows two dominant peaks; a peak at about 2.2 rad/s associated with the 0.32 Hz inter-area mode 1 and a peak at about 3.10 rad/s associated with the 0.52 Hz inter-area mode 2 thus confirming the accuracy of the analysis.

Table 4.12. Effect of two parameter variation on the damping and frequency of inter-area modes

North-south Power transfer (MW)	*Active power generation at Merida power station (MW)*		
	583	*682*	*727*
528	**0.3555 Hz** **ζ = 5.87 %** *0.5062 Hz* *ζ = 2.89 %*	**0.3547 Hz** **ζ = 5.56 %** *0.4918 Hz* *ζ = 1.04 %*	**0.3543 Hz** **ζ = 5.39 %** *0.4840 Hz* *ζ = 0.25 %*
873	**0.3291 Hz** **ζ = 4.79 %** *0.5071 Hz* *ζ = 2.90 %*	**0.3286 Hz** **ζ = 4.54 %** *0.4924 Hz* *ζ = 0.95 %*	**0.3283 Hz** **ζ = 4.41 %** *0.4839 Hz* *ζ = 0.02 %*
1170	**0.2962 Hz** **ζ = -0.62 %** *0.5072 Hz* *ζ = 2.89 %*	**0.2958 Hz** **ζ = -0.78 %** *0.4922 Hz* *ζ = 0.85 %*	**0.2957 Hz** **ζ = -0.87 %** *0.4835 Hz* *ζ = -0.14 %*

The robust stability analysis procedures indicated in chapter 3 were used to account for simultaneous uncertainty. Variations in the north-south intertie power flow and the active generated power at Merida station over a wide range of operating conditions were represented as LFT based parametric uncertainty descriptions. For our computations, μ-analysis tests were performed for the worst case operating condition. The analysis of upper bound in Figure 4.13 shows in both cases a peak larger than one suggesting that the system is unstable. The 0.52 Hz mode 2 shows a higher μ-upper value than the 0.32 Hz mode 1 indicating that the peninsular mode has a more critical behavior than the north-south inter-area mode under the two simultaneous varying parameter ranges under study.

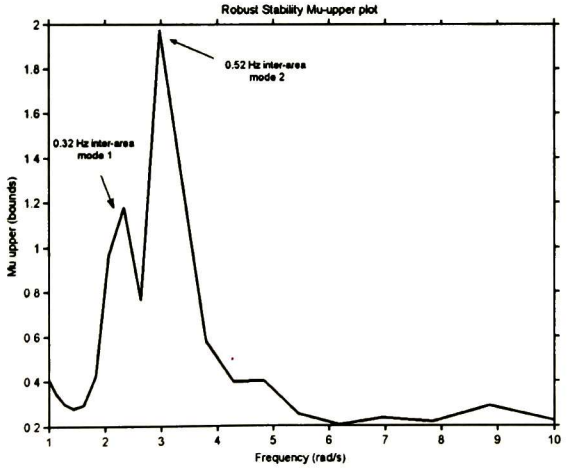

Figure 4.13. μ upper bounds of two simultaneous varying parameters

Table 4.13 shows the estimated and exact equivalent reactance and power flow along with the eigenvalue calculated at the exact parameter. Again, the results are in good agreement with conventional eigenanalysis showing the correctness of the developed procedures.

Table 4.13. Robust stability assessment

μ upper bounds	1.5304, 3.7075
Estimated ω (rad/s)	2.223, 3.102
Exact ω (rad/s)	2.063, 3.040
Estimated (exact) active power at Merida station (MW)	**674 (727)**
Error (%)	*- 7.8*
Estimated (exact) North-South power transfer (MW)	**936 (900)**
Error (%)	*4.0*

4.2.5. Relative importance of simultaneous real uncertainties

A major difficulty in analyzing the effects of simultaneously varying parameters over a range of values is identifying which source of uncertainty is driving any error in model predictions. The complexity and size of conventional approaches make it expensive and difficult to assess the effects of the uncertainties in the predicted stability margins. To more clearly analyze the nature of this problem, conventional linear analysis studies were conducted to validate robust analysis results.

Table 4.14 shows the damping ratio and oscillation frequency of the 0.32 Hz inter-area mode 1 and the 0.78 Hz inter-area mode 4 for the case of two uncertain parameters varying simultaneously. It is clear from Table 4.14, that increasing the north-south power flow the damping ratio of the 0.32 Hz mode is reduced to values near to stability limit and the damping of the 0.78 Hz mode is reduced lightly. On the other hand, increasing the generation of power in the western region destabilizes the 0.78 Hz mode and also, reduces lightly the small signal stability of the 0.32 Hz mode.

A key observation is that, with increased generation in the western region and high north-south power transfer levels, both the 0.32 Hz and the 0.78 Hz modes become unstable. One pertinent question is determining the robust stability condition.

This has several major implications: (*i*) the net system (average) effect is unknown, and (*ii*) using conventional analysis, it is difficult to estimate operating ranges over which the system will satisfy desired operating criteria. Further, determining the worst-case condition under which both modes become unstable is difficult and costly.

Table 4.14. Damping ratio and frequency of the 0.32Hz and 0.78 Hz interarea modes

North-south intertie power flow (MW), 0.32 Hz mode	*Generated Power (MW) in the Western area, 0.78 Hz mode*		
	6043	*6208*	*6298*
530	**0.3565 Hz** **ζ = 7.21 %** *0.7842 Hz* *ζ = 5.20 %*	**0.3565 Hz** **ζ = 7.21 %** *0.7690 Hz* *ζ = 3.65 %*	**0.3557 Hz** **ζ = 7.02 %** *0.6843Hz* *ζ = -0.41 %*
870	**0.3229 HZ** **ζ = 6.26 %** *0.7811 Hz* *ζ = 5.04 %*	**0.3289 Hz** **ζ = 6.21 %** *0.7655 Hz* *ζ = 3.57 %*	**0.3284 Hz** **ζ = 5.96 %** *0.6208 Hz* *ζ = -0.67 %*
1170	**0.2951 Hz** **ζ = 0.83 %** *0.7912 Hz* *ζ = 5.12 %*	**0.2947 Hz** **ζ = 0.73 %** *0.7710 Hz* *ζ = 3.41 %*	**0.2945Hz** **ζ = 0.49 %** *0.6784 Hz* *ζ = -1.08 %*
1202	**0.2910 Hz** **ζ = 0.40 %** *0.7760 Hz* *ζ = 4.87 %*	**0.2906 Hz** **ζ = 0.08 %** *0.7617 Hz* *ζ = 3.38 %*	**0.2909 Hz** **ζ = -0.12 %** *0.6549Hz* *ζ = -1.93 %*

The analysis of the μ plot in Figure 4.14 shows a significant peak near 2.1 rad/s revealing the presence of the 0.32 Hz inter-area mode 1, and a peak at about 3.10 rad/s associated with the 0.52 Hz inter-area mode 2. Moreover, the plot shows relatively smaller peaks at 4.0 rad/s associated with the 0.62 Hz inter-area mode 3, 4.9 rad/s associated with the 0.78 Hz inter-area mode 4, a peak and at 5.8 rad/s associated with the 0.92 Hz Northeastern local mode in addition to a larger peak at about 8.8 rad/s associated with the 1.4 Hz southeastern local mode.

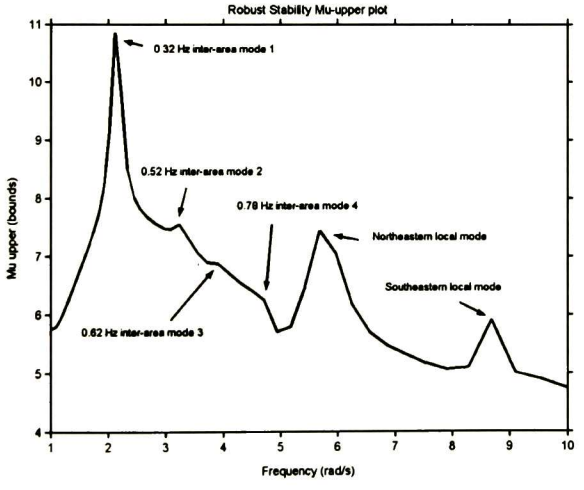

Figure 4.14. μ -upper bounds with two simultaneous varying parameters

Figure 4.15 compares the μ-upper bounds for various selections of uncertainty in the active power generated in the Western system and various levels of transfers in the north-south intertie. The selected operating space is [6043 MW, 6208 MW, and 6298 MW] while the selected power flows across the north-south inter-tie are; *a)* 530 MW, *b)* 870 MW, *c)* 1170 MW, *d)* 1200 MW.

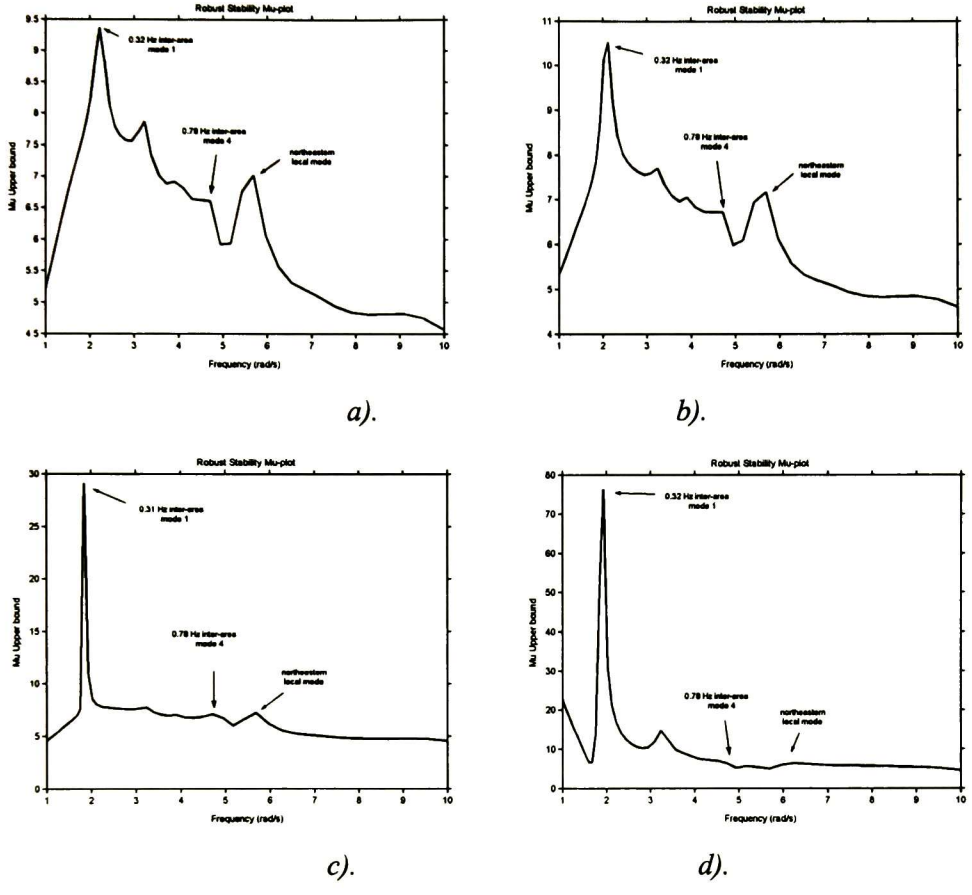

Figure 4.15. μ-upper bounds for the case of single parameter uncertainty. Active power generation in the Western system and several north-south power flows; a) 530 MW, b)870 MW, c) 1170 MW and d)1200 MW

From these plots it can be observed that, cases a) and b) exhibit a similar behavior to the case of two varying parameters (refer to figure 4.14) except for the southeastern local mode which is not showing as a good defined peak. On the other hand, cases c) and d) show a dominant peak of the 0.32 Hz inter-area mode indicating that this mode has the highest

relative importance. In all cases, the 0.32 Hz inter-area mode has the highest μ-upper values indicating a dominant behavior of the power system.

Also of interest, Figure 4.16 shows μ-upper bounds for the case in which the north-south power flow is modeled as an uncertainty (the grid of operating points is given by the interval vector [870 MW, 1170 MW, and 1200 MW] and the robust analysis is computed for three conditions of active power generated in the Western system: *a)* 6043 MW, *b)* 6208 MW and *c)* 6298 MW.

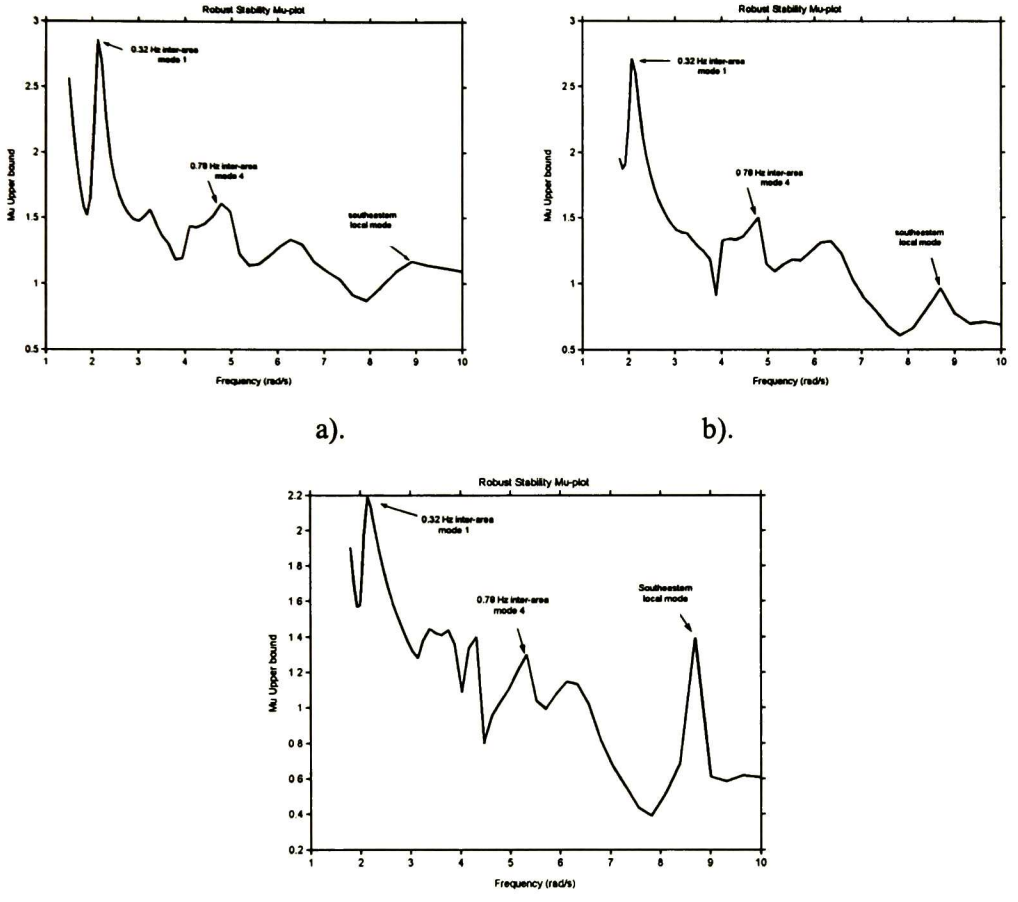

Figure 4.16. μ _upper plots using the north-south power flow as varying parameter with entries range of the 0.78 Hz mode: a) 6043 MW active power generated in the Western system, b) 6208 MW active power generated in the Western system, c) 6298 MW active power generated in the Western system

One notes that increasing the active power in the Western system results in a more energetic participation of the 0.78 Hz inter-area mode and the southeastern local mode in the observed plot. Comparing with Figure 4.14 we see that the 0.32 Hz inter-area mode has the highest μ-upper values but its magnitude is smaller that that obtained for the case of two varying parameters case. Increasing the generated power in the Western system, the μ-upper value of the 0.32 Hz inter-area mode is slightly reduced.

In all results, the 0.32 Hz inter-area mode has the highest μ-upper value indicating a dominant behavior in the power system performance. Thus for instance, in the case of two simultaneous varying parameters the north-south power flow (0.32 Hz inter-area mode) shows a higher relative importance than the Western generated power (0.78 Hz inter-area mode).

4.2.6. Assessment of error sources

Several sources of error can influence the robust stability accuracy. In this section we examine the accuracy and efficiency of robustness analysis by comparing its solutions with the solutions obtained from conventional eigenanalysis.

To illustrate model verification for a typical uncertainty scenario, numerical studies were applied. A crucial parameter in model validation is the number of points in the parameter space to be considered in the analysis. A series of tests was conducted to evaluate the desired number of entries in the operating space. To draw meaningful conclusions from this analysis the damping ratio of the 0.32 Hz mode was computed for various network configurations. Table 4.15 shows the damping ratio and frequency of the 0.32 Hz mode obtained for different north-south intertie reactance values.

Table 4.15. Damping ratio and frequency of 0.32 Hz north-south inter-area mode

Case description	Xeq (pu)	Damping ratio (%)	Frequency (Hz)
1	0.035	19.44	0.2928
2	0.055	10.46	0.2529
3	0.075	2.48	0.2197
4	0.085	- 4.40	0.1916

Table 4.16 compares robust stability simulation results for the case of one varying parameter for various combinations of operating conditions (range entries). Specifically, each operating space takes into account three entries [3].

Analytical predictions in Table 4.16 indicate that inappropriate strategies can result in poor estimate of the limiting operating condition. Simulation results show that straightforward application of the proposed method may result in conflicting estimates when the range entries are changed. Furthermore, small signal analysis and interpretation are highly sensitive to the introduction of uncertainty. In addition, the selection of a given operating range influences the number of varying elements of the system matrix **A** that vary with changing operating conditions, and hence the computational effort.

Table 4.16. Robustness analysis with one varying parameter as a function of the uncertain parameter range

	Range of parameter uncertainty			
	[0.035 0.055 0.075] 1,2,3	[0.035 0.055 0.085] 1,2,4	[0.035 0.075 0.085] 1,3,4	[0.055 0.075 0.085] 2,3,4
Number of varying coefficients of the state matrix [A]	1551	1551	3020	1278
μ upper bound	1.0079	1.2218	2.825	1.893
Estimated ω (rad/s)	1.727	1.768	1.768	1.600
Estimated (exact) interface reactance (pu)	0.0752 (0.0795)	0.0808 (0.0795)	0.0692 (0.0795)	0.0782 (0.0795)
Error (%)	- 5.45	1.61	-12.99	- 1.58

Robustness analysis using three parameters can successfully identify the unstable modes and the worst case scenarios with relative accuracy. However, if higher accuracy is required, the basic technique should be modified.

From the analysis above we suggest that:

- In the absence of reliable estimates for the operating condition we can obtain a rough estimate for the parameter space based on a few (i.e. three) operating conditions. To select one entry associated with an operating condition near the onset

of small signal instability. The case with an error equal to -12.99 % considers two operating conditions near of the onset of dynamic instability.

- A better estimate of the stability margin can be obtained by using a larger number of entries.

4.2.7. Computational aspects

Of fundamental importance to the practical application of the proposed methodology are the computational requirements of the method. Table 4.17 shows the CPU time required for robust stability analysis of the power transfer limit for the north-south corridor. The software is executed using an IBM-PC (Pentium IV/1.5 GHz).

Table 4.17. CPU time requirements for robust stability analysis of the maximum exporting power case

Activities	CPU time (seconds)	% of total time
Computation of state matrices **A**	2010	53
μ analysis functions	857	23
Other functions	930	24
Total CPU time	3797	100

In this study, computation of the state representation for the three operating conditions in Table 4.17 takes about 2010 s. In addition, the time spent on frequency response analysis, and μ-analysis is 857 s whereas the time spent on computing other activities is about 930s, namely the identification of varying coefficients, polynomial fitting and the computation of matrix **M**. The total time to assess the limiting loading condition is 3797 s. We remark, that CPU times may vary according to the characteristics of the study system, system conditions and selected criteria for robust stability assessment.

Of particular relevance, the computational effort to assess the limiting condition of the Mexican system is equivalent to 5 small signal stability simulations using SSAT. It should be emphasized, however, that determining the exact instability condition using conventional small signal analysis may require many simulations depending on the knowledge of the system and the expertise of the analyst. This is particularly true in the case of simultaneous uncertainties occurring simultaneously.

The analysis shows that the computational burden and memory requirements for μ-analysis are reasonable for the analysis of realistic power systems. CPU time requirements appear to compare favorably with those reported in the literature [6] but the nature of test systems used in these studies prevents direct comparison between these approaches.

4.2.8. Model validation

Detailed time domain simulations have been undertaken to validate system results. The stability data used for these studies includes detailed representations of limiters and other nonlinearities.

Figure 4.17 shows the time domain response of unit # 1 of machine Carbon Dos located in the Northeastern network of the system following outage of the unit no. 1 (650 MW) of the Laguna Verde nuclear power station, as a function of the north-south reactance. This contingency is known from previous studies to strongly excite the 0.32 Hz inter-area mode 1.

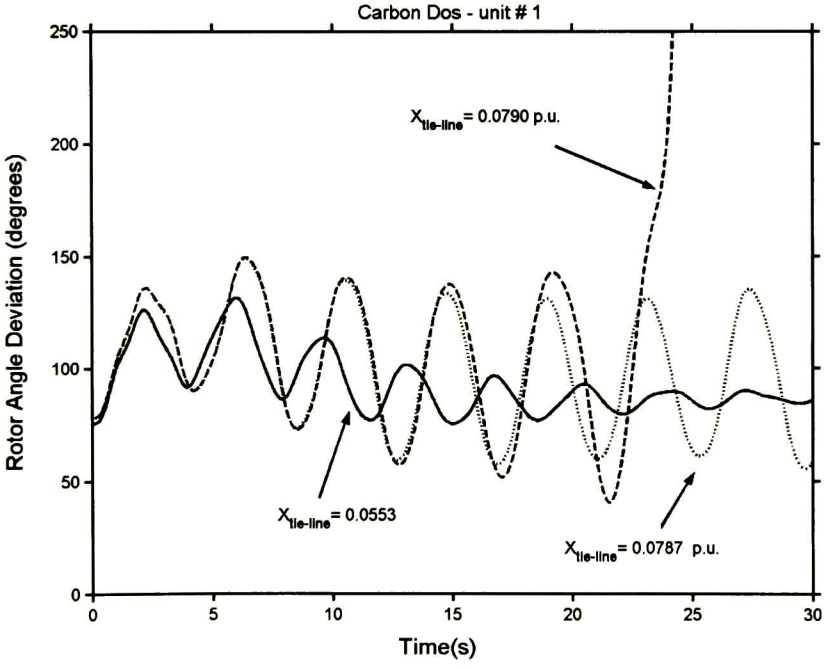

Figure 4.17. Time response of unit # 1 of Carbon Dos thermal power station for various levels of interconnecting reactance

Simulation results agree very well with the determination of small signal stability margins. As shown, the stability limit is close to $X_{tie-line} = 0.0787 p.u.$ in close agreement with small signal stability results in Tables 4.8 and 4.9. Fourier analysis on the other hand (not shown) enables to confirm that the dominant component is the 0.32 Hz inter-area mode 1 as suggested from conventional eigen-analysis.

4.3. Discussion

In this chapter, the proposed analysis technique has been used for stability assessment of two realistic power networks. Simulation results show that the proposed method yields accurate results when compared to corresponding small signal stability analysis and results in reduced computational complexity. Additional applications of robustness analysis hold particular promise for the simultaneous analysis of key varying parameters on nominal stability.

Study experience indicates that the proposed method can accurately be used to assess robust stability of large complex systems; the results of the analysis are seen to correspond closely with the evaluation of small signal stability margins using conventional eigenanalysis. Differences that do exist warrant additional investigation. The analysis shows that small signal analysis and interpretation are highly sensitive to the introduction of uncertainty.

From the results of robust stability analysis, the following general conclusions can be drawn:

a) In all practical cases analyzed, the error estimates remain within 7% of the exact stability limits obtained by conventional small signal analysis. In many cases, however, accuracy in the order of 2-3% was obtained.

b) The fundamental principles of the analytical procedures for stability assessment can be applied to the case in which multiple simultaneous uncertainties are present simultaneously. This is an aspect that deserves further investigation and has not explored in depth here.

c) The present software is suitable for analysis of realistic power networks.

References

[1] M. Klein, G.J. Rogers, and P. Kundur, "A fundamental study of inter-area oscillations in power systems", *IEEE Transactions on Power Systems*, vol. 6, no. 3, August 1991, pp. 914-921.

[2] M. Klein, G. J. Rogers, S. Moorty, P. Kundur, "Analytical investigation of factors influencing power system stabilizers performance", *IEEE Transactions on Energy Conversion*, vol.7, no. 3, September 1992, pp. 382-390.

[3] R. Castellanos, A. R. Messina, H. Sarmiento, "Robust stability analysis of large power systems using the structured singular value theory", *International Journal of Electrical Power and Energy Systems*, vol. 27, no. 3, June 2005, pp. 389-397.

[4] Powertech Labs Inc. "Small Signal Analysis Tool, SSAT", Version 2.1, 2002.

[5] H. G. Sarmiento, R. Castellanos, G. Villa, Aplicación de PSS y TCSC para incrementar la capacidad de transferencia Norte-Sur del Sistema Eléctrico Interconectado Mexicano", (in Spanish), paper CE-C2-28, in: *Tercera reunión Bienal CIGRE*, Irapuato, Gto. MEX, June 2003, pp.1-8.

[6] M. Djukanovic, M. Khammash, V. Vittal, "Application of the structured singular value theory for robust stability and control analysis in multimachine power systems, Parts I and II", *IEEE Transactions on Power Systems*, vol. 13, no. 4, November 1998, pp. 1311-1322.

Chapter 5

Dynamic Security Assessment under Severe Uncertainty

Power system dynamic behavior is becoming more complex and variable. Successful analysis and control of uncertain system behavior requires mathematical tools that are adaptable to the large change of system parameters. Understanding the uncertainties in these parameters and how the uncertainties affect dynamic security, is important in determining the validity of the nominal system model and the development of robustness-based control actions.

Past work on uncertainty modeling has focused primarily on the analysis of single uncertainty in the operation of power systems. In complex systems, however, simultaneous uncertainty estimation is a major concern. A common practice in recent analytical work utilizing robust stability has been to assume that the sources of uncertainty are independent. Such considerations may result in incomplete and often unreliable small signal stability characterization, especially in the study of inter-area oscillations in which variations in operating conditions or control action at various locations in the system may have an interacting effect on the critical modes.

This chapter discusses the development and application of near, real-time uncertainty-based control policies to the problem of evaluating dynamic security assessment in the presence of severe uncertainty in operating conditions. A general formulation for characterizing the effect of simultaneous variations of operating conditions on robust stability is presented. Robustness evaluation techniques are then used to produce on-line preventive and emergency control actions. Such improvements are required for analysis of large-scale uncertain systems, which have large numbers of uncertain parameters.

The efficiency and accuracy of the method is demonstrated by comparisons to detailed conventional eigen-analysis.

5.1. Study focus

Robustness analysis studies of the system in Chapter 4 identified critical transfer limits between areas imposed by low-frequency oscillations. Current operational practices rely on determining the damping ratio of critical modes under a heavily stressed condition. This approach may be very conservative since many uncertainties have to be considered simultaneously.

In the present investigation, we discuss the applicability of robustness analysis for deriving uncertainty-based control polices under severe uncertainty in operating conditions. The objective is to determine worst-case scenarios from which preventive control procedures for dynamic security assessment can be applied to control these modes and to examine how these sources of uncertainty affect the ability of the proposed techniques to forecast and manage large parameter variations. Another related objective is the development of near real-time robustness-based control policies for dynamic security assessment and control.

In this analysis, two critical system parameters were used to assess the influence of uncertainty of operating conditions on the nominal stability of major inter-area modes, namely the power transfer across the Peninsular-Southeastern interface and the power transfer across the North-South interconnection. These operating conditions are known from previous studies to excite the slowest inter-area modes. Models are developed in order to understand the effects of variations in the power transfer levels across these critical interfaces, on the stability of critical modes of the system for various control alternatives.

The analysis consists of three parts. In the first part, the analysis of single uncertainty is used to introduce the need for uncertainty-based control strategies. In the second part, μ-analysis is used to predict the effects of simultaneous uncertainties on small signal stability estimates. Finally, a robustness-based control policy for on-line stability assessment and control is proposed and issues concerning the practical implementation of the method and numerical calculations are discussed.

5.2. The Peninsular-Southeastern interface

The first interface of concern is the East-West interconnection linking the Peninsular system to the Mexican interconnected system. The weak nature of this interconnection

poses a limit to power transfers between the Peninsular and the Southeastern systems and is a major cause of the onset of low frequency oscillations involving two major inter-area modes and a local mode.

Because of its complexity, this system exhibits various sources of significant uncertainty. Figure 5.1 provides a simplified representation of the Peninsular system showing major interfaces, and the most important generating plants. For the case under study, the system has a total load of 980 MW and total generation capacity of 1180 MW.

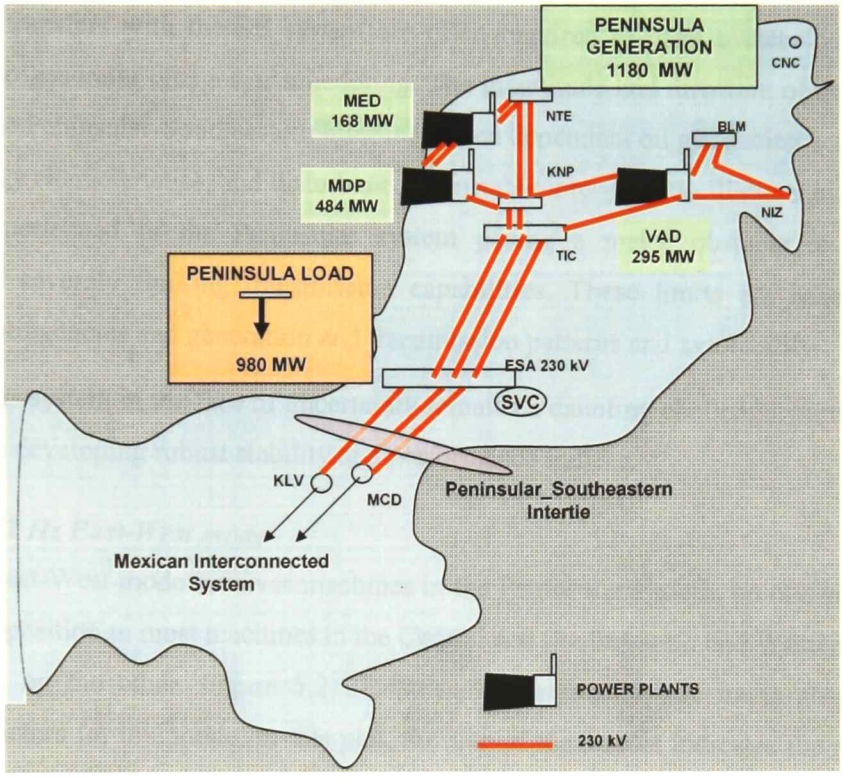

Figure 5.1. Schematic representation of the Peninsular-Southeastern interfaces

The most important load center is located in the Cancun (CNC) zone with a demand of 300 MW. The average demand of the MIS increases annually at a rate of about 5.2%. By contrast, the rate of load growth in the Peninsular system is about 6.6 %.

Paramount to system operation, the most important power station in the region is the Merida (MDP) power station with a capacity of 484 MW. The MDP power station is a

multi-shaft combined-cycle plant, which consists of two gas turbines and one steam turbine. Generation from central Merida region is transmitted over large distances to load centers in the southeastern and central networks of the MIS through the 230 kV tie-line Escarcega-Macuspana as can be appreciated from Figure 5.1. Dynamic voltage support within the study system is provided by a large SVC at the Escarcega (ESA-230) switching station, a major transmission substation located nearly at the centre of the Peninsular-Southeastern interconnection. The Escarcega SVC has a nominal capacity of +300, -90 MVAR. No supplemental modulation controls are presently used in the SVC.

High power transfers with the SE system are often required to meet system needs, for instance due to generator outages or scheduling. The magnitude and direction of the power flow across the Peninsular-Southeastern intertie is often dependent on generation schedules, seasonal energy characteristics, and disturbances. Unstable inter-area oscillations have been frequently experienced in the Peninsular system posing a major obstacle to normal operation and severely limiting transmission capabilities. These limits are based on a number of contingencies and generation and transmission patterns and availability.

Controlling this system in the face of uncertainty remains a daunting challenge, particularly with respect to developing robust stability and performance indices.

5.2.1. The 0.52 Hz East-West mode

The 0.52 Hz East-West mode involves machines in the Peninsular system, on one extreme, swinging in opposition to most machines in the Central and Southeastern and Western areas of the system, on the other. Figure 5.2 illustrates, schematically, the mode shape and participation factors for this mode. In this plot, the size of the arrows indicates the relative participation of a machine in the inter-area mode.

It is seen in Figure 5.2 that the maximum contributions occur in the Western and Peninsular systems. The relative contribution of the MDP and Valladolid (VAD) machines in the Peninsular system to the 0.52 Hz inter-area mode 2 suggests that adding supplementary controls on these units would produce a better dynamic performance on the system. Because of their relative size, however, outage of these units may result in unstable operating conditions thus adding to the overall complexity of the problem. This makes the assessment of small signal stability margins in this system, a complex problem.

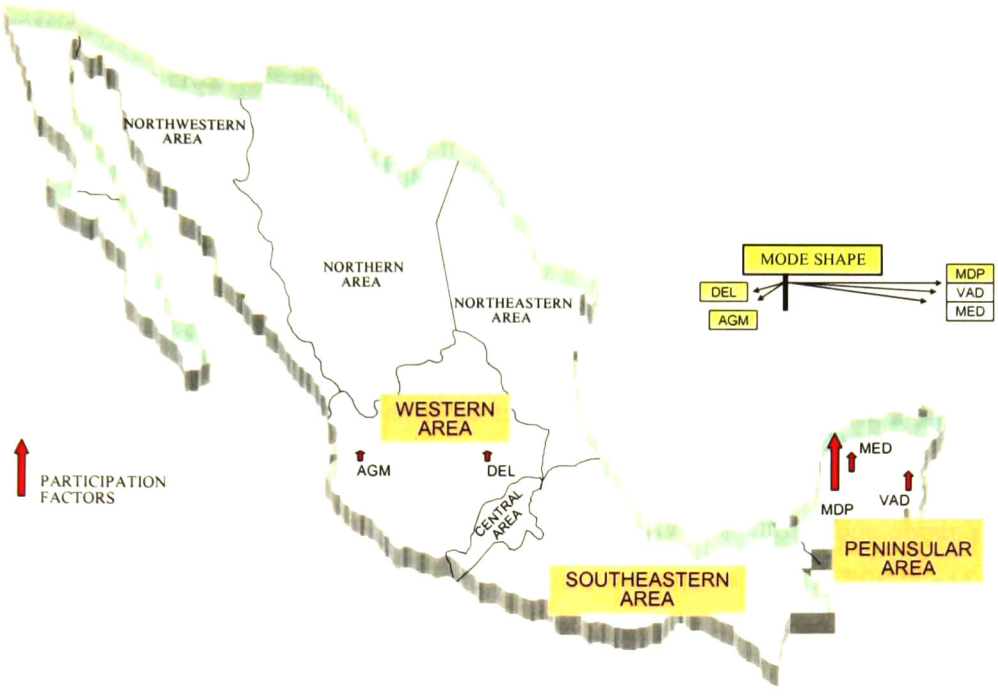

Figure 5.2. Participation factors and mode shape for the 0.52 Hz Peninsular mode

5.2.2. Test scenarios

Planning studies and operating experience have indicated that loss of major transmission resources results in decreased transient and small signal stability margins [1,2]. To mitigate the effects of such events, several control alternatives were identified and studied. Cases of special interest selected for study included:

Test Scenario 1. A modified base case with PSSs on critical machines of the Peninsular area, and

Test Scenario 2. Application of FACTS technology at critical system locations. These include the following:

- 230/300 MVAr dynamic voltage support by static VAR compensation of the 230 kV Escarcega substation (ESA-230kV)
- Thyristor-controlled series-compensation (TCSC) on the Escarcega-MCD 230 kV transmission line

A discussion of these cases in the context of robustness analysis follows. The focus is on the analysis of the effect of uncertainty on operating conditions on the stability of the 0.52 Hz East-West mode as well as to confirm that the designed controllers are robust over a wide range of operating conditions. Uncertainty-based control policies are examined in subsequent sections.

5.2.3. Base case assessment

To assess the base case, conventional eigenanalysis studies were conducted using SSAT. The initial operating condition is the same used throughout Chapter 4 with the entire network being fully represented.

Table 5.1 shows the damping ratio and frequency of 0.52 Hz inter-area mode obtained by varying the amount and direction of the Southeastern-Peninsular power. A PSS is added at unit # 3 of MDP (MDP-U3) to examine the effect of control action on system damping.

Table 5.1. Damping ratio and frequency of the 0.52 Hz East-West mode - PSSs at MDP-U3

Southeastern – Peninsular power flow (MW)**	Eigenvalue	Damping ratio (%)	Frequency (Hz)
- 327	0.0632±j 3.040	0.0	0.4838
- 288	-0.029±j 3.009	0.9	0.4924
- 201	-0.092±j 3.186	2.9	0.5071
-110	-0.153±j 3.249	4.7	0.5171
-15	-0.208±j 3.278	6.32	0.5217
33	-0.229±j 3.277	6.99	0.5216
82	-0.245±j 3.265	7.50	0.5196
192	-0.250±j 3.223	7.72	0.5130
252	-0.233±j 3.185	7.29	0.5069
342*	-0.233±j 3.185	6.13	0.4968

* Last solved power flow condition.

**A negative sign indicates reversed power flow conditions.

Figures 5.3 and 5.4 show, respectively, the corresponding damping ratio and frequency of the 0.52 Hz inter-area mode for the case with and without control measures included. Each plot corresponds to a different combination of supplementary controls in the Peninsular area.

Depending on the level of power transfers and the magnitude and direction of power flows, normal, preventive or remedial actions are necessary to maintain system stability. These include:

- SVC control action at Escarcega on the Peninsular-Southeastern corridor
- The application of PSSs at dominant machines, and
- Discrete supplementary control actions

As shown from the analysis of the damping ratio of the Peninsular mode in Figure 5.3, adding PSSs at units # 1 and 3 of MDP power station, results in increased damping ratios for the 0.52 Hz inter-area mode even for large Southeastern-Peninsular flows.

By contrast, the use of SVC voltage support at the 400 kV Escarcega (ESA-230kV) substation on the Southeastern-Peninsular interconnection is seen to enhance damping of the inter-area mode only when the power flow is reversed. The small-signal stability limit (MGPen limit) in Figure 5.3 is estimated to be about 327 MW and represents the maximum inter-area power transfer from the Peninsular system to the MIS.

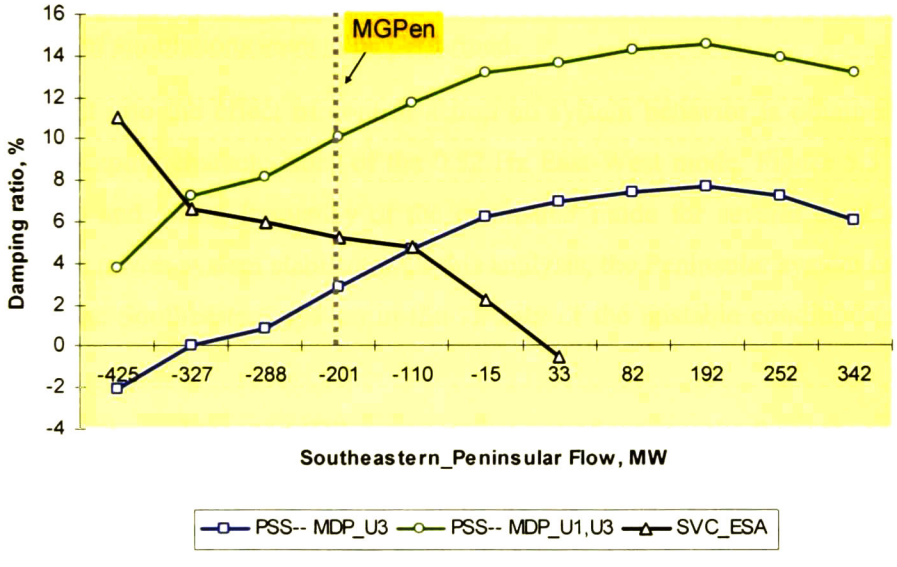

Figure 5.3. Damping ratio of the 0.52 Hz East-West mode for various control alternatives

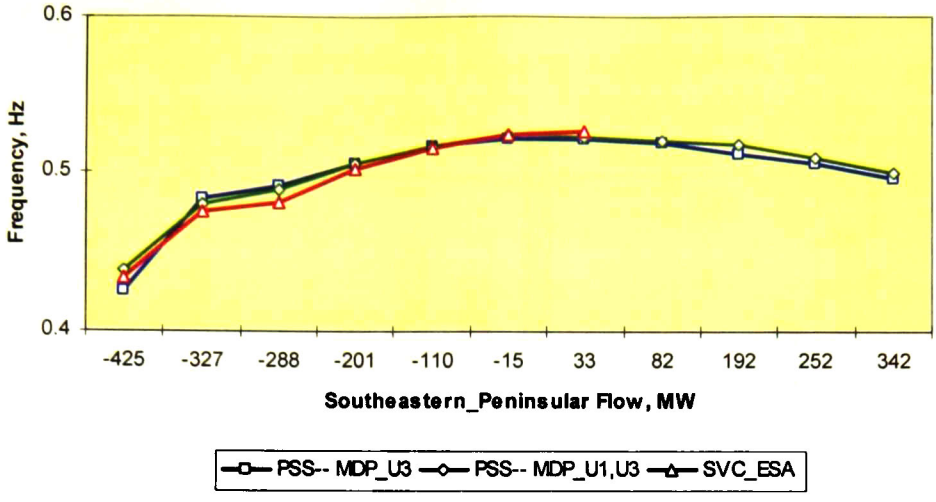

Figure 5.4. Oscillation frequency of the 0.52 Hz Peninsular mode as a function of the Southeastern-Peninsular tie-line power transfer

Figure 5.4 suggests that transfer levels in excess of 330 MW from the Peninsular region to the Southeastern system result in a complex behavior associated with the 0.52 Hz Peninsular mode. It should be stressed, however, that for any operating scenario considered, it will always be difficult to estimate stability margins using conventional analysis since a large number of simulations have to be performed.

Further insight into the effect of control action on system behavior is obtained from the analysis of damping characteristics of the 0.52 Hz East-West mode. Figure 5.5 shows the damping ratio and swing frequency of the peninsular mode for several combinations of machines with power system stabilizers. In this analysis, the Peninsular system is exporting 110 MW to the Southeastern system in the vicinity of the unstable condition (see Figure 5.4).

For the case with machines at MDP power station out of service, the frequency of the 0.52 Hz East-West mode increases from 0.52 Hz to 0.71 Hz. It is also interesting to observe from Figure 5.5, that adding PSSs to units # 4 and 5 of VAD station, the damping of the 0.71 Hz inter-area mode increases from 1.9 to 7.29 % that is considered satisfactory.

These complex operating conditions motivate consideration of approximate analytical techniques to determine stability margins.

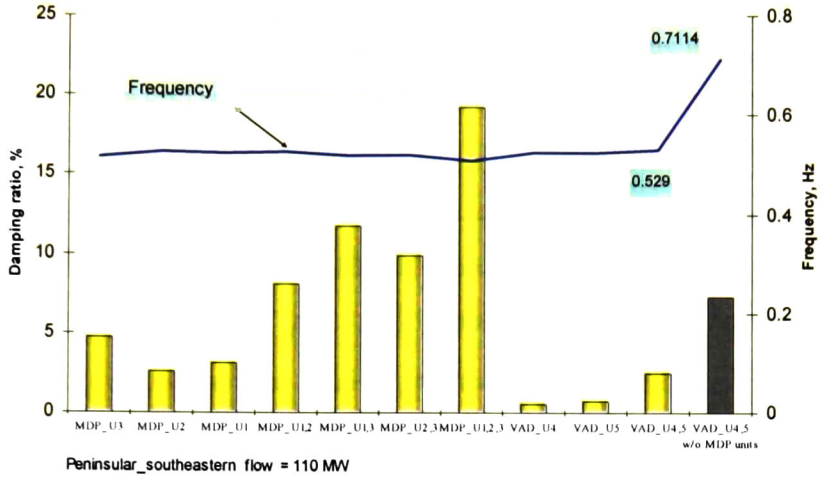

Figure 5.5. Damping ratio and frequency of the 0.52 Hz East-West mode

We next turn our attention to the application of robustness analysis and discuss the development of dynamic security assessment techniques for test scenarios 1 and 2. Comparisons are also provided with conventional analysis.

5.2.4. Test Scenario 1: robust stability analysis with PSSs at MDP

The uncertainty algorithm detailed in the previous chapter was used to determine robust stability limits. For this purpose, the power transfer across the interface was modeled as a structured uncertainty and included in the nominal system representation. Transfer and operating limits were then determined for various control alternatives.

Table 5.2 shows the behavior of the 0.52 Hz East-West mode as a function of the total power flow across the Southeastern-Peninsular interface. From these studies, the limiting operating condition corresponds to a total power flow of about 327 MW.

Table 5.2. Damping ratio and frequency of the 0.52 Hz inter-area mode as a function of the intertie power transfer

Peninsular-Southeastern transfer (MW)	Eigenvalue	Damping ratio (%)	Frequency (Hz)
110	-0.153±j 3.249	4.7	0.5171
201	-0.092±j 3.186	2.9	0.5071
288	0.0290±j 3.009	0.9	0.4924
327	0.0632±j 3.040	**0.0**	0.4838

Using the method described in the previous section, a grid of operating conditions was constructed using expected operating conditions. To more explicitly incorporate uncertainty in the system model, a grid of operating conditions was then determined from the parameter space.

From experience in our case studies in Chapter 4 we know that the range of variations (parameter space) of interest can be sufficiently accurately approximated by a set of three operating points, i.e. $\mathbf{p}_1 = [p_{11} \quad p_{12} \quad p_{13}]$, where the first value corresponds to the nominal operating condition and p_{12} and p_{13} are two other selected operating conditions.

Table 5.3 compares the exact power transfer level at which instability is detected with the estimated power flow using μ-analysis. From μ-results in Table 5.3, the estimated robust stability limit is about 280 MW. The error in the maximum power flows estimate is about 7.5 %, which is still within a reasonable tolerance. It is important to note, however, that the accuracy of the method can be improved by taking an additional operating condition as discussed in Chapter 4.

Table 5.3. Test Scenario 1. One parameter variation robust stability assessment with a PSS at MDP-U3

μ upper bound	4.07
Estimated (exact) ω (rad/s)	3.11 (3.04)
Estimated (exact) power flow (MW)	280 (327)
Inter-area mode 1/damping	0.0001± j 3.04, ζ = 0.0 %
Error (%)	7.5

5.2.5. Test scenario 2: effect of controlled series compensation

In this scenario, a TCSC was located on the 230 kV Escarcega substation of the ESA-MCD 230 kV line in the Peninsular system to enhance the Peninsular-to-Southeastern The TCSC's fixed compensation level is set to 10 %. Reference [2] provides details of the control structure adopted in the studies.

Following a similar procedure to the case considered above, the Southeastern-Peninsular real power flow was treated as a varying parameter and the stability limit was determined using conventional analysis.

Table 5.4 depicts the damping of the inter-area mode as a function of the Peninsular-Southeastern power transfer level, whilst Table 5.5 provides the estimate using robust analysis. For comparison, the frequency computed at the exact limiting condition (250 MW) using a conventional small signal stability program is also included. It can be seen that uncertainty analysis gives a reasonable prediction of the maximum loading condition. The error in this case is in the order of 5.8%.

Table 5.4. Damping ratio and frequency of the 0.52 Hz inter-area mode for various power transfers

Peninsular-Southeastern (MW)	Eigenvalue	Damping ratio (%)	Frequency (Hz)
110	-0.4866±j 3.2085	14.90	0.5106
201	-0.0823±j 2.8356	3.71	0.4513
288	0.0632±j2.8105	1.89	0.4473

Table 5.5. Estimated value of critical parameters. Test scenario 2

μ upper bound	6.09
Estimated (exact) ω (rad/s)	2.868 (2.827)
Estimated (exact) power flow (MW)	236 (250)
Inter-area mode 1/damping	-0.0006± j2.827, ζ = 0.02 %
Error (%)	- 5.8

The analysis of the μ plot in Figure 5.6, on the other hand, shows two dominant peaks; a peak at about 0.32 Hz associated with the interaction of most machines in the north and south systems (north-south mode), and a peak at about 0.52 Hz associated with the East-West mode. The magnitude of the peaks for the 0.32 Hz mode and the 0.52 Hz mode is greater than 1, showing that the system is robustly unstable. It is also of interest to note that, magnitude of the 0.32 Hz component is nearly equal to that of the 0.52 Hz peak, thus emphasizing the importance of multiple uncertainties. A third mode at 7.55 rad/s (1.2 Hz) is also perceptible close to the instability condition, representing a local oscillation to the Peninsular system.

To verify these findings, the nature of this mode was analyzed using eigenanalysis. Table 5.6 shows the damping ratio and frequency of the 1.2 Hz local mode as a function of the inter-area power transfer. Note that, while the damping of the mode decreases with increased transfer levels the mode remains stable as suggested by robustness analysis.

The identification of critical modes close to instability is a useful characteristic of the method that allows accurate tracking of the behavior of critical modes over a given frequency interval.

Table 5.6. Damping ratio and frequency of the 1.2 Hz local mode for various power transfers

Peninsular_ Southeastern (MW)	Eigenvalue	Damping ratio (%)	Frequency (Hz)
110	-0.514±j 7.699	6.67	1.225
201	-0.346±j 7.636	4.53	1.215
288	-0.259±j 7.544	3.53	1.201

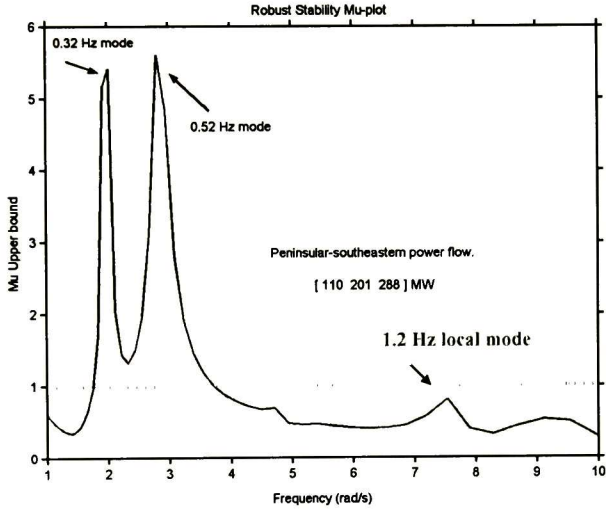

Figure 5.6. μ upper bound for robust stability assessment of limiting power flow

On the basis of this analysis, the notion of uncertainty-based control dynamic security assessment (DSA) is defined and techniques to define preventive and emergency control procedures are discussed. A secondary objective addresses the temporal changes in the uncertainty and parameter interactions within the study area.

5.3. Dynamic security assessment – N-1 contingency condition

As discussed in the last section, system security may be considered as the ability of a power system to survive contingencies with a safety factor or margin [3]. In practice, the computation of the stability margin is based on the system operating condition and the

nature of the disturbance. A critical level for a given parameter can be used to define a critical region or measure of DSA. Thus for instance, small signal stability can be considered as an indicator of the robustness of the power system at a given operating condition [4]. To be of practical use, however, this indicator must be related to typical parameter measures by the human operator, for instance power transfer levels and has to be updated as system operating conditions change.

In this section, we propose the definition of robustness-based preventive and emergency control zones or system-operating states associated with the operation of the system under high uncertainty. Techniques to expand the secure operating range based on control action are discussed. The analysis is limited to variations in operating conditions, adjustments in the control settings of existing controllers and network contingencies, since the analytical formulation requires the number of states to remain constant during the study. The extension of this approach to account for generator outages or other contingencies resulting in a transition of the state model, to another reduced order model, would lead to a reformulation of the state model valid for the post-contingency condition.

Given a system operating condition, a two-stage approach is proposed for dynamic security assessment:

(i) The parameter of interest is varied for both, an *n* condition, i.e. the pre-contingency condition, and the critical contingency case, or *n-1* condition.

(ii) Then, using the proposed robust method, uncertainty-based estimates are used to define the operating range at which the emergency zone starts.

With this approach, one is not limited to considering one varying parameter, and may in fact consider various uncertainty conditions simultaneously. One additional advantage of this method is that it allows for an intuitive algorithm for assessing the relative importance of each uncertainty in system performance.

To illustrate this operation strategy we consider two test scenarios: i) a base case with PSSs on several units of the Peninsular area (*n*-condition), and ii) a case with a PSS on MDP-U3, (n-1 system condition). For each operating scenario, the damping ratio was computed as a function of the inter-tie power transfer.

By obtaining several critical flows, a secure operating region can be defined in which all operating points are stable and well damped. These solutions, depicted graphically in Figure 5.7, are computed using conventional eigenanalysis techniques. This provides a new visualization of the robustness analysis problem that guarantees both, robust stability and performance.

According to the discussion in the previous subsection, we define three operating states as follows:

1. The first level of operation corresponds to the normal operating state in which damping remains within acceptable margins, i.e. greater than 5%. Starting with a normal operating point (point A) in Figure 5.7, a sequence of small-signal stability (SSS) studies are needed to compute the trajectory of the mode of concern for various inter-area power transfers.

2. The second level of operation is an alert state. As discussed below, the system enters an alert state when the damping of the mode of concern is below a pre-specified damping ratio margin; this corresponds to the limiting small signal stability condition for the critical contingency case, in this case 327 MW. Under these conditions, the dispatcher must take manual actions to reestablish the normal operating state and to prevent the system from entering the emergency state. These actions can include generation disconnection, load disconnection or other decisions that reduce the emerging power oscillations. The normal operating zone finishes when the alert zone starts, at approximately 100 MW. In this case, the small-signal stability margin is about 230 MW.

3. The third and final level of operation is the emergency state in which automatic control remedial actions are designed to take place.

In the n condition, the above approach ensures that the system has reasonable small signal stability margin over the range of the Southeastern-Peninsular intertie power transfers of interest. One further advantage of this scheme is to have control strategies for operating changes associated with the transition from the n condition to the n-1 condition. As a result, operating in both the normal and the alert states, the system will be small signal stable whilst operating in the normal zone the system will be small signal secure.

The above arguments provide a self-consistent approach to the choice of control strategies which will satisfy the required robustness criteria, i.e. minimum damping.

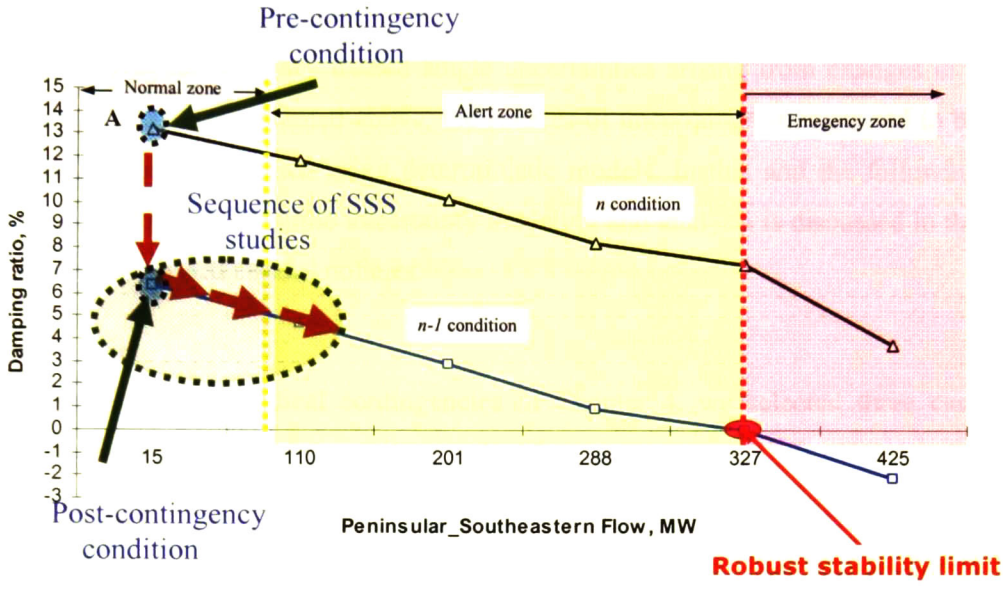

Figure 5.7. Illustration of robust stability regions in terms of normal, alert and emergency zones or operating regions

The procedure outlined above to define the normal and alert operating conditions, however, is not practicable for a number of reasons.

- For any operating scenario it is difficult to estimate small signal stability margins. It is also difficult to assess how the process variables or parameters influence each other.
- This approach is too computationally intensive to be practically used in numerical simulations and for real-time control.
- The analysis may overlook mode shifting associated with destabilization of local modes. This is especially true for the 1.2 Hz local mode.

To circumvent these limitations, local and wide-area control actions based on robustness analyses that improve the efficiency of the above approach are discussed in the subsequent section in the context of uncertainty theory. Criteria are also developed to translate this

information into an assessment of the robustness of the system. The focus of this study is to find good design solutions in the presence of multiple interacting uncertainties.

5.4. Robustness-based analysis in the presence of multiple uncertainties

In the discussion thus far, we have treated single uncertainties arising from changes in a given parameter of concern. As noted above, the sources of uncertainty are assumed to be independent and have been treated using deterministic models. In this and the following three sections, the subject of multiple uncertainty modeling and analysis is discussed in the context of uncertainty-based control policies.

5.4.1. Case studies

Based on the evaluation of critical contingencies in Chapter 4, we selected three case studies with two parameters varying simultaneously. These are:

Case 1. A case with both, high north-south power transfer levels and high Peninsular-Southeastern power transfer levels. In this case, the operating space is defined by the vector of power flows across the north-south interface ($\mathbf{p}_1$ = [530 MW, 870 MW and 1170 MW]) and vector of power flows across the Peninsular-Southeastern interface ($\mathbf{p}_2$ = [110 MW, 200 MW 288 MW]).

Case 2. A case with both high north-south power transfers ($\mathbf{p}_1$ = [530 MW, 870 MW, 1170 MW]) and increased active power generation in the Western system ($\mathbf{p}_2$ = [6043 MW, 6208 MW, and 6298 MW]).

Case 3. A case with combined high Peninsular-Southeastern power transfers ($\mathbf{p}_1$ = [110 MW, 200 MW and 288 MW]), and increased active power generation in the Western system ($\mathbf{p}_2$ = [6043 MW, 6208 MW, and 6298 MW]).

Robust stability analysis results for the cases described above are shown in figures 5.8(a)-(c) for these values of uncertainty. Note that, the large uncertainty in parameter values results in considerable variations in worst-case scenarios thus emphasizing the importance of robustness analysis.

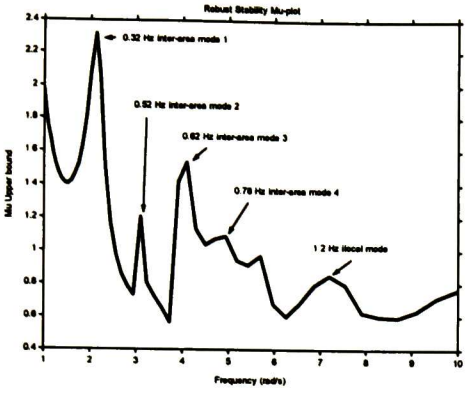

a) Case 1

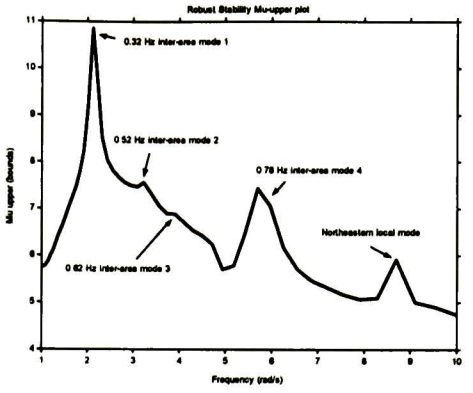

b) Case 2

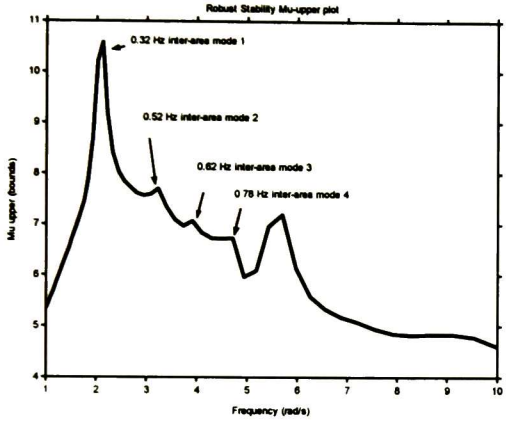

c) Case 3

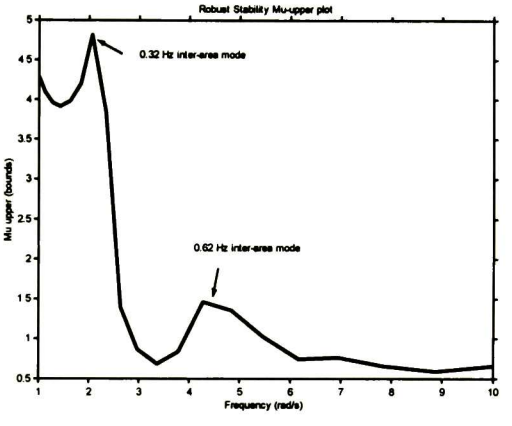

c) Case 4

Figure 5.8. μ-upper plot for case studies of concern

From the application of μ-analysis in Figure 5.8, the following conclusions can be drawn:

- In all three cases, robustness analysis identifies a dominant, unstable mode at about 0.32 Hz associated with the north-south mode. The magnitude of the peaks at a given frequency provides an indication of the importance of the uncertainty in operating conditions. The bigger the magnitude of the peak associated with a given parameter, the larger the importance associated with the uncertainty in the parameter. (?, memo)
- Cases 1, 2 and 3 on the other hand suggest multiple instability conditions in which robust stability can not be guaranteed for several major inter-area and local system

modes. For cases 1 through 3, the analysis identifies instability for four inter-area modes (0.32 Hz, 0.52 Hz, 0.62 Hz, and 0.78 Hz). Instability is also evinced for the 7.55 rad/s local mode to the Peninsular system (Case 1) and a local mode to the Northeastern system (8.8 rad/s).

- Case 4 on the other hand, detects a more localized behavior in which stability is not guaranteed for the 0.32 Hz north-south mode and the 0.62 Hz inter-area mode.

Finally, by relating these results to the zones with more influence on the dominant modes, the areas that are more vulnerable to system instability can be detected, and preventive and corrective remedial actions can be developed more efficiently.

Having estimated μ bounds for the cases of concern, we perform a detailed investigation of the use of automated robustness analysis algorithms and extend its range of applicability to the analysis of multiple, interrelated uncertainties. In the sections to follow, we describe the application of the developed procedures to the problem of evaluating robust stability regions of interrelated uncertainties.

5.4.2. Dynamic security assessment

Using the results of the previous steps, we applied the developed technique to computing robust stability margins. The analysis is needed for our subsequent robustness analysis investigation.

Our analysis extends the formulation presented in section 5.3, and that in Ref. [5] in two main ways:

- The procedure is automated thus avoiding the use of previous knowledge on system behavior, and thus the need for repetitive small-signal calculations and
- The approach performs the computation of robust stability limits in a single step thus saving lengthy iterative evaluation of stability

In order to construct and efficient tool to determine robust stability limits in Figure 5.7, a two stage approach was developed: (i) Using an initial operating condition, p_1, the operating space was determined using two (additional) forecasted operating conditions.

This approach results in a grid of nine operating conditions, and (ii) robust stability conditions are determined using μ-analysis.

Figure 5.9 shows robust stability assessment for the four cases above determined using the proposed approach. The results of the analysis are seen to correspond closely with the evaluation of robustness in Figure 5.7 further confirming the validity of the procedures.

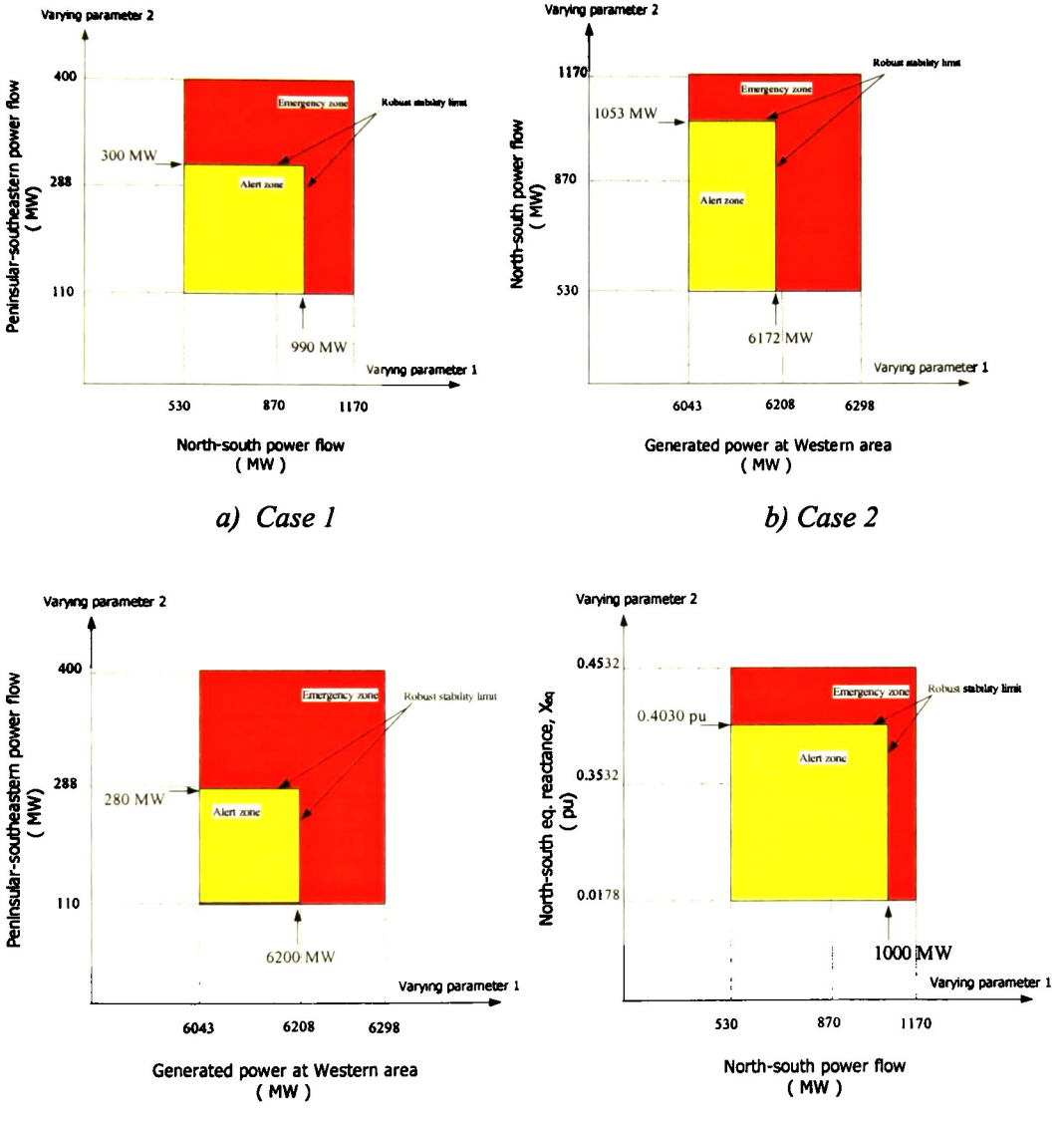

Figure 5.9. Dynamic security assessment for cases in Figure 5.8. n-condition.

For each condition and varying parameter, the relative size of the yellow areas (alert state) provides a measure of the distance to the instability condition (robust stability limit). In interpreting these results, we remark that the initial operating conditions have damping ratios greater that 5%. As a result, all four cases are initially operating in the alert zone.

For more general operating conditions, however, the initial operating point would be in the normal operating state (green zone).

Two strong advantages of this approach are it's efficiency being roughly equivalent to the analysis of a single operating conditions, and the fact that the analysis of multiple interrelated uncertainties becomes feasible. This technique also offers an increased appreciation of a number of related concepts in the area of real-time control and points to the need for online small-signal security assessment.

5.4.3. Computational considerations

The proposed approach offers significant improvements over the approach in Figure 5.7, generating detailed information on the nature and size of operating regions. Figure 5.10 provides details of the cost of computer time for full-scale robustness analysis.

Of the total cost of computer time, about 90% is devoted to obtaining the power flow solution and constructing the state matrix (i.e. 10% for each operating condition in the operating space). It should be stressed that about 10% of the computational cost is spent on determining the robust stability limit.

In words, robustness analysis amounts to determining the robust stability limit for a single operating condition. More importantly, the computational effort for the proposed method increases only linearly with the number of operating conditions. This shows the efficacy of the method for analyzing very large systems.

Further, as noted above, conventional analysis is very sensitive to the expertise of the analysis carrying out the simulations.

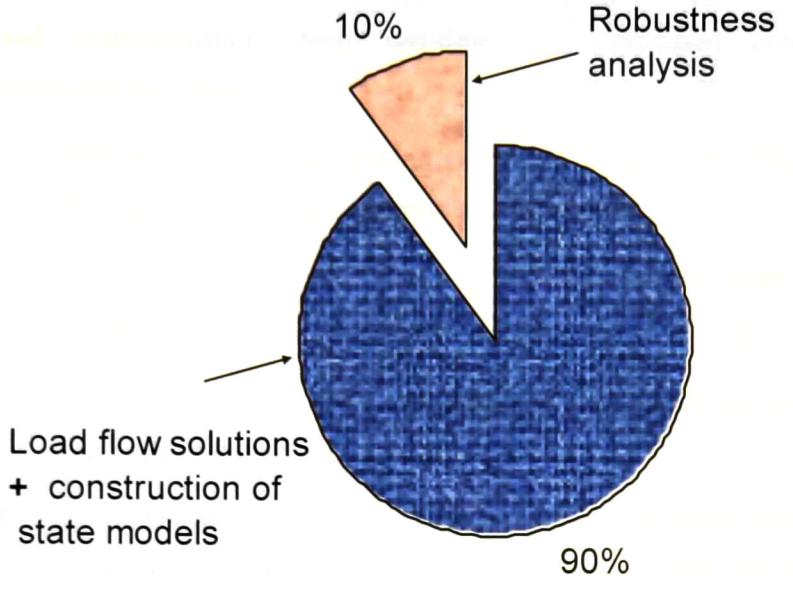

Figure 5.10. Computational effort for modeling uncertainty in two parameters simultaneously

Next, the notion of uncertainty-based dynamic security assessment is defined and a near, real-time control strategy is proposed that accounts for system contingencies. A secondary objective addresses the temporal changes in the uncertainty and parameter interactions within the control system. Case 1 is selected because of the most complex dynamics involved but the developed procedure is general and can be used to characterize any selected operating scenario.

5.5. Real time, uncertainty-based dynamic security assessment

The concept of dynamic security proposed in section 5.3 can be easily generalized to deal with multiple uncertainties in a real-time environment. In this section, we proposed a systematic framework to extend robustness analysis near, real-time and provide better information about preventive and emergency dynamic security assessment.

In our previous formulation, a vector of m varying parameters $\mathbf{p} = [p_1 \quad p_2 \quad \cdots \quad p_m]$ was considered for robustness analysis. Motivated by this algorithm, we explore the utilization of Scada (System Control and Data Acquisition) monitoring systems to determine the range of varying parameters and computing robust stability margins.

Following the scheme outlined in section 5.3, Figure 5.11 shows a schematic of the proposed implementation. Near real-time robustness-based control policies are implemented in four steps.

Step 1. Obtain the base case operating condition from on-line (Scada) measurements. This provides the base-case power flow solution.

Step 2. For each operating condition, a set of forecasted (i.e. three expected operating conditions) are used to define the operating space $\mathbf{p}_k = [p_{11} \quad p_{12} \quad \cdots \quad p_{1ne}]$.

Step 3. Using this representation, small signal stability margins are determined using the approaches outlines in section 5.3.

Step 4. If the system is expected to enter an insecure operating condition, the operator takes action to reestablish the normal operating state. Alternatively, automatic discrete supplementary control actions can take place based on planning strategies.

The goal is to be able to anticipate, on an on-line environment, system contingencies that make system operation insecure and to develop robustness-based remedial actions. These four steps are elaborated in our subsequent analysis.

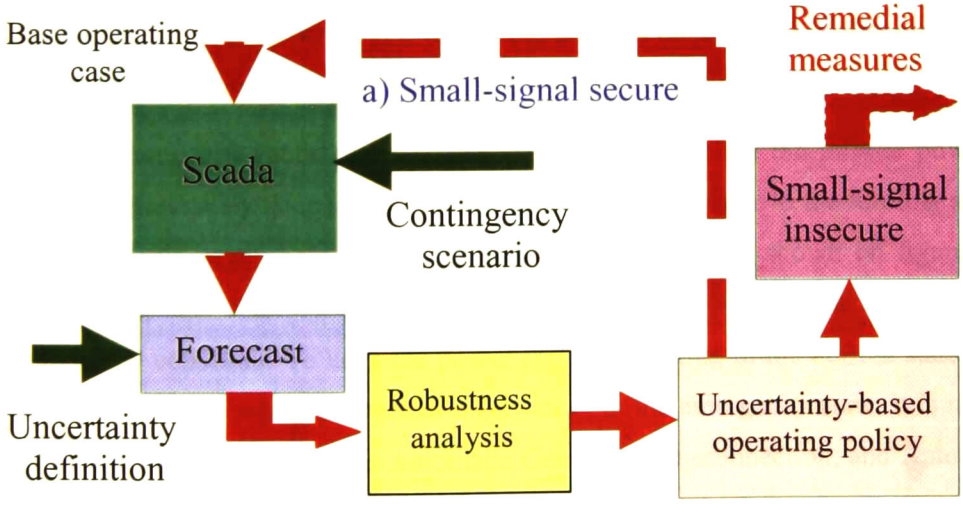

Figure 5.11. Proposed robustness-based framework for DSA and control

There are two key issues concerning this approach. The first one is defining accurate regions for normal and alert operating conditions based on robustness analysis. The other key issue in applying this formulation for determining remedial actions is finding representations of the system which allow for the efficient characterization of multiple, interrelated uncertainty.

Using the definition of operating states in section 5.3, the normal, alert and emergency operating zones can be defined as follow. In the first step, we increase the power flow across the critical intertie for three cases: i) the n condition, i.e. the pre-contingency condition, ii) the critical single contingency case, or n-1 condition, and iii) the critical double contingency case, or n-2 condition.

Because of the speed of the proposed robustness analysis technique, the methodology can be used efficiently to anticipate dangerous contingencies and alert the operator to take emergency and preventive actions to mitigate such events. Ideally, such an approach could be used to take control actions on-line. This is, however not discussed here.

For illustration, consider a combination of uncertainty involving two varying parameters acting simultaneously in which the north-south power flow and the north-south interconnecting reactance are allowed to vary between known upper and lower bounds.. In this scenario, the north-south power flow takes the values [530 MW, 870 MW, 1170 MW] and, the north-south intertie reactance takes the values [n=0.01766 p.u, n-1=0.3532 p.u., n-2=0.4532 p.u] (full network, one circuit out and two circuits out). PSSs on CDB thermal power station are considered for the control of the 0.32 Hz north-south mode.

Using the proposed robustness analysis criteria, we calculate the intertie power flow at which the emergency zone (red region) begins; this corresponds to the limiting small signal stability condition at about 1000 MW and 0.04030 pu, as is shown on figure 5.12. We remark that, this stability limit takes into account the n-2 design criteria, or double contingency condition. To keep the power system operating in the normal state, and avoid the loss of stability when the system is operating in the emergency zone, it is necessary to design discrete controls such as Automatic Generation Disconnection, and Automatic Load Shedding.

Generalizing the approach of section III, the secure region determines the area of all stable (and secure) operating points for the system for which robust performance is guaranteed. In a similar vein, the alert zone (yellow area) starts when the intertie power flow is below the specified damping ratio margin, i.e. 5 %. In turn, operation in the alert condition, the dispatcher must take manual actions to avoid that the system reaches the emergency condition. Finally, as indicated in Figure 5.12, using the n-1, criterion the normal operating zone (green region) finishes where the alert zone starts, at approximately 870 MW.

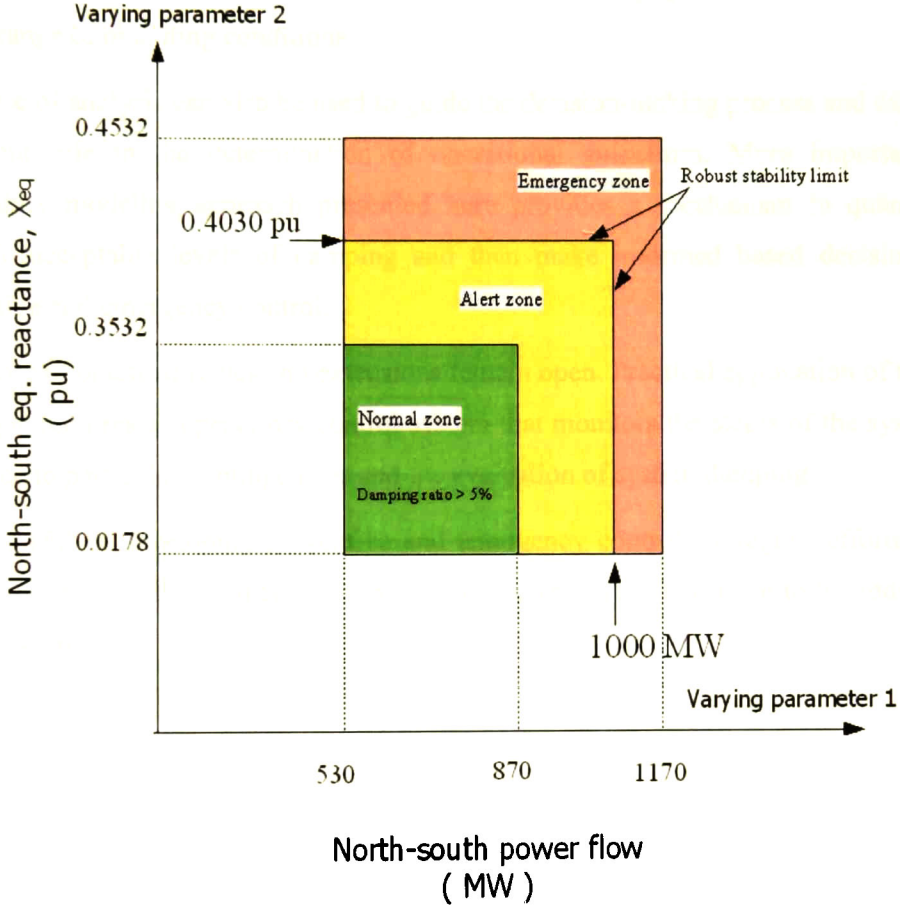

Figure5.12. Conceptual representation of robust stability domains for two varying parameters.

In the *n*-condition, the above approach ensures that the system has a minimum damping over the entire range of parameter variations. One further advantage of this scheme is to have control strategies for operating changes associated with the transition from the *n* condition to the *n-1* or *n-2* condition.

Hence, operating in the alert zone, the system will be small signal stable whilst operating in the normal zone the system will be small signal secure as discussed above.

5.6. Concluding remarks

In this chapter, robustness analysis has been extended to account for multiple uncertainties occurring simultaneously. The method presented here provides a simple, systematic and powerful methodology for the analysis of complex networks with significant sources of interrelated uncertainties and enables to confirm if existing system controllers are robust over a range of operating conditions.

This type of analysis can also be used to guide the decision-making process and can play an important role in the determination of operational guidelines. More importantly, the uncertainty modeling approach presented here provides a mechanism to quantitatively evaluate acceptable levels of damping and then make informed based decisions about preventive and emergency control.

A number of practical issues and extensions remain open. Practical application of the above technique requires a supervisory control system that monitors the status of the system with reference to particular contingencies and the evaluation of system damping.

To be useful in developing preventive and emergency control strategies, efforts are also needed to improve the quality of estimates. These are issues that have to be addressed by future research.

References

[1] R. Castellanos, A. R. Messina, H. Sarmiento, "Robust stability analysis of large power systems using the structured singular value theory", *International Journal of Electrical Power and Energy Systems*, vol. 27, No. 3, July 2005, pp. 389-397.

[2] H. G. Sarmiento, R. Castellanos, G. Villa, Aplicación de PSS y TCSC para incrementar la capacidad de transferencia Norte-Sur del Sistema Eléctrico Interconectado Mexicano", (in Spanish), Paper CE-C2-28, in: *Tercera Reunión Bienal CIGRE*, Irapuato, Gto. MEX, June 2003.

[3] Tomas E. Dy Liacco, "Real-Time Computer Control of Power Systems", *Proceedings of the IEEE*, vol. 62, no. 7, July 1974, pp. 884-891.

[4] Magdy E. Aboul-Ela, A. A. Sallam, James D. McCalley, A. A. Fouad, "Damping controller design for power oscillations using global signals", *IEEE Trans. on Power Systems*, vol. 11, no. 2, May 1996, pp. 767-773.

[5] M. Djukanovic, M. Khammash, V. Vittal, "Application of the structured singular value theory for robust stability and control analysis in multimachine power systems, Parts I and II", *IEEE Transactions on Power Systems*, vol. 13, no. 4, November 1998, pp. 1311-1322.

Chapter 6

Conclusions and Recommendations

This Chapter summarizes the main conclusions drawn from the application of the developed procedures to test systems and provides an overview of the main contributions of the research.

Suggestions for suture work are also given in the context of the present work.

6.1. General conclusions

The analysis of stability robustness of complex systems with respect to real parameter variations is an important problem. Operating and controlling these systems in the face of severe uncertainty remains a daunting problem for which very few results have been presented.

Uncertainty in the operation of power systems may result in reduced reliability and in many cases, in underperformance of system controls. The ability to quantify the impact of uncertainty leads to improved system operation and control and provides information which is needed in determining stability limits. In addition, accurate structured uncertainty descriptions are needed in the design of robust control to variations in system operating conditions and the development of robustness-based control policies.

Standard procedures for robust stability analysis of uncertain systems existing in the literature are not suitable for robustness analysis of large-scale systems. A significant disadvantage of existing μ-formulations is the high computational cost associated with the SSV/LFT formulations. Moreover, traditional methods of analysis are limited in their ability to treat multiple uncertainties arising from correlated parameter variations.

In this dissertation, a novel framework for robust stability analysis and control of large, uncertain power systems has been developed and presented that circumvents the above limitations. The proposed technique is based on structured singular value theory which allows computation of an effective measure of robustness in the presence of real parametric uncertainty and can treat and analyze most types of uncertainties, common in power system applications. This approach can be used to analyze multi-machine power systems of

realistic dimensions and results in computational requirements that outperform existing approaches. Further, the derived formulations are suitable for real-time dynamic security assessment.

A distinct feature of this approach is that it allows not only robust stability assessment but also an estimation of the critical value of the uncertainty parameter for which the system becomes unstable. This is especially important when several uncertainties are treated simultaneously. Another advantage is the ability to identify the relative influence of the uncertain parameters in the robust performance measure.

The successful use of μ theory depends to a great extent on its relationship with LFT-based description. In the work conducted in this dissertation, an efficient analytical technique to derive LFT-based uncertainty descriptions of large-scale systems is outlined. The method overcomes some of the limitations of computational complexity, resolution and interpretation of uncertain linear systems. Further, the formulation can determine worst-case operating conditions arising from the representation of several uncertainties occurring simultaneously in the control loop. Ultimately, this approach promises to be valuable for the analysis and control of nonlinear dynamic systems.

There are two main advantages to this approach:

1. Because the uncertain representation is derived directly from a small signal stability software, the modeling capacity is that of the software. This allows the study of systems of realistic dimensions, often characterized by several thousand states.
2. The method eliminates the need for reduced-order representations and thus enables the full structure of the system to be preserved. In this way, the uncertainties associated to reduced order approximations to small-signal dynamics are eliminated.

Extensive numerical studies have been presented to demonstrate that accurate results can be obtained. Simulation results indicate that the proposed method can accurately be used to assess robust stability of large complex systems. Differences that do exist warrant additional investigation.

These results are encouraging and suggest the potential for using in conjunction with more advanced analytical techniques for μ computation as the basis for obtaining a dynamical-system based model of system in an on-line environment.

The analysis shows that small signal analysis and interpretation are highly sensitive to the introduction of uncertainty. Both conventional linear analysis and detailed time domain simulations have been undertaken to validate robust stability results, which show good agreement.

Simulation results with various power systems clearly indicate the efficacy of the proposed procedures in predicting stability robustness. Numerical simulations show that the method produces accurate results within 5% of the exact solution. These results are considered to be acceptable, especially in view of the wide range of changes in operating considered in the studies. While further applications of the method are in progress, it is found to work well for a variety of complex problems.

The importance of these results lies in their usefulness in determining the conditions under which the system may become unstable. These techniques are thought to have potentially important applications to analyze robust stability and robust performance of power systems and other physical processes. This latter development is part of future work.

6.2. Suggestions for further research

The development of robustness evaluations techniques represents the first attempt in applying real SSV theory to a complex, large-scale system. As a result, improvements are expected in almost all aspects of modeling and implementation of the technique. More specifically, the results presented in this research indicate that a number of improvements can be made in modeling and characterization methods for multiple, uncertain parameters.

The following aspects require further investigation:

(a). Numerical results suggest that better numerical algorithms for calculating tight bounds on μ for the resulting high-order real parametric uncertainty model are needed. Currently available software tools for calculating lower bounds on real μ fail for this problem.

(b). The extension of the proposed μ-analysis approach to consider robust performance issues merits considerations in the analysis of control and design problems and is the subject of current research by the author. Further, robust tuning of power system controllers deserves further investigation.

(c). Finally, although structured singular values are useful measures of robustness, their interpretation is sometimes difficult. Techniques are therefore needed to interpret robustness measures in ways that are familiar to power engineers.

Additional applications of robustness analysis hold particular promise for the simultaneous analysis of key varying parameters on nominal stability. Other aspects such as the extension of the above algorithms to design system controllers and the improvement of μ computations might be worthwhile in the context of robust control and analysis of uncertain systems.

As pointed out in the foregoing, the research here represents one of the first attempts in applying the recently developed μ-theory for analyzing the robustness properties of large-scale linear state-space power system models. In the large-scale application of the method to realistic power system models, several sources of error have been identified that limit the applicability of the proposed technique to accurately determine robust stability limits. These include (i) errors arising from the determination of the LFT-based representation using least-squares optimization, (ii) errors arising from the computation of upper bounds for real problems, and (iii) other sources of error arising from the numerical implementation of the proposed technique.

Efforts are needed to address and treat these problems.

CENTRO DE INVESTIGACIÓN Y DE ESTUDIOS AVANZADOS DEL I.P.N.
UNIDAD GUADALAJARA

El Jurado designado por la Unidad Guadalajara del Centro de Investigación y de Estudios Avanzados del Instituto Politécnico Nacional aprobó la tesis

Valoración de la estabilidad robusta de sistemas de potencia de dimensión grande utilizando la teoría de valor singular estructurado

del (la) C.

Rafael CASTELLANOS BUSTAMANTE

el día 17 de Noviembre de 2006.

Dr. Arturo Román Messina
Investigador CINVESTAV 3C
CINVESTAV Unidad Guadalajara

Dr. José Javier Ruíz León
Investigador CINVESTAV 3B
CINVESTAV Unidad Guadalajara

Dr. Antonio Ramírez Treviño
Investigador CINVESTAV 2C
CINVESTAV Unidad Guadalajara

Dr. Emilio Barocio Espejo
Profesor Investigador Titular C
Universidad de Guadalajara

Dr. Jorge Guillermo Calderón Guizar
Investigador Categoría K Nivel 4
Instituto de Investigaciones
Eléctricas